# DETECTION AND PROCESSING OF FOETAL ELECTROCARDIOGRAMS

## A REPRESENTATIVE EXAMPLE FOR THE PROCESSING OF BIOLOGICAL SIGNALS

J. H. VAN BEMMEL

PROMOTORES:

Prof. dr. A. J. H. VENDRIK

Prof. ir. B. P. Th. VELTMAN

# DETECTION AND PROCESSING OF FOETAL ELECTROCARDIOGRAMS

## A REPRESENTATIVE EXAMPLE FOR THE PROCESSING OF BIOLOGICAL SIGNALS

PROEFSCHRIFT

TER VERKRIJGING VAN DE GRAAD VAN DOCTOR
IN DE WISKUNDE EN NATUURWETENSCHAPPEN
AAN DE KATHOLIEKE UNIVERSITEIT TE NIJMEGEN,
OP GEZAG VAN DE RECTOR MAGNIFICUS
MR. W. C. L. VAN DER GRINTEN, HOOGLERAAR IN DE FACULTEIT
DER RECHTSGELEERDHEID, VOLGENS BESLUIT VAN DE SENAAT
IN HET OPENBAAR TE VERDEDIGEN OP 2 OKTOBER 1969 TE 16.00 UUR

DOOR

JAN HENDRIK VAN BEMMEL

GEBOREN TE ROTTERDAM

1969
GRAFISCH BEDRIJF SCHOTANUS & JENS UTRECHT N.V.

*Aan mijn Ouders*
*Aan An en Christine*

# ACKNOWLEDGMENTS

The present work was performed at the Institute of Medical Physics TNO, Utrecht, in cooperation with the Department of Obstetrics and Gynaecology of the University of Nijmegen.

To Ir. D. H. Bekkering, Director of the Institute of Medical Physics TNO, and Ir. J. Kuiper who initiated the investigation, I want to convey my thanks for their encouragement and continuous support.

It is a pleasure to thank H. van der Weide for his competent and active contribution in developing the instruments for clinical use and in the collection and presentation of the data.

I am greatly obliged to S. J. Hengeveld and B. Versteeg who carried out most of the analyses and processing of the signals.

The author acknowledges the interest of Professor Dr. J. L. Mastboom, Head of the Department of Obstetrics and Gynaecology of the University Hospital of Nijmegen.

I wish to express my sincere gratitude to Professor Dr. L. A. M. Stolte and Dr. T. K. A. B. Eskes, formerly associated with this Department, and Dr. L. A. M. Peeters who gave much help and advice concerning the obstetrical part of this investigation.

To the entire staff of the Institute of Medical Physics TNO I am very indebted for their collaboration; not at least to J. Riethorst and J. G. J. Lommen of the Electronic Workshop, to H. W. de Soete of the Mechanical Workshop, to H. W. A. Vennix for the drawings, to Mrs. H. Wijnands and her staff for their excellent secretarial help and to R. M. Zondag and N. P. P. Haagen of the photography department.

I would like to mention the very interesting discussions with Professor Dr. A. J. H. Vendrik, Head of the Department of Medical Physics of the University

of Nijmegen and to thank him for his warm interest and his stimulating criticism in preparing the manuscript. To Professor Ir. B. P. Th. Veltman, Technological University of Delft, I am deeply obliged for the friendly advices he gave me.

The author wishes to express his profound gratitude to Professor B. McA. Sayers and Dr. P. Vahl, Imperial College of Technology, London, for reading the manuscript and making many helpful suggestions.

# CONTENTS

## SUMMARY

The foetal electrocardiogram (FECG) is one of the few signals that flow from the foetus to the outside world. It can be obtained with abdominal-, intra uterine- or scalp electrodes. Its detectability is hampered by the small signal-to-noise ratio (SNR).

The purpose of this study is the analytical and quantitative description of the detection and the processing of foetal electrocardiograms in order to prepare a subsequent signal transformation, the interpretation and the patient treatment.
It also is an example of the processing of a complex biological signal.

1. A general introduction into the subject is provided. Some aspects relevant to the processing of biological signals are considered: a priori information, disturbance and variability, parameter estimation and interpretation and treatment or action after the signal processing. Basic signal processing methods, that stem from statistical communication theory and time series analysis used in this study are briefly treated: convolution, smoothing, correlation, matched filtering, Fourier transformation, power spectrum estimation, detection and coherent averaging.

2. The foetal heart is considered as a signal source. A first approximation model of the foetal heart and its surrounding tissues is given and related to communication theory where a transmitter, a channel and a receiver can be identified. Lead systems for the recording of the foetal ECG are discussed.

3. The different elements are described out of which the recorded signal is composed — the maternal and the foetal ECG, the additive and the modulating noise. The signal is analysed with respect to its frequency, time and amplitude aspects and other statistical properties to gather general a priori information about the signal.

4. An on-line method is described by which the foetal heart rate can be computed instantaneously, starting from signals with visible foetal ECG complexes amidst noise and maternal ECG. The procedure uses threshold detec-

tion after band pass filtering and utilizes the statistical properties of the series of foetal RR-intervals by comparing subsequent intervals. A flow diagram of the method is discussed and the accuracy of the result is evaluated approximately by considering the properties of the stochastic processes that generate the foetal heart beats and the disturbance.

5. The shape of the foetal ECG complex can be computed from abdominal recordings with the aid of signal detection and estimation techniques. The foetal ECG complex is detected by optimal filtering and anti-coincidence circuitry. Coherent averaging is used and an artificial maternal electrocardiogram is constructed. The accuracy of the computed result is given analytically by calculation of the noise variance.

6. When foetal QRS complexes are not visible or are not detectable accurately enough to compute the instantaneous foetal heart rate, correlation techniques offer possibilities to overcome this problem. The foetal RR-interval can be detected after filtering, square law envelope detection and autocorrelation. To demonstrate the presence of a foetal signal the crosscorrelation function is computed between the preprocessed abdominal ECG and an artificially constructed maternal signal. An analytical approximation is given of the variance after processing.

7. Some clinical and physiological aspects are discussed concerning the analytic methods that have been developed. A further processing of the series of computed RR-intervals in second order distributions and histograms is discussed to acquire insight in the short term irregularity of the foetal heart. A transformation to polar coordinates of the second order interval distribution corrects for shifts in the absolute values of the RR-intervals. The order of the series of intervals is tested by comparison with distributions after shuffling.

8. Concerning the processing of the foetal ECG in practice some more detailed information is given about the preceding chapters in form of block diagrams and processing schemes. Analog, digital and hybrid methods are used for the processing. Both general purpose and special purpose computers and instruments have been used and developed. The need to preprocess the signals before entering the digital computer is stressed.

# CHAPTER I

# INTRODUCTION

## 1.1 Description of the subject

This work describes the analytical and quantitative aspects of the detection and processing of foetal electrocardiograms and their practical realization. The purpose of such studies is to make available the detailed information on which clinical interpretation may ultimately be based. Furthermore the work described here provides a typical example of the possibilities in processing a complex biological signal.

It is well known that a physiological process may have a complex structure and function so that extensive detailed information is needed for its understanding. In practice, this fact is responsible for many difficulties since it is rare that all necessary information can be acquired. This applies also to assessing the condition of the foetus since here again it is difficult to assemble all necessary information. The foetal electrocardiogram (FECG) is one of the few signals that flow from the unborn child to the outside world, and consequently the processing of FECG's is of great value in seeking insight into the condition of the foetus.

The maximal amplitude of a foetal electrocardiogram, recorded during pregnancy with abdominal electrodes, is about 10 to 50 microvolts. This magnitude is much smaller than in the typical adult ECG but in some stages of pregnancy the FECG may be much smaller still. In addition all disturbances are larger than the foetal signal. The detectability of the FECG is therefore hampered not so much by the small absolute magnitude of the signal but because of the large relative magnitude of interfering disturbances as well as by the non-stationary nature of both wanted signal and interfering noise.

Although a correct signal recording is very important in obtaining an optimal signal-to-noise ratio (SNR), technical aspects such as shielding, grounding, impedance considerations, electrical isolation of the patient and so on are not treated in this study, since much about these aspects can be found elsewhere.

A central problem in processing the FECG is the need for improvement of the existing SNR, in order to permit a subsequent signal transformation, from

which clinical interpretation and any consequent therapeutic measure can follow. In this study mainly the physical and technical aspects are treated; clinical and physiological aspects of the methods that have been developed are only briefly mentioned.

It is hoped that a quantitative basis has been presented which will facilitate further research into the correlation between foetal, perinatal or even neonatal condition of the child and the results of the information processing.

The study starts with a description of some aspects of physiological signals (chapter 1.2) and ends with basic signal processing methods used in other chapters (chapter IX). The foetal heart is considered as a signal source and the tissues as a transmission channel (chapter II); the recorded transducer signal is analysed with respect to its different components in order to gather a priori information to guide development of the necessary processing methods (chapter III).

The processing of the FECG consists in the computation of the instantaneous foetal heart rate (chapter IV), the estimation of the FECG waveshape (chapter V), the computation of the mean foetal RR-interval from disturbed FECG's (chapter VI) and the separation of short term irregularities from the basic heart rate (chapter VII). Some clinical and physiological aspects of the processing are mentioned in chapter VII; it is tempted that this chapter can be read on its own.

Technical aspects are treated in chapter VIII.

## 1.2 General considerations with respect to the processing of physiological signals

The purpose of the processing of physiological signals is generally the reduction of a redundant transducer output flow to a few parameters that have to be relevant to the problem to be solved, in order to prepare a subsequent interpretation and (human) action. It means that only those parameters need to be extracted from the transducer output signal, that give insight into the signal source or the underlying physiological process.

The processing of the information consists of three stages:

1. the measurement and signal recording.
2. the improvement of the signal-to-noise ratio (SNR), signal transformation and data reduction.
3. the recognition, interpretation and decision.

These three phases of the signal handling might be intermingled when attacking

a specific problem. Ideally, however, the information processing is carried out in a closed loop, with still a fourth stage added to it:

4. the treatment (see Figure 1).

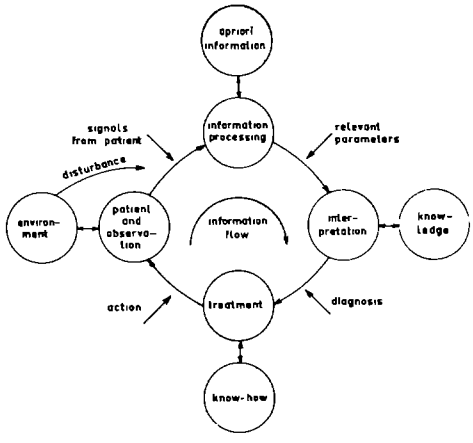


Figure 1. The closed loop, in which the information processing is carried out. Especially for the foetal electrocardiogram the disturbance from the environment plays an important role in the handling of the information flow.

## a priori knowledge

The whole processing can be done most effectively, only when as much a priori knowledge as possible has been assembled and is used concerning the signal and its source. It is thus inappropriate to try to describe generally the processing of physiological signals as if for this purpose there could exist any general scheme. Before a useful scheme can be designed, the signal must be analysed with respect to its different aspects, its source and pathways must be characterized and the physiological relevance of the resulting information taken into account.

Some examples are:

*knowledge of depolarization time*

The length of the QRS segment of most ECG's of adults is about 100 msec. It indicates the depolarization time of the ventricles; large deviations of this duration are apparently due to physiological causes. The foetal heart is quite small in relation to the adult cardiac muscle and it is therefore understandable that the foetal QRS segment lasts shorter than that of the adult. Hence a method exists to discriminate between foetal and maternal ECG's in the frequency domain (see chapters III and IV).

*properties of QRS-complexes*

The spatial velocity of an adult vectorcardiogram (VCG) has its absolute maximum value somewhere within the QRS-complex.
This phenomenon can be used to locate QRS-complexes in the automatic screening of VCG's (see Figure 2).

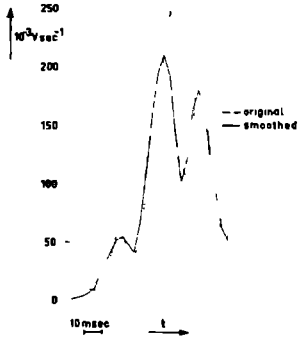


Figure 2 The modulus of the spatial velocity of a vectorcardiogram as a function of time before and after digital filtering.

*knowledge of FECG wave shape*

For the detection of the foetal electrocardiogram (FECG) it is useful to know the shape of the FECG complex beforehand, since use can be made then of optimal filtering techniques for the location of foetal peaks and a gain in signal-to-noise ratio is then obtained (see chapter VI).

## disturbance and variability

It is almost never possible to classify unambiguously a signal from a physiological process by means of its extracted parameters, because these parameters can seldom be determined with a sufficiently high accuracy. The cause of this insufficient accuracy is twofold: biological variability is an inherent property of such signals and disturbance is always superimposed on the signals. The main causes are the variability with time and the interindividual variability of the information sources. Nearly every physiological signal is generated by a process of which the properties and parameters change as a function of time. The foetus may for instance move rather freely below the electrodes during the recording of its ECG so that the FECG parameters vary continuously as a function of time (see Figure 11).

Also from a statistical point of view the signals are rarely ergodic. An

electro-encephalogram, when recorded under conditioned circumstances even contains components that consist of harmonics or repetitively occurring spikes and is influenced by unknown and unmastered factors. Further, in terms of the signal-space concept, the variability between physiological processes of different individuals (e.g. the de- and repolarization processes of heart muscles) results in the signal-space in an overlap of the regions which describe signals drawn from normal and abnormal processes, so that a certain percentage of diseases cannot be recognized intrinsically. On account of the non-stationarity of the processes the observation time of the signals has to be short even when all controllable circumstances that influence the process and thus the signal are kept constant.

The second reason for the sometimes very low accuracy of the parameters is the superimposed disturbances. Together with the physiological signals one always records small and sometimes large amounts of random noise and other disturbing signals. The latter is especially true for the foetal ECG. The noise, being the random component, is fortunately mostly uncorrelated with the signal. Other disturbing signals may however be largely correlated with the signal that we wish to process and even originate from the same or related sources. Since the observation time must be kept short on account of the non-stationarity of the process, it is difficult to eliminate the influence of the disturbance sufficiently in order to obtain a small enough noise variance.

*computation of disturbed FECG wave shape*

The shape of the foetal ECG is completely masked by the electromyogram and the maternal ECG. Accurate shapes can only be determined by a statistical method that eliminates both the noise and the maternal disturbance (see chapter V).

*SNR improvement by correlation methods*

Detection of the foetal heart rate from FECG's during pregnancy is impossible, because of the very small SNR, unless the repetitive character of the FECG complex against the random nature of the noise can be recognized by correlation methods (see chapters IV and VI).

**parameter estimation and interpretation**

Signal parameters have thus to be estimated for a time-varying or non-stationary signal in a random noise background. The signal itself often has a stochastic character too; some aspects of the signal may be stochastic or it may have a completely random character. In the latter case the processing reveals parameters that are only describable in statistical terms.

It sometimes happens that nearly nothing is known about the process except for the signals flowing to the outside world, and that these signals can only be measured by passive methods, without the possibility of influencing the process at will. Computation of significant parameters is then possible by a mutual comparison of several information streams. By comparing different signals of the same nature (transversal, from many patients for instance) or by observing one signal as a function of time (longitudinal, e.g. in follow-up studies) it is possible to extract only those parameters that change significantly.
This can often be done by classical signal analysis or -transformation methods. Of course it is then important to search for the physiological meaning of such changes since this is the ultimate aim of the analysis and the processing.

When several signals can be obtained from the same source it is always meaningful to search for interrelations even when the signals are statistically not comparable at all. It could happen that the determination of the relationship leads to insight into their common origin or even reveals the fact that one of the signals is responsible for the generation of the other. Understanding of the process is sometimes much facilitated when it is feasible to stimulate the process with an input signal. This increases the possibility that the recorded signals can be interpreted since all other (mostly unknown) inputs and disturbing factors can be eliminated by using a suitable "probe" signal which can unequivocally be identified. This of course has to do with the fact that we have then enlarged our a priori knowledge about the system by offering it controlled inputs; it permits the application of system analysis and control theory for such problems.

Physiological systems are nearly all non-linear, but even when these systems would be describable in linear terms, physiological information about the process would still be needed, in order to make possible an interpretation in physiological terms.

It can thus be stated, that the processing method for the estimation of relevant parameters must be firmly grounded in physiological and physical a priori knowledge about the process.

*relation between vagal tension and RR-intervals.*

Although the shape of a foetal ECG can be considered as more or less constant over a short period of time, its occurrences exhibit a statistical character. The intervals between foetal R-waves are related to vagal effects on the heart muscle. A lowering heart rate (bradycardia) during birth can be interpreted as resulting from a higher vagal tension which could be caused by a changing oxygen saturation of the foetal blood or a high activity from baroceptors.

*changing ST-T parameters*

During severe foetal distress it can sometimes be noted that the ventricle repolarization of the FECG changes as compared with complexes earlier computed during the birth process (see Figure 3).

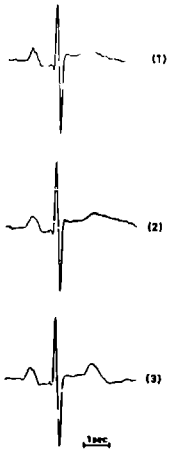


Figure 3. Change in ventricular repolarization of a foetal ECG complex during birth in severe foetal distress. The time lapse between (1) and (2) is 45 minutes and between (2) and (3) 30 minutes.

*changing systolic parameters*

It appears that the interval between the onset of the foetal QRS complex and the second foetal heart sound is much shorter for children with severe Rh-antagonism.

These differences are statistically highly significant. The phenomenon is of medical importance, while it can also be explained in physiological terms [1].

*irregular heart rate*

Sequential foetal RR-intervals are normally rather constant. Arrhytmic contractions of the heart muscle showing a large beat-to-beat variation (see chapter VII) can be an indication of foetal distress.

**treatment**

The action stage is only reached when we dispose of reliable parameters. With independent parameters it is possible to build up a parameter-space in which the devolpment of the processes can be characterized as a function of time [2]. A trend in a patient's condition can then be represented by a shifting or wandering condition vector in this space. The trajectory can be extrapolated

and predicted when the bandwidth of this vector space-walk is limited. The smaller the bandwidth, the longer the time course over which can be extrapolated. Then it is possible to extend one's attention beyond the therapeutic situation towards the prevention.

*diagnosis of foetal distress*

The condition of a foetus during birth may be represented by several parameters: basic cardiac rhythm, stability of the heart rate, intra-uterine pressure, foetal blood pH, ST-depression etc.

Changes in the condition of the child can be recognized when all these factors are properly weighted and combined; foetal distress can then sometimes be diagnosed (see chapter VII).

## statistical processing methods

Many procedures, used in communication and detection theory, are of great value for the processing of biological signals. Some of these will be used in the next chapters for the processing of the foetal electrocardiogram. The basic theory of such methods will shortly be outlined in the Appendix (chapter IX) in so far it fits in with the subject of this study (see Figure 4). Besides the well-known linear and non-linear processing techniques that can be applied in the search for significant parameters in and between biological signals, some other, heuristic, procedures have often to be developed for the effective description and understanding of physiological processes and phenomena.

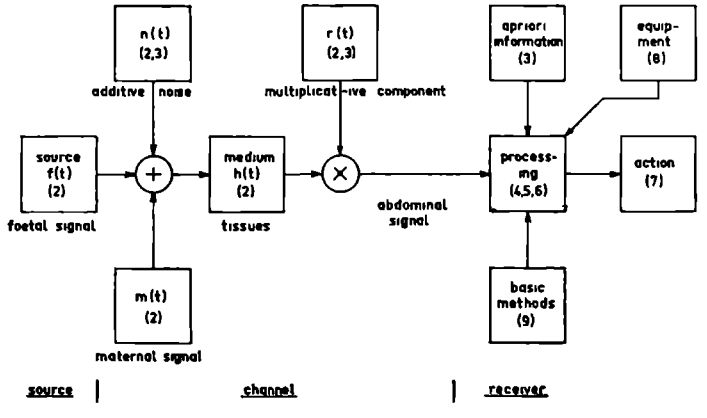


Figure 4. Processing scheme and communication model for the FECG. The figures between brackets refer to chapter numbers.

The more insight there exists into the physiological process itself, the better a processing method can be devised.

## References

1. Peeters, L. A. M., J. H. van Bemmel, "Fetal hypodynamic cardiac insufficiency in erythroblastosis fetalis", Am. J. Obstet. and Gynec., Vol. 104, 1969, p.p. 883-888.
2. Sayers, B. McA., "Prospects for biomedical applications of communication engineering", Lecture at the Int. Electr. Conf., Toronto, september 1967.

# CHAPTER II

# THE FOETAL HEART AS A SIGNAL SOURCE

## 2.1 Physiological and physical considerations

*Tissues*

The foetus lies safely stowed in the uterus, which means that it is electrically and mechanically shielded from the outside world. This is indeed the reason that only a small amount of information flows from the foetus to the outer world. Figure 5 gives a representation of the distinct tissue layers that are between the foetal heart and outside. The only detectable signal that flows actually from the foetus to the abdominal wall is the electric field potential from its heart, the foetal ECG, and later in pregnancy its heart sounds too.
This is the main reason that the processing of foetal heart signals is of potential value for the obstetrician, since these instantaneous signals may tell him about the condition of the unborn child. The difficulty in acquiring information about the child is not only restricted to signals such as these, but applies also for instance to biochemical information, when only passive data acquisition methods are used and abdominal punctures, for example, are not done.

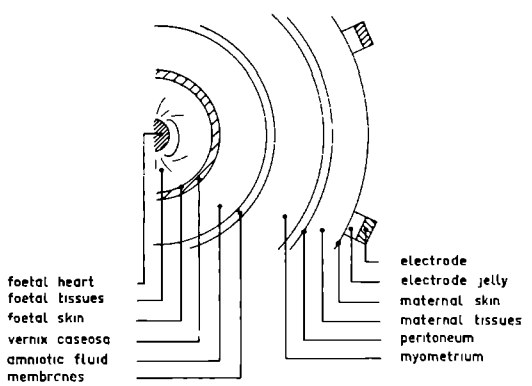


Figure 5. Schematic spherical representation of the different tissue layers around the foetal heart.

As indicated in Figure 5, the foetus lies encapsulated in the innermost of a system of shells each with a different structure. The tissue that encloses the

unborn child is accordingly very inhomogeneous: the electrical properties of the tissue layers differ considerably [1]. The foetal tissue itself can be considered as a rather good and homogeneous conductor for electric currents, comparable with that of an adult. On the foetal skin there is, however, mostly a fatty layer, the vernix caseosa, which isolates the child for the greater part from the well conducting fluid. Next come two firm membranes, the chorion and the amnion, (both bad conductors for ions) followed by the uterine muscle, the peritoneum and the maternal abdominal tissues. The conduction path ends at the maternal skin in electrode jelly and electrode.

*First approximation model*

Due to inter- and intra-individual variability it is not possible to describe as a function of the stage of pregnancy accurately enough the size and mutual position of the various conductors and isolators and the position of the foetal heart in relation to tissues and electrodes. It would be feasible to say something about quantitative aspects only in statistical terms and even then only generally. It is possible to describe in general terms the electric situation around the foetal heart. At the same time it can be indicated, why in abdominal signals the foetal ECG is so small, whereas in intra-uterine or scalp recordings the foetal ECG is mostly much larger and the maternal ECG scarcely observed at all. Further it can then be explained how it occurs that low frequency components (such as T-waves) are only occasionally observed (see chapter V).

In principle it is possible to set up a three dimensional model in a spherical or cylindrical homogeneous conductor as has been done for the adult heart [2]. Although it is quite well possible to formulate such a problem, its analytical or numerical solution is not easy to obtain. Furthermore such a model would be very little related to the real physiological situation. This is the reason for choosing a simple but enlightening one-dimensional model. Figure 6 gives, as an analogon of Figure 5 a picture of the tissues around the foetal heart in the form of an electrical network consisting of resistive and capacitive elements, with two current generators, $I_F$ and $I_M$, for the foetal and the maternal hearts. The poorly conducting vernix caseosa and the membranes are represented as RC-elements. Since the quantities $R_1$, $C_1$, $R_2$ and $C_2$ are of importance in their ratio to the other impedances, these other impedances have been called purely resistive [3] of the same value R. In the middle of the model the foetal heart functions as a current generator. The different electrode positions are indicated as $A_1$—$A_2$, $A_1$—$D_2$ and $D_1$—$D_2$ respectively for abdominal-, scalp- and intra-uterine leads (directly attached to the foetus).

The voltages between the electrode positions can be expressed in terms of the impedances present.

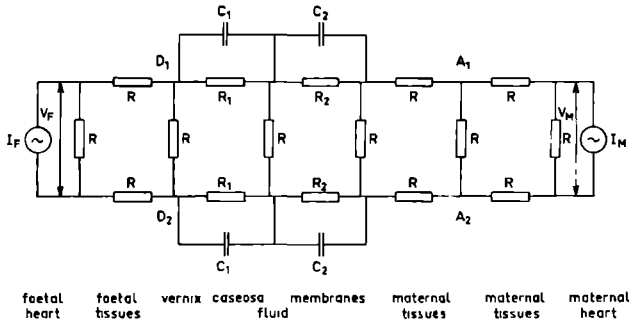


Figure 6. One-dimensional model composed of resistors and capacitors of the tissues around the foetal heart. The maternal and foetal hearts are represented as current sources. The points $A_1A_2$, $A_1D_2$ and $D_1D_2$ refer to electrode positions for abdominal, scalp and intra-uterine leads respectively.

It can be seen directly from Figure 6 that direct currents and low frequencies are attenuated by the differentiating RC-networks from the foetal signal source to the electrodes A. This is the reason why the foetal ECG shows little evidence of low frequency components, especially when $R_1$, $R_2 \gg R$. An analytical expression for $V_{AA}$ is easily obtained, although here it is of no value in giving the frequency response of the network, since the parameters are quantitatively unknown. However, in order to get an idea about the amplitudes of voltages at the electrodes we will further simplify the network, omitting the capacitors and assuming $R_1 = R_2 = 10\ R$ and $V_F = V_M$. Then it follows directly (for abdominal leads) that

$$V_{AA} \approx 25.10^{-5}\ V_F + 3.10^{-1}\ V_M$$

from which can be seen the enormous attenuation of the foetal signal. The voltage between $A_1$ and $D_2$, $V_{AD}$, becomes (scalp leads):

$$V_{AD} \approx 15.10^{-2}\ V_F + 15.10^{-2}\ V_M$$

and for the voltage between $D_1$ and $D_2$ (intra-uterine leads):

$$V_{DD} \approx 3.10^{-1}\ V_F + 25.10^{-5}\ V_M$$

From these simply obtained results we see the main reason why foetal ECG's measured at the abdomen are nearly always low level. Only when the high resistances have become low, is it possible to measure strong foetal R-waves. This is true when the vernix layer has disappeared in very late stages of pregnancy [1].

## 2.2 Communication theoretical aspects

Since hereafter techniques and methods are used, which are partly common property in the area of communication theory, we will outline the parallels existing between fundamental problems in statistical communication theory and research into the properties of the foetal heart; differences also of course exist.

In communication problems one usually identifies a signal source, a transmission channel plus a noise source and a receiver where, after decoding of the symbols, the message has to be interpreted (Figure 4). Finally also some action based on the received message will usually result. A parallel of this communication problem can be seen in many physiological problems; certainly it holds for the foetal ECG situation, comprising a transmitter or a physiological signal source (the foetal heart), a channel (the tissues) plus disturbance (among other things, the electromyogram) and a receiver (the physician). The signals involved have to be processed in order that they will render useful and interpretable information. Based on the acquired information some action could be taken.

There exist however several differences: the receiver cannot construct his own symbols, which would allow an appropriate bandwidth, orthogonal codes and suchlike to be used. The receiver can neither activate the signal source, nor stimulate or trigger the transmission, but must be satisfied with observational (passive) measurements of the underlying process.

Since initially the transmitted signal is completely unknown, it is not distinguishable from the channel disturbance. Thus a deformation of the signal by the channel will initially not be recognized. Only when the signal source can be observed over a long period, can the nature of the signal be traced with statistical methods.

### *Channel properties*

The properties of a transmission channel in a physiological system may vary as a function of time, just as in technical communication problems. These changes may be very fast, for example caused by muscle contractions or respiration, or slow, e.g. due to the growth of foetus and uterus. Also the position of the signal source in relation to the receptor may change, since during the greater part of the pregnancy the child can move freely below the electrodes.

It is therefore advisable to put the recording electrodes as near to the foetal heart as can be permitted in order to obtain a reasonable signal-to-noise ratio and minor channel influence on the signal. A further improvement of this SNR is reasonable only when at the recording side all that is possible has been done

to acquire an optimum signal. Only then does it pay to use advanced processing techniques to attempt to achieve any further improvement of the SNR or to effect a transformation of the signal prior to the phase of interpretation and consequent action.

## 2.3 Lead systems

When the electric field due to the processes of depolarization in the foetal heart is thought of as a dipole layer and if the surrounding tissues are assumed to be spherically-symmetric, then it is possible to calculate what has to be the optimum position of the electrode system for the recording of a foetal ECG with a high SNR. For simplicity it is assumed that the foetal heart lies embedded in an infinitely extended homogeneous medium.
When it is further assumed that the wavefront of electric depolarization in the foetal heart at some instant has a shape S and consists of a dipole layer with a moment $\underline{m}$ per unit area of S (see Figure 7), then the total potential at P is [4]:

$$V_P = \int_S \frac{\mathbf{m} \cdot \mathbf{r}}{r^3} ds \tag{2.1}$$

where r is the vector from P to the surface element ds.

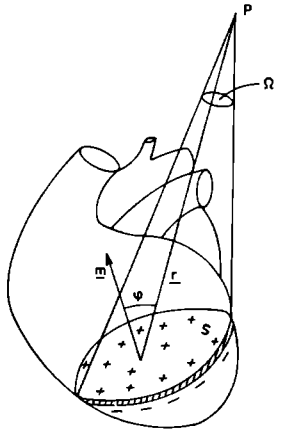


Figure 7. Simple representation of the electric field in the foetal heart by a dipole layer S of strength m per unit area, which subtends a solid angle $\Omega$.

When the vector length 'r is large in relation to the magnitude of S, then (2.1) can be written for the potential difference between two points $P_1$ and $P_2$:

$$V_{P_1P_2} = |m'| \ (\Omega_1 - \Omega_2) \tag{2.2}$$

$\Omega$ is the solid angle under which S is seen from P.
$V_{P_1P_2}$ is maximal when $\Omega_1$ is maximal positive and $\Omega_2$ is minimal.

The position of the electrodes $P_1$ and $P_2$ has thus to be such that the foetal heart is between the electrodes and the electrodes are as near to the foetal heart as possible. We have seen that the latter is favourable for the SNR as well.

It is important to ensure that the electrodes are not placed at both sides of large abdominal muscles, since on the ground of the reasoning above the noise will then become most intense. A suitable lead position locates one electrode near to the umbilicus and the other one above the symphysis [5].

It also follows from the arguments outlined above that using scalp leads, a mostly very small maternal ECG is recorded, since the two electrodes are placed symmetrically with respect to the maternal heart, so that in (2.2):

$$\Omega_1 \approx \Omega_2 \text{ and } r_1 \approx r_2,$$

although the tissue layers between both electrodes and the maternal heart are not completely identical.

Furthermore it can also be seen that the angle $\Omega$ can only be wide enough when the foetal heart is large enough, i.e. when the foetus itself is several months old. Prior to that time the cross section of the dipole layer is too small to allow detection of a foetal ECG amidst the background noise.

## References


1. Bolte, A., K. D. Bachman and G. Kühn, "Die fetalen Herzaktionspotentiale und ihre diagnostische Bedeutung", Archiv für Gynäkologie, vol. 203, 1966, p.p. 133—163.
2. Yeh, G. C. K., J. Martinek and C. V. Nelson, "The electrophysiology of the heart", Annals of the New York Academy of Sciences, vol. 65, 1957, p.p. 1003—1006 and p.p. 1014—1050.
3. Schwan, H. P., "Electrical properties of tissue and cell suspensions", Advances in Biology and Medicine, vol. 5, Academic Press, 1957, p.p. 147—209.
4. Rutherford, D. E., "Vector methods", Oliver and Boyd, Edinburgh, 9th Ed. 1959, p.p. 78—101.
5. Peeters, L. A. M., "The foetal electrocardiogram", Thesis, University of Nijmegen, 1968.

# CHAPTER III

## ANALYSIS OF THE ELECTRIC SIGNAL FROM THE FOETAL HEART

To be well informed about the foetal heart during pregnancy or birth, it is necessary to improve the existing signal-to-noise ratio (SNR), which is mostly very small.

To develop techniques for the improvement of this SNR, analysis of the kind of signals involved is a first requirement, since optimal processing is only possible when much apriori knowledge about the signals and their origin is available and used. The components present in an abdominal recording will now be analysed with respect to their information content. Based on the result, procedures can then be designed, which will separate the information about the foetus from the disturbing components in the complex signal.

The abdominally recorded electrocardiogram of a pregnant woman generally contains four components:

$$a(t) = r(t)\ \{m(t) + f(t) + n(t)\} \tag{3.1}$$

where $a(t)$ represents abdominal signal
$m(t)$ represents maternal electrocardiogram (ECG)
$f(t)$ represents foetal ECG (FECG)
$n(t)$ represents additive noise, mainly consisting of electromyogram
$r(t)$ represents multiplicative disturbance, especially due to movements, e.g. respiration.

It is assumed that the means of the signals of (3.1) between brackets equal zero:

$$\bar{m}(t) = \bar{f}(t) = \bar{n}(t) = a(t) = 0 \tag{3.2}$$

and that

$$\overline{r(t)} = 1. \tag{3.3}$$

For abdominal signals it is mostly true that

$$\overline{m^2(t)} \gg \bar{f}^2(t) \geqq \bar{n}^2(t) \tag{3.4}$$

The bar stands for averaging in the time domain.

Figure 8a gives an example of an abdominal recording of an ECG in which the four components are clearly visible. In case of a scalp lead recording,

Figure 9a, the maternal ECG will hardly be seen (see chapter II). Formula (3.1) is a simplified version of a more complex one, in which the foetal signal f(t) is also modulated by some multiplicative component. The different terms will be examined below as to relevant apriori information.


Figure 8. Abdominal recording of the foetal electrocardiogram. (a) The original signal a(t). (b) The filtered signal a(t) (15—60 Hz).

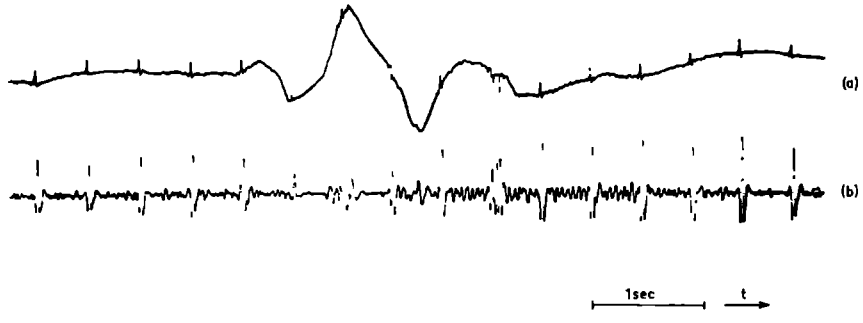


Figure 9. Recording of the foetal electrocardiogram during birth with scalp electrode. (a) The original signal. (b) The filtered signal (15—60 Hz).

## 3.1 The frequency domain

The recorded spectral bandwidth of the adult electrocardiogram is standardized from about 0.15—100 Hz [1].

In Figure 10 examples are given of the power spectra of a randomly chosen adult and foetal QRS-complex, derived by computation using formula (9.22). If one were interested only in the presence or absence of the FECG, the bandwidth above could be reduced drastically. In that case, any interference signal

outside this narrowed bandwidth would also be filtered out. The peak with the largest power content in the ECG, the R-wave or the whole QRS-complex, functions as a measure to define such a filter that enhances the foetal SNR. It appears that generally the highest power density in the frequency spectrum of a QRS-complex of an adult lies between about 10 and 30 Hz; that of a foetal QRS-complex lies mostly somewhat higher: between about 15 and 40 Hz. This can be understood from the different durations of the adult and foetal QRS-segments: resp. about 100 and 60 milliseconds.

Then, after passing the abdominal signal through a linear filter with a bandwidth from about 15 to 40 Hz, the maternal R-wave amplitude will have become smaller in relation to the foetal R-wave amplitude and the noise outside this frequency band will have been filtered out. As the QRS-complex in the ECG is the part with the highest frequency content, significant responses in the filtered signal to P- and T-waves are not seen Fig. 8b and 9b show a filtered version respectively of an abdominal and an intra-uterine FECG. The noise is present over the whole frequency range of the ECG. The verly low frequency noise arises from movements of electrodes and has usually a rather high power density during birth, even when using a scalp electrode. Disturbance in the higher frequency range is normally caused by muscle activity, the electromyogram (see Figure 10).

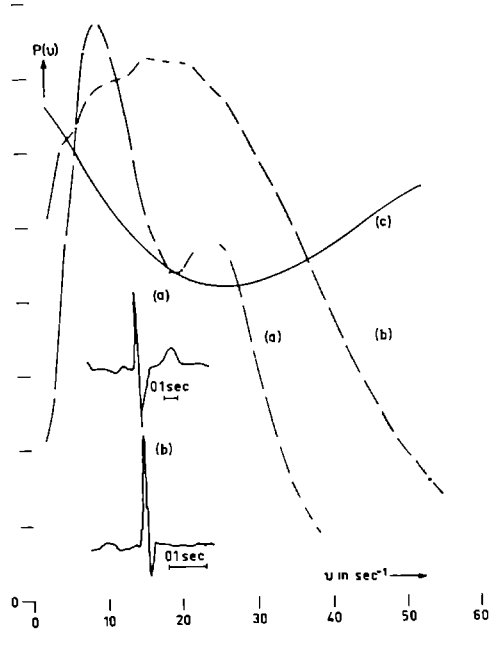


Figure 10 Power spectra of the QRS-parts of an adult ECG (a), a computed foetal ECG (b) and of a commonly occurring noise component (c) The original ECG complexes are also shown

## 3.2 Amplitude Properties

The peak of the maternal R-wave in an abdominal recording nearly always exceeds that of the foetus. After filtering, the foetal R-wave is in favorable cases larger than the interference which is always present (see Figure 8). Starting from the filtered signal the foetal R-waves can then be separated from the noise and the maternal ECG in the amplitude domain. Of course it is only sensible to use methods which improve the existing SNR, when the interference has been diminished as much as possible during recording (see chapter II).

Foetal signal power and thus the foetal SNR are statistically strongly related to the stage of pregnancy, as has been shown by Bolte et al. [2].

Even during a short interval the amplitude of the foetal QRS-complex may vary strongly, because of changing position of the foetus. Figure 11 shows an example of an abdominal FECG, where the foetus apparently changes its position below the electrodes.

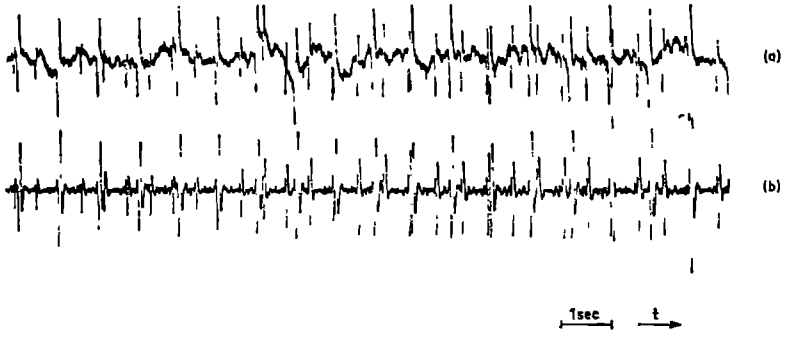


Figure 11. Recording of an abdominal FECG. The foetus suddenly changed its position below the electrodes, so that the R-wave amplitude increased in a few seconds. (a) is the unfiltered and (b) the filtered signal a(t).

The noise originates mostly from muscle activity. The amplitude density distribution of the noise is assumed to have a Gaussian character, which will be true to a good approximation. Especially during labour the additive disturbance is very non-stationary because of the noisy electromyogram during contractions.

The modulating factor r(t) from Formula (3.1) is not very important for the processing. Only sometimes do the abdominal respiration or other movements influence the envelope of the abdominal signal. The factor r(t), as can be seen from Figures 8 and 22, is an example of an exceptionally strong influence of respiration on the maternal ECG.

## 3.3 Statistical Properties

*Repetition rate*

The maternal ECG occurs with a mean interval $T_M$, anywhere between about 0.5 to 1.0 seconds. As is well known there is an effect due to respiration on the maternal heart rate, so that fluctuations around the mean heart rate are partly due to the signal r(t).

The foetal heart rate fluctuates during pregnancy usually between 130 and 150 beats per minute. During birth however, large deviations from this basic rhythm may occur. Figure 12 shows an interval distribution of foetal R-waves during pregnancy, whereas Figure 13 represents a very broad one, computed from a foetal ECG recorded during birth.

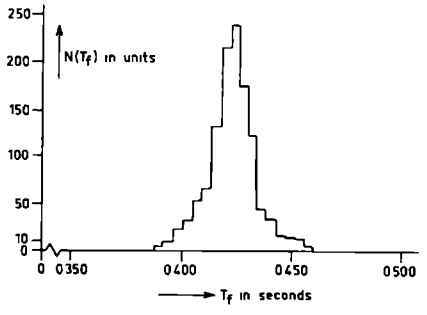


Figure 12. RR-interval histogram for an abdominal foetal electrocardiogram, with a small variations in RR-interval duration.

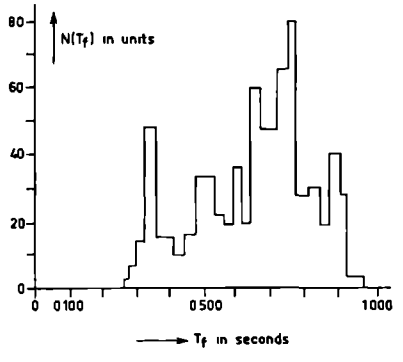


Figure 13. RR-interval histogram for a FECG recorded during delivery with a scalp electrode. Note the enormous variations in RR-interval duration.

The upper limit for the human foetal heart rate can safely be taken as 300 beats per minute, whereas in normal cases a lower limit of 40 beats per minute is amply sufficient.

*PQRST-complex*

It may be assumed that the PQRST-complex of a normal adult does not change appreciably in shape during an observation time of minutes or even hours, when the subject stays in the same position and condition. On the other hand, the shape of the foetal ECG may vary considerably with time when the foetus can move freely below the recording electrodes and the foetal heart axis changes its direction. The latter has consequences for the processing of the foetal ECG (see chapter V).

## References

1. Kossmann, C. E. et al., "Recommendations for standardization of leads and of specifications for instruments in electrocardiography and vectorcardiography", Report of committee on electrocardiography, American Heart Association, Circulation, vol. 35, 1967, p.p. 583—602.
2. Bolte, A., K. D. Bachman and G. Kühn, "Die fetalen Herzaktionspotentiale und ihre diagnostische Bedeutung", Archiv für Gynäkologie, vol. 203, 1966, p.p. 133—163.

# CHAPTER IV

# DETECTION OF THE INSTANTANEOUS HEART RATE

In this chapter an on-line method is described, which computes from abdominal-, intra-uterine- or scalp leads (or phonocardiograms) the instantaneous foetal hart rate after improvement of the foetal SNR [1]. The output of the instrument developed to this end, is the RR-time interval or the heart rate in beats per minute, represented as a voltage, and a numerical display with a possibility of punching or printing the computed results.

## 4.1 Statement of the problem

The foetal ECG is, for a short time, almost periodic, so the two intervals lying between three consecutive R-waves, will not differ very much from each other. In the case of an ideal abdominal lead, the maternal R-waves of the filtered signal are often larger than the foetal peaks, while the noise has an envelope amplitude, small in relation to that of the peaks of the foetal ECG (see Figure 8). Separation of the foetal ECG complexes from the rest of the signal components can to a large extent be done in the amplitude domain, by seeking only those foetal R-wave peaks, which are in between two amplitude levels. Two amplitude comparators $C_M$ and $C_F$, which compare the maternal and foetal R-wave amplitudes with reference levels $V_M$ and $V_F$ (with $|V_M| > |V_F|$), can now give the indication whether a maternal, or a maternal plus a foetal R-wave is present (see Figure 14). Sometimes, however, the disturbance will be so considerable, that it will surpass the foetal or even the maternal R-wave peaks.

If the peak amplitude of the disturbance lies between the two reference levels, such a peak can be mistaken for a foetal R-wave. Responses to interference peaks, statistically speaking and assuming a stationary noise process, occur randomly. Thus it is possible to distinguish between noise peaks and foetal R-waves by means of time domain information. The SNR, here defined as the ratio of the number of foetal peaks to the number of noise peaks per unit time must not be too small, since only a small part of the time-domain information is utilized to compute the correct foetal RR-interval. At the same time it may happen that foetal R-waves are missed, since a foetal R-peak might have been cancelled

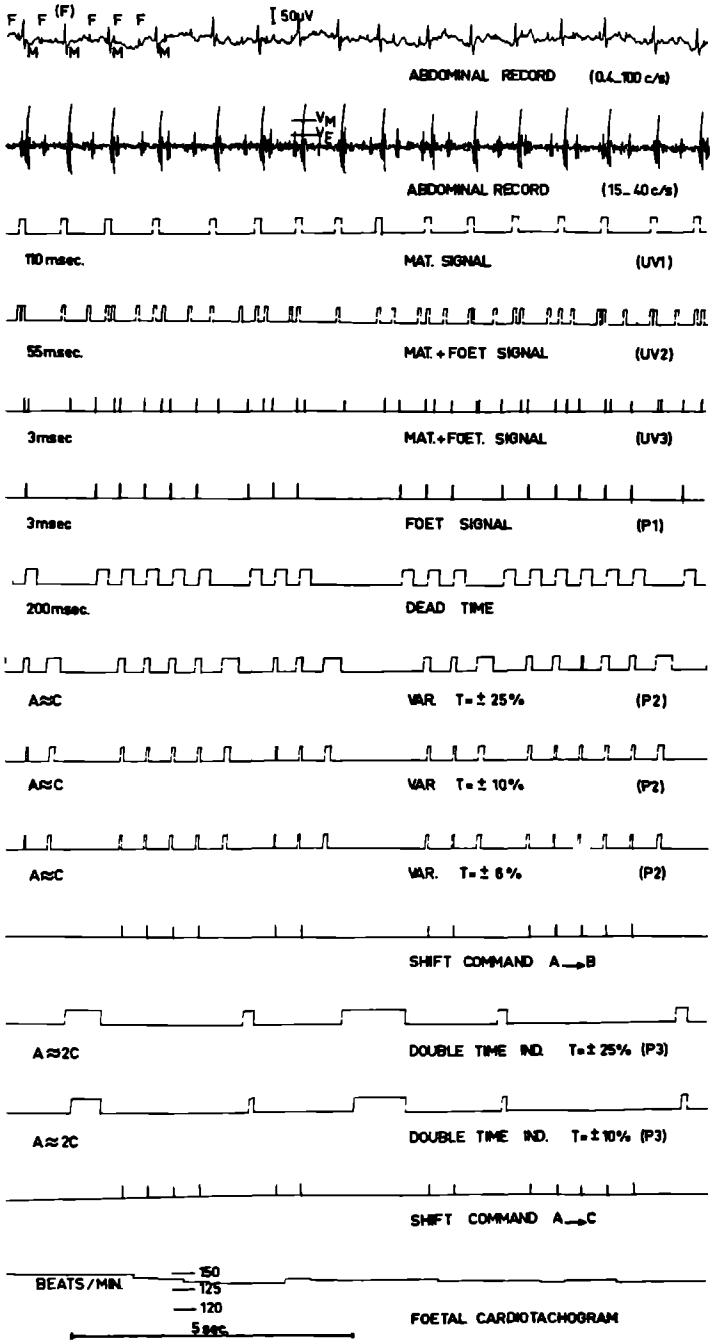
F F (F) F F F
M M M M
50 µV
ABDOMINAL RECORD (0.4–100 c/s)
VM
VF
ABDOMINAL RECORD (15–40 c/s)
110 msec.
MAT. SIGNAL (UV1)
55 msec.
MAT. + FOET SIGNAL (UV2)
3 msec
MAT. + FOET. SIGNAL (UV3)
3 msec
FOET SIGNAL (P1)
200 msec.
DEAD TIME
A≈C
VAR. T = ± 25% (P2)
A≈C
VAR T = ± 10% (P2)
A≈C
VAR. T = ± 6% (P2)
SHIFT COMMAND A→B
A≈2C
DOUBLE TIME IND. T = ± 25% (P3)
A≈2C
DOUBLE TIME IND. T = ± 10% (P3)
SHIFT COMMAND A→C
BEATS/MIN.
150
125
120
5 sec.
FOETAL CARDIOTACHOGRAM

by a noise peak of opposite phase, occurring at the same instant that a foetal QRS-maximum appears (see section 4.5).

It is necessary to have an on-line processing method because it is important in some cases that a decision can be taken immediately on the basis of information acquired in the very recent past of the signal. The decision, whether or not a certain response to the comparator $C_F$ is due to a foetal R-wave, can be taken by comparing a measured foetal RR-interval with the supposed known past of the signal.

It is known that the foetal heart rate lies between 40 and 300 beats per minute, so that after recording a presumed R-wave a pause ("dead time") of at least 0.200 second can be taken, while the next FECG complex can be expected within 1.500 seconds.

After the signal has been filtered and passed through the amplitude comparators, a pulse can be obtained which indicates a foetal ECG or a noise peak of the same order of magnitude as the foetal R-wave peak. Now and then foetal R-waves have disappeared due to coincidence with maternal R-waves or large interference peaks. Furthermore foetal information may have become lost because a foetal R-wave appeared within 0.200 second after a noise peak that gave rise to a response of the foetal comparator.

## 4.2 Threshold detection

After amplification the abdominal signal is led to the filter (Figures 14 and 15).

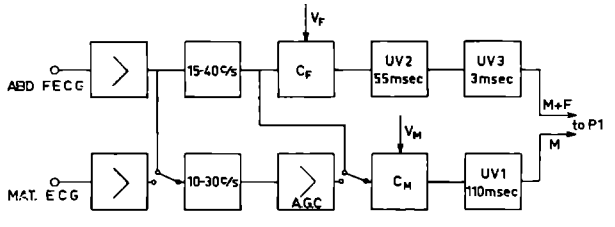


Figure 15. Block diagram for the extraction of foetal signals from an abdominal lead. The inputs and outputs of the different blocks can be seen in the upper six traces of Figure 14 (UV stands for monostable multivibrator. The amplifier A.G.C. contains automatic gain control circuitry). The switches allow use of a separate maternal ECG and a filter for the maternal R-wave detection.

Figure 14. Time sequence for Figures 15, 16 and 52. The sequence starts with the upper trace showing an abdominal FECG a(t), and ends with the bottom trace showing the resulting foetal cardiotachogram.

If desired a separate recording is made of the maternal ECG, when, for example, the maternal R-wave is not large enough to be distinguished from the foetal R-peak. Both before and after response of comparator $C_M$ the foetal information is blocked for +55 msec and —55 msec, to ensure that comparator $C_F$ will not pass any incorrect information arising from responses to maternal QRS-complexes. Three monostable multivibrators ($UV_1$, $UV_2$ and $UV_3$) take care of this. The outputs of $UV_1$ and $UV_3$ are fed to an anti-coincidence gate $P_1$. The pulse series resulting from $P_1$ contains only foetal information and incorrect responses to large noise spikes

## 4.3 Statistical processing of the pulse series

The information sought about the foetal heart must be acquired by further processing of the pulse series from $P_1$, from which the sequence of foetal R-waves and the intervals between successive beats must be determined in order to compute the instantaneous foetal heart rate. The almost periodic character of the foetal heart beat, against the random properties of the interference pulses, now makes it possible to extract the foetal information from the pulse series $P_1$ (Figure 14).

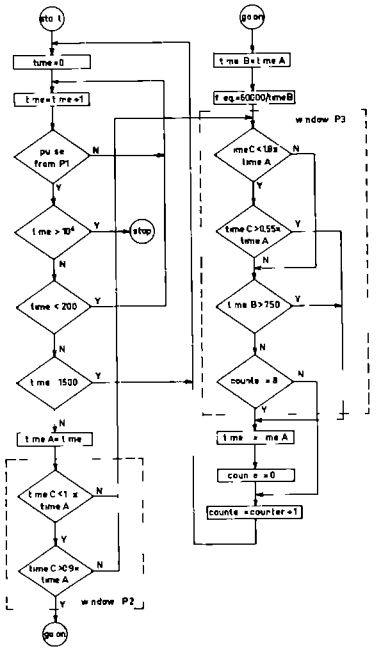


Figure 16 Flow diagram for the processing of foetal RR intervals after R-wave exactraction The integer variable "time" is assumed to be incremented every millisecond The characters Y and N stand for "Yes" and "No" after the decision in the diamond shaped blocks

The procedure developed to this end, indeed, shows the qualities of time locked systems. The nature of the pulse series lends itself particularly well to digital computer processing, resulting in a histogram, an expectation density function or suchlike (see chapter VII).

Since for clinical purposes it is desirable to have available an indication of instantaneous heart rate, an on-line method has been designed that makes use of the similarity of two sequential foetal RR-intervals. The advantage of such a method lies in its rapid presentation of results to the physician and the fact that the method can be practically realized with a small size instrument. A flow diagram of the method is given in Figure 16. With the latter Figure it is possible to follow exactly the statistical processing of the pulse series and the decisions to be taken. A more detailed block diagram is provided in chapter VIII (Figure 52), where the instrument will be discussed.

## 4.4 The flow diagram

The flow diagram of Figure 16 will briefly be explained in this section. The indicated times are measured in milliseconds. The first loop is traversed after "time" = 0. The integer variable "time" is incremented by one unit during each loop until a foetal "pulse" arrives. When the measured time has been large ($>$ 10 sec.), then it is assumed that no pulses are produced by $P_1$ of Figure 15 and the computation can be stopped. When the measured time has been less than 200 msec (the upper limit of a heart rate of 300 beats per minute) we continue the time measurement as if no foetal pulse had occurred. When the latter decision has also been passed by "NO", an abnormal low foetal heart rate ($<$ 40 beats per minute i.e. time $>$ 1500) is checked. When all the conditions have been satisfactorily fulfilled, "time A" is given the value of the measured time, which is then further processed. The time is then compared with "time C", which during processing is normally equal to the preceding time interval, and has to be within $\pm$ 10 % of it (window $P_2$). The variable "time B" is thereupon made equal to "time A" and the reciprocal of "time B" is put into "freq.", the foetal heart rate in beats per minute. A second window ($P_3$) checkes if "time C" lies between 0.55 and 1.8 times "time A", or if "time B" is more than 750 msec., or if the "counter" is equal to 8.

In fact the window $P_3$ follows very large deviations from a basic instantaneous foetal heart rate. However, intervals that are nearly double or half those of the preceding interval are not accepted as true foetal RR-intervals, since a coincidence may have occurred with a maternal QRS-complex. During the start-up period "time C" has a value, which has not been determined by some preceding interval.

For that reason a counter has been included in the scheme: only when eight sequential times a pulse has arisen from $P_1$ and when during that time the variable "time A" has not once been made equal to a measured time, "time C" is given the value of the ninth interval, however short or long it may be.

During foetal bradycardia it may happen that between the maternal pulse series and interference, only an occasional foetal interval can be measured. This is the reason that for foetal intervals longer than 750 msec (or heart rates lower than 80 beats per minute) "time C" is continuously given the value of the preceding measured time.

When one of the latter requirements has been met, the "time A" is taken over by "time C", the "counter" is made zero and again incremented. The measured intervals $T_{F_i}$ have then to satisfy the equations:

$$0.9\, T_{F_i} \leqq T_{F_{i+1}} < 1.1\, T_{F_i} \tag{4.1}$$

and

$$0.55\, T_{F_i} \leqq T_{F_{i+1}} < 1.8\, T_{F_i} \tag{4.2}$$

It is thus possible to filter out most of the erroneous pulses that have crept into the pulse series from $P_1$. The pulse series results finally in an improved one, from which the foetal RR-interval can be measured more accurately than without the comparisons shown in the flow diagram.

## 4.5 Number of correct measurements

The presentation of the heart rate in numbers and the decision to store "time A" in "time B", can be the result of a successful comparison between two foetal intervals or between two interference pulse intervals which by chance were equal. In the case of non equal intervals no measurement is carried out. Starting from the method described above, the chance of a correct, a wrong or no measurement can be calculated. When the foetal peaks occur at fixed time intervals $t_k$ it would be unnecessary to introduce in the windows $P_2$ and $P_3$ a variation of 10 percent. The detection method could thus gain in accuracy, because one would only have to look for a single interval $t_k$. Such an interval being found, the time measurement would then have been finished immediately.

The foetal heart rate, however, is only approximately periodic. Consequently, variations in $P_2$ and $P_3$ need to be introduced. For a calculation of the reliability of detection it does not matter if $t_k$ is taken as constant, because a foetal peak is certain to fall within the time window around $t_k$. To obtain a numerical result from the calculation, the ratio $\Delta A/A$ is assumed to be 0.1, $\Delta A$ being the variation in A ("time A"). So the window $P_2$ is open when $C = A \pm 10$ percent.

Furthermore, it is assumed that no foetal R-waves are cancelled out as a result of coincidence with maternal QRS-complexes. Thus in the following calculations the window $P_3$ plays no important role. The occurrence of the interference pulses is further thought to be random, and it is assumed that the interference pulse series intervals are distributed according to an exponential distribution.

This is a reasonable assumption, since the time that the random waveform n(t) of equation (3.1) remains above the level $V_F$ is relatively short compared with the time interval between two different excursions above $V_F$, when $V_F^2/n^2(t)$ is large. In such cases one may view the excursions above $V_F$ as a random process of independent point events in time, at a mean rate $t_n$. It is well-known that such a process has an exponential distribution function [2]. Even for stationary Gaussian processes with narrow-band spectra, it can be shown that the intervals between high-level crossings are distributed to an exponential distribution [3].

The expected number of crossings per unit time $t_n^{-1}$ through the level $V_F$ with positive slopes can be expressed in terms of the correlation function of n(t) [4]:

$$t_n^{-1} = \frac{1}{2\pi}\left[-\frac{C_{nn}''(0)}{C_{nn}(0)}\right]^{\frac{1}{2}} \cdot \exp\left[-\frac{V_F^2}{2\,C_{nn}(0)}\right] \tag{4.3}$$

where $C_{nn}(\tau) = n(t) \cdot n(t-\tau)$, the autocorrelation function of n(t), and $C_{nn}''(\tau)$ is the second derivative of $C_{nn}(\tau)$. For a spectrum $G(\nu)$ of n(t) between 15 and 40 Hz it follows that

$$C_{nn}(0) = \int_{15}^{40} G(\nu)\, d\nu = \sigma_n^2$$

$$C_{nn}''(0) = -4\pi^2 \int_{15}^{40} \nu^2 G(\nu) d\nu$$

Thus equation (4.3) becomes for a rectangular spectrum between 15 and 40 Hz:

$$t_n^{-1} = 1/3\ \sqrt{825}\ \exp\left[-V_F^2/2\,\sigma_n^2\right] \tag{4.4}$$

This means that for respectively

$$V_F = 1, 2, 3 \text{ and } 4 \text{ times } \sigma_n$$

a mean interference pulse rate can be expected of 17, 4, 0.3 and 0.08 pulses per second.

The optimal SNR is determined by this consideration: the number of false alarms decreases when a high level $V_F$ is chosen. It is clear, however, that foetal pulses are misdetected when $V_F$ is too high.

The mean number of detected foetal pulses per unit time can be approximated by

$$t_f^{-1} = t_k^{-1} \int_{V_F}^{\infty} \frac{1}{\sqrt{2\pi}\,\sigma_n} \exp\left[-\frac{(x-A)^2}{2\sigma_n^2}\right] dx \qquad (4.5)$$

where $t_k$ is the foetal RR-interval and A the peak of the foetal R-wave, which is thought to have a rectangular shape. The integral (4.5) represents the probability that the amplitude x is larger than the threshold $V_F$. With a reasoning, usual in detection theory [5], the optimum level $V_F$ for given signal characteristics will be calculated.

The number of false alarms during one second is apparently $t_n^{-1}$, whereas the number of misdetections equals

$$t_m^{-1} = t_k^{-1} \int_{-\infty}^{V_F} \frac{1}{\sqrt{2\pi}\,\sigma_n} \exp\left[-\frac{(x-A)^2}{2\sigma_n^2}\right] dx = \tfrac{1}{2}\, t_k^{-1} \left[\operatorname{erf}\left(\frac{V_F - A}{\sigma_n \sqrt{2}}\right) + 1\right] \qquad (4.6)$$

with $\frac{2}{\sqrt{\pi}} \int_0^{\alpha} e^{-x^2}\, dx = \operatorname{erf}(\alpha)$

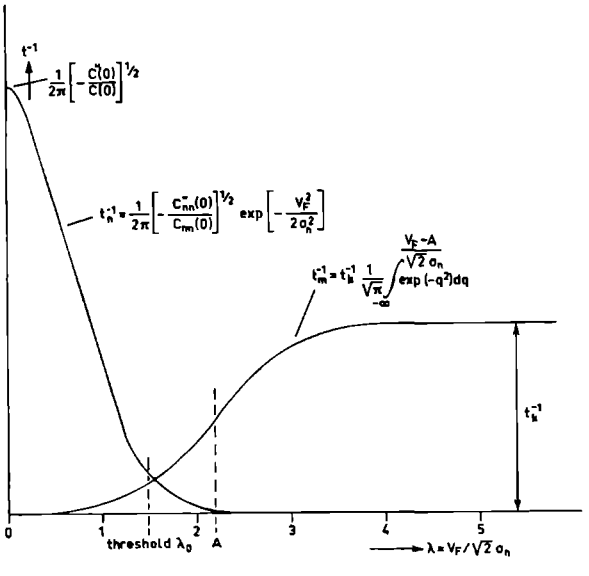


Figure 17. Number of wrong interpretations $t_n^{-1}$ (false alarms) and $t_m^{-1}$ (misdetections) as a function of the detection level $\lambda$.

The total number of wrong interpretations during one second is then

$$W = t_n^{-1} + t_m^{-1} \tag{4.7}$$

which is a function of $V_F$ (see Figure 17).

Differentiation of (4.7) with respect to $V_F$ and setting equal to zero to obtain the condition for the extremum of W gives with the normalized values:

$$\frac{V_F}{\sigma_n \sqrt{2}} = \lambda \text{ and } \frac{A}{\sigma_n \sqrt{2}} = a: \quad \exp[2a\lambda - a^2] - 40\, t_k \lambda \sqrt{2\pi} = 0 \tag{4.8}$$

For the limits of the function (for $a \downarrow 0$ and $a \to \infty$) it can be calculated that a minimum number of wrong interpretations W is reached for respectively $\lambda = \infty$ and $\lambda \approx a/2$). It means that for large SNR's (e.g. $a > 3$) the best level $\lambda$ that can be chosen is at half the foetal pulse height, $V_F = A/2$.

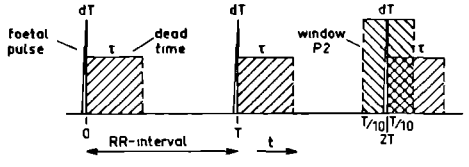


Figure 18. Foetal pulse sequence with dead times $\tau$ and window $P_2$.

An estimation can now be made of the results from the processing method, after the detection stage, with the following assumptions (see Figure 18):

1. If a pulse originates from $P_1$, a second one cannot occur for $\tau$ (0.200) seconds.
2. The pulse series from $P_1$ is supposed to be the sum of a truly periodic foetal pulse series (f) at distances $t_k$ and a Poisson distributed series of interference pulses (n).
3. If in "time C" an interval of duration T is stored, and in "time A" an interval T ± 10 percent, then the decision to store "time A" into "time B" can be taken; in other words a measurement can be carried out.
4. The contents of "time A" are always stored into "time C" on command of every pulse from $P_1$, so that equation (4.2) is omitted and gate $P_3$ is not thought to be present.
5. The limits of $t_k$ are

$$0.200 < t_k < 1.500 \text{ (seconds)} \tag{4.9}$$

6. Poisson's distribution for the interference pulses n is [2]:

$$\Pr\{p=m\} = \left[\frac{T}{t_n}\right]^m \frac{\exp(-T/t_n)}{m!} \tag{4.10}$$

The left hand side of the equation specifies the probability that the number of interference pulses, p, measured during an observation time T, equals m. $t_n$ is the mean interval of the interference pulse series.

There are 8 possible combinations for a sequence of three pulses drawn from the foetal (f) and interference (n) sequences:

TABLE 1

| combinations | 1st | 2nd | 3rd | pulse result | |
|---|---|---|---|---|---|
| (1) | f | f | f | correct | |
| (2) | f | f | n | ~ correct | $2T = 2t_k$ |
| (3) | f | n | f | | |
| (4) | n | f | f | correct | |
| (5) | n | n | n | incorrect | $2T \neq 2t_k$ |
| (6) | n | n | f | | |
| (7) | n | f | n | | |
| (8) | f | n | n | | |
| time | 0 | T | 2T | | |

A measurement is performed when a transfer from "time A" into "time B" takes place. From Table 1 it may be seen that both correct and wrong combinations can be found from the sequences indicated. No measurement at all is performed when $\Delta T > T/10$.

The probability of a good measurement or that of a wrong one can now be calculated using Table 1.

*Probability of a correct interpretation, (1)*

The total observation time is $2(t_k - \tau)$

During the dead time $\tau$ all pulses are suppressed. The probability that during the observation time no interference pulse n occurs at all is, with (4.10):

$$\Pr\{p=0\} = \left[\frac{2(t_k-\tau)}{t_n}\right]^0 \exp\{-2(t_k-\tau)/t_n\} = \exp\{-2(t_k-\tau)/t_n\} \quad (4.11)$$

The probability that the first pulse of the series of three consecutive pulses is indeed a foetal pulse is:

$$\Pr\{\text{foetal pulse f}\} = \frac{t_k^{-1}}{t_k^{-1} + t_n^{-1}} = \frac{t_n}{t_k + t_n} \tag{4.12}$$

$t_k^{-1}$ and $t_n^{-1}$ are respectively the foetal and the mean interference pulse rate. Combination of the two probabilities (4.11) and (4.12) in a product yields the combination (1) of Table 1.

$$\Pr\{\text{combination (1)}\} = \frac{t_n}{t_k + t_n} \exp\left\{-2\frac{t_k - \tau}{t_n}\right\} \tag{4.13}$$

The probabilities of the combinations (2), (3) and (4) are negligibly small as compared with that of (1), because the appearance of a pulse n now enters nearly at the same time as a foetal pulse f.

*Probability of a wrong interpretation, (5)—(8)*

The four probabilities which contribute will be calculated separately. The probability of finding an interference pulse n is:

$$\Pr\{\text{interference pulse n}\} = \frac{t_k}{t_k + t_n} \tag{4.14}$$

The probability of finding on two occasions no pulse n during the observation interval can be determined from (4.10):

$$\Pr\{p = 0\} = \exp\{-2(T - \tau)/t_n\} \tag{4.15}$$

The probability of finding a pulse n during dT is:

$$\Pr\{\text{interference pulse at dT}\} = t_n^{-1} \cdot dT \tag{4.16}$$

Finally, the probability that an interference pulse occurs between 2T—T/10 and 2T+T/10 is:

$$1 - \Pr\{p = 0\} = 1 - \exp\{-0.2\ T/t_n\} \tag{4.17}$$

The probalibility of finding no foetal pulse f during the observation time is:

$$\Pr\{\text{no foetal pulse f during } 2T - \tau\} = \frac{t_k - (2T - \tau)}{t_k} \tag{4.18}$$

This is only valid when

$$t_k > 2T \tag{4.19}$$

The probability for combination (5) can then be written as the product of all results (4.14) to (4.18):

$$\Pr\{\text{combination (5)}\} = \frac{t_k}{t_k + t_n} \exp\left\{-2\,\frac{T-\tau}{t_n}\right\}\left\{1 - \exp\left(\frac{-0.2\,T}{t_n}\right)\right\}^{\frac{t_k - (2\,T-\tau)}{t_k}} \frac{dT}{t_n} \tag{4.20}$$

Because the time T may vary from 0.200 to $t_k/2$ seconds the equation (4.20) has to be integrated.
For simplification the subterms are written as:

$$\alpha = \frac{T}{t_n},\ \beta = \frac{t_k}{t_n},\ \tau = 0.200 \text{ and } \lambda = \frac{1}{1+\beta} \exp\left\{2\,\frac{\tau}{t_n}\right\} \tag{4.21}$$

The complete probability of a wrong interpretation of a pulse sequence (5) is then:

$$\lambda \int_{\tau/t_n}^{\beta/2} \exp\{-2\,\alpha\}\ [1 - \exp(-0.2\,\alpha)]\left(\beta + \frac{\tau}{t_n} - 2\alpha\right) d\alpha \tag{4.22}$$

The same reasoning can be held for the combination (6)—(8), so that only the final answers will be given.

For combination (6):

$$\lambda \int_{\tau/t_n}^{\beta/2} \exp\{-2\,\alpha\}\ 0.2\,\alpha\, d\alpha \tag{4.23}$$

For combination (7):

$$\lambda \int_{\tau/t_n}^{\beta} \exp\{-2\,\alpha\}\ \{1 - \exp(-0.2\,\alpha)\}\, d\alpha \tag{4.24}$$

For combination (8):

$$\lambda \int_{\tau/t_n}^{\beta/2} \exp\{-2\,\alpha\}\ \{1 - \exp(-0.2\,\alpha)\}\, d\alpha \tag{4.25}$$

On the basis of the equations (4.22)—(4.25) the following answer is obtained:

$$\Pr\{\text{combinations (5)} - \text{(8)}\} = \frac{1}{1+\beta}\left[\exp\left[0.4\,\frac{\beta}{t_k}\right]\exp\left[-\beta\right]\right.$$
$$\left\{-0.05\left(1+\beta+2\,\frac{\beta}{t_k}\right)+\frac{1}{121}\left(5+11\,\frac{\beta}{t_k}\right)\exp\left[-0.1\,\beta\right]+\right.$$
$$+\left.\frac{5}{11}\exp\left[-1.2\,\beta\right]-0.5\,\exp\left[-\beta\right]\right\}+\left\{0.05\left(11+10\beta-1.6\,\frac{\beta}{t_k}\right)-\right.$$
$$\left.\left.-\frac{5}{121}\left(12+11\beta-2.2\,\frac{\beta}{t_k}\right)\exp\left[-0.04\right]\frac{\beta}{t_k}\right\}\right]. \qquad (4.26)$$

*Probability of no interpretation*

No measurement takes place if the two measured time intervals differ more than 10 percent from each other. This probability is known to be: 1 minus the probabilities as calculated in equations (4.13) and (4.26).

Figure 19 represents the probabilities of correct, wrong and not-performed measurements of foetal pulse series. The ratio of noise pulse density to foetal pulse density is plotted on the abscissa, the probability itself on the vertical, logarithmic scale.

The same computations can be carried out for the case where the foetal interval was measured by one pulse interval only, without comparison with the preceding one (see also Figure 19).

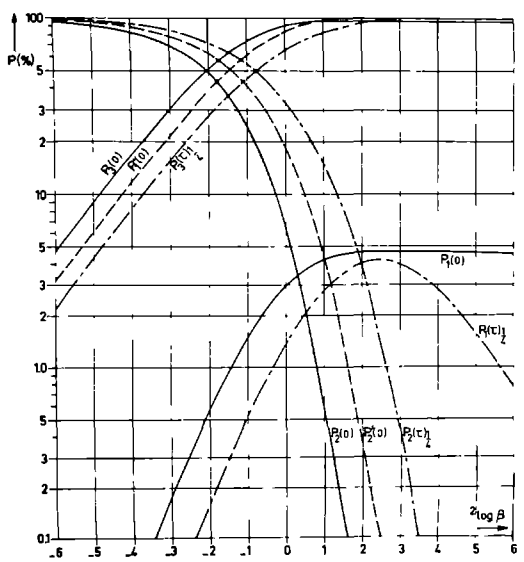


Figure 19. Probability of wrong ($P_1$), correct ($P_2$) and no measurements ($P_3$) as a function of $\beta$ (interference pulse density/foetal pulse density).
P(0) is the probability in percent for a comparative time measurement and no dead time. $P(\tau)\frac{1}{4}$ is the same for a dead time of 0.200 second and a pulse density of 4 per second, P'(0) is the probability in percent for a direct time measurement without comparison. Note then the absence of $P_3'(0)$.

For $\tau = 0$ and $\tau = 0.200$ the probabilities are calculated for a pulse density ratio $\beta = 2^r = \pm 5, \pm 4, \ldots, 0$.

For illustration $t_k$ has been taken as 0.250 sec with $\tau = 0.200$. It can be seen that the number of wrong interpretations has apparently decreased when the comparative method is used in place of a direct interval measurement.

The method described offers an improved reliability in measuring foetal RR-intervals. This greater reliability does of course not lie in a higher number of good results, but in the decreased percentage of wrong measurements.

When the window $P_3$ is allowed to operate the calculated probability (4.26) would decrease further. Although the Poisson distribution is an approximation of the real stochastic process, its assumption remains valid for the time considered, between three sequential foetal pulses. In reality the mean $t_n$ varies rather strongly, especially during labour and over a long time of observation the noise must be viewed as a non-stationary process. This non-stationarity makes no difference to the results of the processing method followed, since the advantage of comparative calculations is obvious and independent of the kind of distribution function; the probability of incorrect measurements still decreases when comparative calculations are used.

In an experimental arrangement it is possible to use more "times C" in order to compare more than two sequential intervals $t_k$. Further advantage will result from such a procedure, but less than proportionally with the number of comparisons.

In practice, however, it is very obvious, when a wrong measurement has been performed, since the result is usually greater in error and completely outside the range of the most recent measurements. This has to do with the fact that the method has properties of time locking. Figure 21a gives an example of such incorrect measurements in a continuous series of correct interpretations. It is noticeable that the equipment seems to remain in a waiting loop before taking a new correct measurement, after having taken a wrong one, while its output voltage is constant during that time. Consequently the wrong measurements can easily be discerned by eye.

## 4.6 Results of the processing

The result of the method is the instantaneous RR-interval as a function of time, i.e. the cardiotachogram. This RR-interval is a measure of the instantaneous foetal heart rate which, especially during labour, is liable to change to a great extent. These large, rapid changes, naturally, introduce an extra complication

when comparative measurements are to be performed in the manner described. This is in fact the reason for introducing the rather large variation of ± 10 percent in window $P_2$.

Figure 20 shows a part of a continuous RR-interval measurement (cardiotachogram) for a widely varying heart rate during labour. The lead in this example is an intra-uterine one, as described by Hon [6]. Sometimes the variation in the instantaneous heart rate is so large that even the limits of ± 10 percent are not sufficient and a broader time window must be applied. In the case of extra systoles, of course, no time window can be used at all.

Figure 21 shows a cardiotachogram computed from an abdominal recording. Here the variation in the heart rate is not so large and sudden as the variation during delivery, but the SNR is much worse than in the case of direct leads.

For the procedure to be described in chapter V also, the above method has advantages, because occurrence of foetal complexes can be determined very accurately by means of the time window from $P_2$.

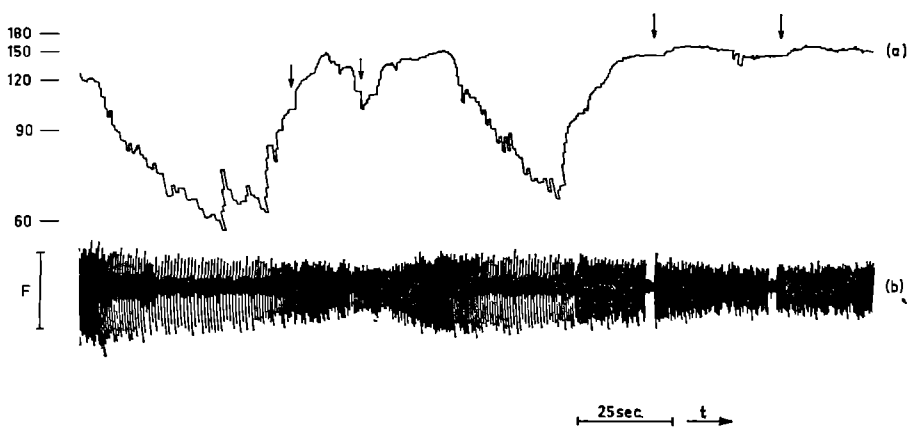


Figure 20. Example of a strongly varying foetal heart-rate during delivery, (a) is the instantaneous cardiotachogram and (b) the filtered foetal ECG, recorded with scalp electrode. Note that the instrument "waits" now and then until a comparison has been made between two intervals (a few places are indicated by arrows).

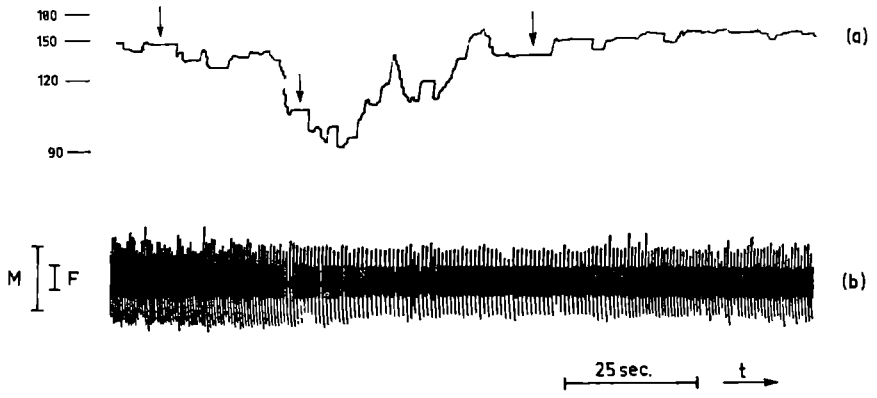


Figure 21. Example of a foetal instantaneous cardiotachogram (a), recorded with abdominal electrodes during delivery. (b) is the filtered signal a(t). Note that sometimes, because of interference between foetal and maternal complexes, no comparative measurement can be performed (a few such places are indicated by arrows).

## References

1. Van Bemmel, J. H. and H. van der Weide, "Detection procedure to represent the foetal heart rate and electrocardiogram", IEEE Trans. on Bio-Med. Engineering, BME 13, no. 4, 1966, p.p. 175—182.
2. Cramer, H., "Mathematical methods of statistics", Princeton University Press, 1946, p.p. 203—206.
3. Rice, J. R. and F. P. Beer, "First-occurrence time of high-level crossings in a continuous random process", Journal of the Acoustic Society of America, Vol. 39, no. 2, 1966, p.p. 323—335.
4. Rice, S. O., "Mathematical analysis of random noise", Dover publications, New York, 1954, p.p. 133—294.
5. Selin, I., "Detection theory", Princeton University Press, 1965.
6. Hon, E. H., "Instrumentation of fetal heart rate and fetal electrocardiography", Am. J. Obstet. and Gynecol., vol. 86, 1963, p.p. 772—784.

# CHAPTER V

# DETECTION OF THE SHAPE OF THE FOETAL ECG

The waveform of the foetal electrocardiogram can be recorded by means of several lead techniques. Recording from the foetal scalp or breech with a clip electrode [1] has the advantage of yielding a large foetal R-wave in relation to the maternal QRS-complex. At the same time it offers standardization of electrode placement with regard to the foetal heart axis. The disadvantage of the method lies in its limited applicability, viz. in the case of ruptured membranes and a dilatation of some centimeters.

Abdominal recording has no such limitation; it is always possible during the major part of the pregnancy. Its disadvantage is the often restricted amplitude of the foetal R-wave compared to that of the disturbances. The foetal ECG complex is always so disturbed by the maternal electromyogram that foetal P- and T-waves are only rarely visible. The almost periodic maternal PQRST-complex also interferes with the abdominal recording. The shape and amplitude of the recorded foetal ECG will vary considerably when the position of the foetus changes with respect to the electrodes. When the cephalic position of the child is sufficiently fixed, the shape of the FECG, recorded during the last weeks of pregnancy using electrodes positioned along the median line has been claimed to be comparable to the neonatal ECG in standard lead II [2].

In this chapter a method will be outlined by which it is possible to compute the shape of the foetal ECG from abdominal-, intra-uterine- or scalp-leads [3].

## 5.1 Statement of the problem

The interfering signals as mentioned above, which disturb the abdominal foetal ECG record must be eliminated by some manipulation of the signal. For this purpose the well-known technique of averaging is used. Hon was the first to use it for the scalp lead [4], but an averaging or integration technique has been applied by others to the abdominal signal as well. Favret's method [5], which requires a digital computer, consists of subtracting a mean maternal ECG-complex from the abdominal lead, at those locations in the recording where a maternal ECG-complex is found, before averaging the foetal ECG-complexes. In con-

sequence of this, foetal R-peaks that originally coincided with maternal QRS-complexes would become just as readily detectable as R-waves which do not so coincide. Others [6], [7], using average response computers, averaged only those foetal PQRST-complexes, of which the foetal R-waves did not coincide with the maternal QRS-complex. In general, however, when averaging techniques are applied to abdominal signals it is wise to pay attention to the following factors.

1. The maternal ECG-complex is often not constant in magnitude due to modulating disturbance (see chapter III and Figure 22). Consequently, after subtraction of an averaged maternal complex, a residual part of the maternal signal remains. This hampers the exact determination of the locations of the foetal R-peaks in the signal, especially in the immediate vicinity of a maternal QRS-complex. Furthermore it is rather difficult to detect those foetal R-waves which coincide with maternal QRS-complexes, because the waveforms of both ECG-complexes are statitstically not orthogonal (see (5.11) below).

2. Since both the maternal and foetal ECG-complexes occur almost periodically, a statistical dependence in occurrence between these two ECG's is noticeable, certainly during finite times of observation. This interdependency is artificially enlarged to a great extent when averaging is restricted to only those foetal ECG-complexes which do not coincide with maternal QRS-complexes. For example, in this way the probability of influencing the averaged foetal QRS-complex by maternal P- and T-waves, but not by maternal QRS-complexes, is increased. Owing to this dependency between the maternal and foetal ECG an averaged foetal ECG complex arises, in which the maternal ECG is not averaged out, so a very disturbed base line is often seen.


Figure 22. Effect of the modulating disturbance on an abdominal FECG (a), in which the four components of formula (5.1) can be clearly seen, (b) is the artificial maternal ECG computed from (a).

These considerations result in the need to observe the following principles in

the determination of the averaged foetal ECG-complex when utilizing only one abdominal lead of the FECG and the usual averaging procedures.

1. Only those foetal complexes should be averaged for which no coincidence exists between the foetal R-wave and the maternal QRS-complex.
2. The contribution of the maternal ECG in the averaged foetal PQRST-complex must be eliminated by a proper correction method.

## 5.2 The processing method

On the basis of the stated considerations a processing method has been developed with which the averaged foetal complex can be determined with great accuracy from the abdominal lead.

### *1. location of foetal R-waves*

The locations of the foetal R-waves are detected according to the method described before (chapter IV).

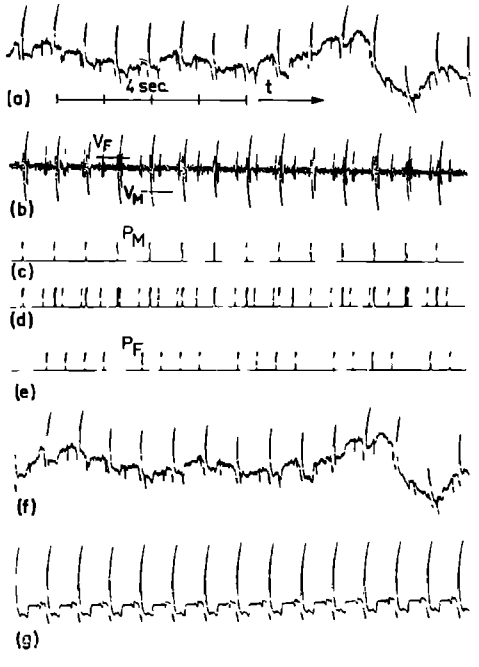


Figure 23. Time sequence for the computation of the abdominal FECG complex (see section 5.2.).

The signal, originating from an abdominal lead of the FECG (Figure 23a, original signal) is filtered into an appropriate frequency band (Figure 23b). Next the maxima of the maternal and foetal R-waves are detected using two detectors $C_M$ and $C_F$ with levels $V_M$ and $V_F$ (Figure 23b) and two differentiating circuits, utilizing the unequal amplitudes of the maternal and foetal R-waves. Combining the outputs of $C_M$ (Figure 23c) and $C_F$ (Figure 23d), a pulse series $P_F$ is generated, which exactly indicates the places in the recording, where maxima of the disturbed foetal R-waves occur (Figure 23e). It is clear that foetal R-waves which coincide with maternal QRS-complexes, are entirely eliminated by this method.

*2. the artificial maternal ECG*

By utilizing the output of the detector $C_M$ (Figure 23c) the pulse series $P_M$ is available, indicating the locations of the maxima of all maternal R-waves in the original signal. Using an average response computer (ARC) and a delaying mechanism for the original signal, on command of the pulse series $P_M$ an averaged maternal ECG-complex is acquired, in which electromyogram, modulating disturbance and foetal ECG are considerably suppressed. So, after some averaging time, a clean maternal PQRST-complex is present in the memory of the ARC. Thereupon, on command of the pulse series $P_M$ the memory of the ARC is sequentially read out.

In this manner an artificial maternal ECG is generated (Figure 23g) which runs completely synchronously with the maternal ECG in the delayed original signal. It is, as far as the maternal ECG m(t) is concerned, completely identical with the delayed original signal (Figure 23f), but free of all disturbance n(t) and r(t) and free of foetal ECG. It is assumed (see chapter III) that the shape of the maternal PQRST complex does not change during the observation time. These two signals (Figure 23f and 23g) are recorded on magnetic tape. With these signals, now synchronously available, the following operations are carried out.

*3. the averaged foetal ECG-complex*

On command of the pulse series $P_F$ (as in Figure 23e) the delayed original signal (Figure 24a) is averaged, as described for the maternal ECG in paragraph 2. Consequently, a result arises as presented in Figure 24c. This is the uncorrected averaged foetal PQRST-complex. When, however, in parallel with processing the original signal, the artificial maternal signal (Figure 24b) is also averaged on command of $P_F$, the curve of Figure 24d appears. This is the contribution of the maternal ECG to the uncorrected averaged foetal PQRST-complex.

The corrected foetal ECG complex (Figure 24e) can now be constructed by algebraic subtraction of the two curves, after multiplication of the correction curve (Figure 24d) with the correct amplification factor $\alpha$. This factor $\alpha$ is the square root of the ratio of the power in the averaged maternal complex computed from the original and the artificial signal (Figure 24f and g).

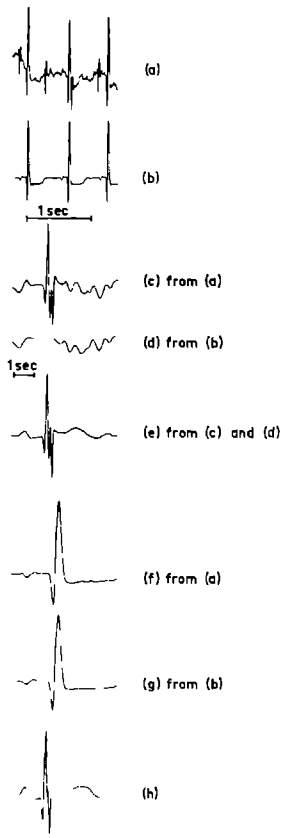


Figure 24. Computation of the mean foetal ECG complex. (a) and (b) are the original and artificial signals a(t) and m(t) respectively. (c) is the uncorrected FECG complex, (d) is the correction for it, from (b).
(e) is the corrected FECG complex.
(f) and (g) are the averaged maternal complexes from (a) and (b) respectively and (h) is the neonatal FECG complex (lead II).

For comparison one complex of the neonatal ECG is also shown. The resemblance to the averaged foetal abdominal ECG-complex is obvious (Figure 24h).

## 5.3 Description of the signal parameters

The problem of computation of the foetal ECG waveform involves both signal detection and extraction.

The latter is in fact a problem of parameter estimation; this estimation only takes place at those times when the signal is detected.
Consequently the computation is divided in two parts:

1. Detection or location of foetal complexes in the abdominal signal (cf. paragraph 5.4).
2. Parameter estimation by elimination of additive noise and correction for maternal ECG (cf. paragraph 5.5).

Schematically the procedure is represented in Figure 25 where the foetal parameters are estimated only after processing the input signal in a double detection circuit and estimation of the parameters of the maternal ECG-complex. In this and following paragraphs the processing method will be described in mathematical and quantitative terms [8].

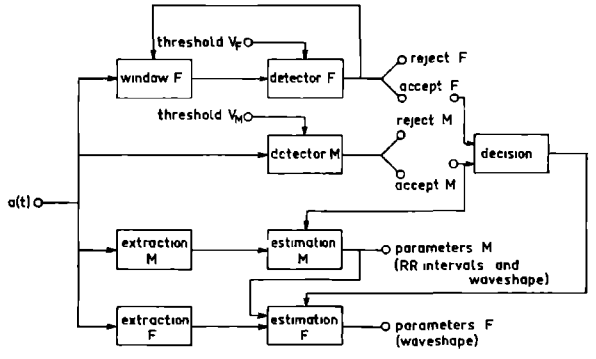


Figure 25. Detection and parameter estimation of both maternal and foetal ECG for the computation of the FECG wave shape.

The abdominal signal can be written in terms of (3.1):

$$a(t) = r(t)\ \{m\ (t) + f(t) + n(t)\} \qquad (5.1)$$

It is assumed that the mean of all components except r(t) is zero and that the mean of r(t) is equal to 1. Further it is supposed that both the maternal ECG and the foetal ECG occur almost periodically with respectively:

| | | | |
|---|---|---|---|
| mean periods | $T_M$ | and | $T_F$ |
| shapes of ECG-complex | M(t) | and | F(t) |
| defined for | $\lvert t\rvert < \frac{T_M}{2}$ | and | $\lvert t\rvert < \frac{T_F}{2}$. |
| with maxima at | $t = 0$ | | $t = 0$ |

The pulse series $\mu(t)$ and $\varphi(t)$

indicate respectively the occurrence of a complex

$$M\,(t-t_m) \qquad \text{and} \qquad F\,(t-t_f)$$

in the abdominal ECG.

Finally it is assumed that the signal properties do not change during the observation time, 2 T, of a(t).

## 5.4 Location of foetal complexes

The techniques that can be used for determination of foetal complexes in the abdominal recording, the pulse series $\varphi(t)$, are for a large part comparable with those used in detection theory.

The location of foetal complexes could be computed optimally using maximum likelihood estimation [9], with peak detection after matched filtering of the signal [11]. The shape of the signal is, however, never known a priori, so that these filtering techniques would only be usable in a second stage of the processing method, when more knowledge had been gained about the waveform of the foetal ECG.

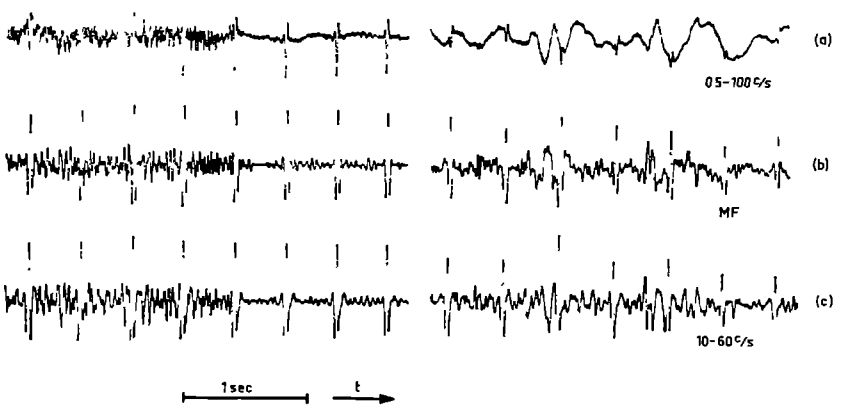


Figure 26. Reduction of noise and low frequency components by matched filtering and band pass filtering.
(a) is the original foetal ECG, recorded with scalp electrode,
(b) is the output of a filter, matched for optimal detection of FECG and maximal SNR.
(c) is the output of a 24 dB band pass filter between 10—60 Hz.

A direct method for SNR improvement (in this chapter the SNR = ratio of foetal signal power to noise power) is to filter the abdominal signal in a bandwidth from about 10 to 60 Hz, utilizing the a priori information about the power spectra of the signal components (see chapter IV). Not only can the additive noise n(t) be reduced by that procedure, but the low frequent maternal ECG components (P- and T-waves) are filtered out as well. An example of both matched filtering and band pass filtering is shown in Figure 26, where it is seen that noise and low frequency disturbance is filtered out. Threshold detection of the filtered signals has been described in chapter IV. It appears that for a sufficiently high SNR nearly all foetal peaks are detected. Still, error-free determination of maxima of f(t) (slightly modulated by the r(t) term from (5.1)) is impossible, due to the n(t) term and the residual influence of m (t). The calculation which now follows will be confined to determining the influence of n(t) on the accuracy of the location of maxima. For that reason a simplified version of formula (5.1) will be used:

$$a(t) = f(t) + n(t) \tag{5.2}$$

If the noise term were absent, a peak in a(t) would indicate exactly the location of a maximum F(0) of a complex $F(t - t_f)$ at $t = t_f$.

The f(t) signal has a finite bandwidth (e.g. 0—200 Hz). The maximum F(0) will be approximated by a second degree function of time around $t = t_f$ in a Taylor expansion:

$$f(t) = F(0) + \dot{F}(0)\ (t - t_f) + \ddot{F}(0)\frac{(t - t_f)^2}{2!} \tag{5.3}$$

where

$\dot{F}(t) = \dfrac{dF(t)}{dt}$ and $\dot{F}(0) = 0$, because it is an extremum.

The noise is also written in a Taylor expansion for all t:

$$n(t) = n(t_f) + \dot{n}(t_f)\ (t - t_f) + \ddot{n}(t_f)\frac{(t - t_f)^2}{2!} + \ldots \tag{5.4}$$

(5.2) combined with (5.3) and (5.4) yields:

$$a(t) = F(0) + n(t_f) + \dot{n}(t_f)\ (t - t_f) + \left\{\ddot{F}(0) + \ddot{n}(t_f) + \dddot{n}(t_f)\frac{2!}{3!}(t - t_f) + \ldots\right\}\frac{(t - t_f)^2}{2!} \tag{5.5}$$

When the SNR is large enough (e.g. $> 10$), then all derivatives for $t \approx t_f$ in the third term at the right hand side except $\ddot{F}(0)$ may by neglected. Differ-

entiation of (5.5) with respect to time gives the location of the new, disturbed maximum as

$$t = t_f - \frac{\dot{n}(t_f)}{\ddot{F}(0)} \tag{5.6}$$

The variance of the location error is

$$\bar{\sigma}_t^2 = \overline{(t - t_f)^2} = \frac{\overline{\{\dot{n}(t_f)\}^2}}{\{\ddot{F}(0)\}^2} \tag{5.7}$$

(The bar stands for averaging in time).

Because n(t) has a Gaussian distribution, the $\dot{n}(t)$ derivative and the location error $\sigma_t$ are also Gaussian. $\ddot{F}(0)$ is a given signal constant, dependent on the spectral properties of F(t). The higher the frequencies which F(t) contains, the sharper is the maximum and the larger is the $\ddot{F}(0)$ term, as can easily be seen from the Fourier transform of F(t).

Assuming that the noise has originally a white spectrum with a variance of $n^2(t) = \sigma_n^2$ ($\mu$V)$^2$ in the bandwidth from 0 Hz to 200 Hz, we can express the variance $\sigma_t^2$ for a given FECG waveform (e.g. the one of Figure 27) with a peak of 20 $\mu$V as:

$$\overline{\{\dot{n}(t_f)\}^2} = 4\pi^2 \frac{\sigma_n^2}{200} \int_{15}^{40} \nu^2 \, d\nu \tag{5.8}$$

where $\nu$ has the dimension of sec $^{-1}$.

It can be calculated from F(t) in Figure 27 that $\ddot{F}(0) = 0.5$, so that (5.7) with (5.8) yields:

$$\sigma_t \approx 12.10^{-5} \, \sigma_n \text{ sec.} \tag{5.9}$$

It means that for example an original variance of (8 $\mu$V)$^2$ produces a location error of 0.3 msec.

The inaccuracy in the location for weak disturbances is appartenly a linear function of the square root of the noise variance. With the aid of an estimate of the signal shapes, and optimal filtering techniques, the variance can be made smaller, although for interpretation of final results an accuracy as calculated in (5.9) is amply sufficient. For (very) large disturbances the calculation is not applicable, because the assumption SNR $>$ 10 is no more valid. Of course, the signal is then subject to large interference so that even coherent averaging (cf. section 5.5) is no longer practicable within the short observation time of the a(t) signal, for which the signal properties are constant.

When the disturbance is so large that peak detection is no longer possible, or

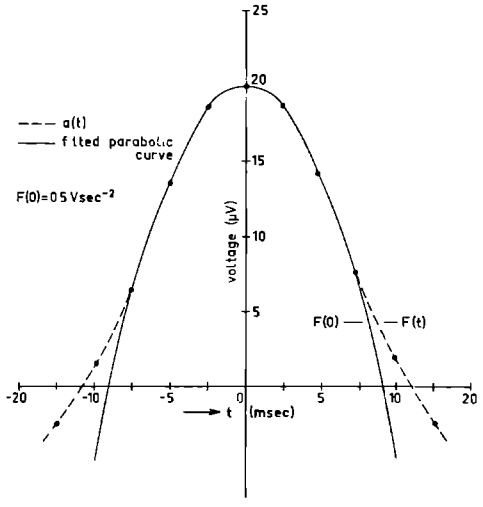


Figure 27. Fitting a parabole to a foetal R-wave to obtain an estimation of the second derivative of the FECG maximum.

even when the foetal complexes are no more or not yet visible in the abdominal recording, it is possible (within certain limits) only to be informed of the presence of foetal ECG's. Then auto- and cross-correlation techniques, after non-linear amplification of a(t), can indicate the presence of f(t) in a(t) and give the mean interval $T_F$ as well (see chapter VI).

## 5.5 Elimination of noise and correction for maternal ECG

*Noise*

Coherent averaging techniques are used to reduce the influence of the noise. By this procedure, the SNR increases linearly with the number of summed or averaged complexes F(t). This averaging may be thought to be a convolution procedure (see Formula 9.1) between pulse series $\varphi(t)$ and signal a(t) of (5.2):

$$F_1(t) = \int_{-T}^{T} \varphi(\tau)\, a(\tau - t)\, d\tau = \varphi(t) * a(-t) \qquad (5.10)$$

The SNR is increased according to $N_F = 2\,T/T_F$, i.e. the number of summed foetal complexes. This, as known, is only true when the noise is stationary and independent [10]. It means, for example, that an original variance of $(8\ \mu V)^2$, after averaging of 100 complexes, becomes $(0.8\ \mu V)^2$.

*Maternal influence*

The simplified formula (5.2) is only usable when discussing the influence of the noise term n(t) on the location of foetal maxima. Formula (5.1) will be used for calculation of the maternal ECG disturbance in (5.10) assuming r(t) = 1. This disturbance can be very large, because of the finite integration time 2T and the appreciable maternal signal power. Furthermore it might be possible that the two pulse series $\mu(t)$ and $\varphi(t)$ are correlated (mathematically, not physiologically), e.g. by a constant ratio $T_M/T_F = R$. When for example R = 2, then at certain places in the resulting averaged waveform (5.10) there might be present a strong clustering of maternal signal, which gives rise to a considerably disturbed baseline.

*Coincidence*

Signals F(t) and M(t) are generally not orthogonal. It means that the cross-correlation function between F(t) and M(t) is non-zero:

$$\overline{F(t)} \,.\, \overline{M(t-\tau)} \neq \overline{F(t)} \,.\, \overline{M(t)} = 0 \qquad (5.11)$$

This implies that detection of $F(t - t_f)$ is impossible when a maternal ECG complex concides with a foetal one, even when we use optimal linear filtering techniques. As a consequence of this it is not possible to obtain a complete pulse series $\varphi(t)$. So another pulse series (Figure 28) is computed instead:

$$\varphi_1(t) = \varphi(t) - \mu_1(t) \qquad (5.12)$$

where $\mu_1(t)$ is the pulse series arising from those maternal complexes $M(t - t_m)$ that coincide with foetal complexes $F(t - t_f)$, for their QRS parts only.

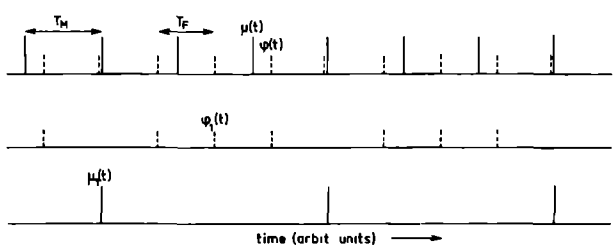


Figure 28. Schematic representation of the maternal, $\mu(t)$, and foetal, $\varphi(t)$, pulse series, $\varphi_1(t)$ is the non-coinciding foetal pulse series and $\mu_1(t)$ is the coinciding maternal pulse series.

In fact, pulse series $\mu_1(t)$ is a part of both series $\varphi(t)$ and series $\mu(t)$. Convolution of $\varphi_1(t)$ with a(—t) gives:

$$F_2(t) = \varphi_1(t) * a(-t) = \varphi_1(t) * m(-t) + \\ + \varphi_1(t) * f(-t) + \varphi_1(t) * n(-t) \tag{5.13}$$

The first term at the right hand side of this equation can be written as:

$$M_1(t) = \varphi_1(t) * m(-t) = \varphi(t) * m(-t) - \mu_1(t) * m(-t) \tag{5.14}$$

This equation shows the considerable influence of maternal signal in (5.13), due to the strong correlation between $\mu_1(t)$ and m(t).

*Artificial ECG and correction*

The influence of the second term in (5.14) will now be calculated. Whereas, in general, it is true that:

$$\bar{M}^2(t) \gg F^2(t) \text{ and } \gg n^2(t) \tag{5.15}$$

it is quite possible to locate maternal maxima, i.e. pulse series $\mu(t)$, using the method mentioned in section 5.4, above. Furthermore it is in any case possible to compute $\mu(t)$ from a separate maternal lead in which both f(t) and n(t) are negligibly small.

Convolution between $\mu(t)$ and a(—t) gives the rather noise-free maternal ECG complex:

$$M(t) = \mu(t) * a(-t) \tag{5.16}$$

With (5.16) we can compute an artificial maternal ECG, completely the same as the one in (5.1) buried in other signals, except for its modulating factor:

$$m(t) = \mu(t) * M(t) \tag{5.17}$$

Finally, a convolution procedure between m(t) from (5.17) and $\varphi_1(t)$ from (5.12) yields:

$$\varphi_1(t) * m(-t) = M_1(t) \tag{5.18}$$

The results of (5.18), subtracted from those of (5.13) leave:

$$F(t) = F_2(t) - M_1(t) \approx \varphi_1(t) * f(-t) \tag{5.19}$$

In Equation (5.19), the noise term has been neglected. As calculated in paragraph 1 of this section, its variance is:

$$n_1^2(t) = \bar{n}^2(t)/N \tag{5.20}$$

where N represents the number of non-coincident foetal ECG-complexes during the observation time.

F(t), as represented in (5.19), is the final result of the processing method after

filtering, peak detection, computation of the artificial signal, two-fold coherent averaging and subtraction. Of course, the result from (5.19) is still inaccurate when there is a strong modulating factor r(t).

The maternal power has then to be measured instantaneously for every complex $M(t—t_m)$ in (5.1) in order to obtain r(t) and the signal m(t) in (5.17) must be multiplied with this factor. In practice, this procedure has never appeared to be necessary, since the rest of the maternal disturbance was always smaller than the remaining noise variance.

## 5.6 Results of the processing

Figure 24 presents a result of the procedure utilized with an abdominal FECG; in this record the several signals mentioned can be recognized. It appeared that abdominal foetal ECG complexes may differ considerably one from the other. Only occasionally can the cause of an apparently abnormal pattern be clearly demonstrated.

To give an impression of the improvement of SNR, several averaged foetal ECG complexes, each for a rather short integration time and taken from one patient, are plotted in Figure 29.

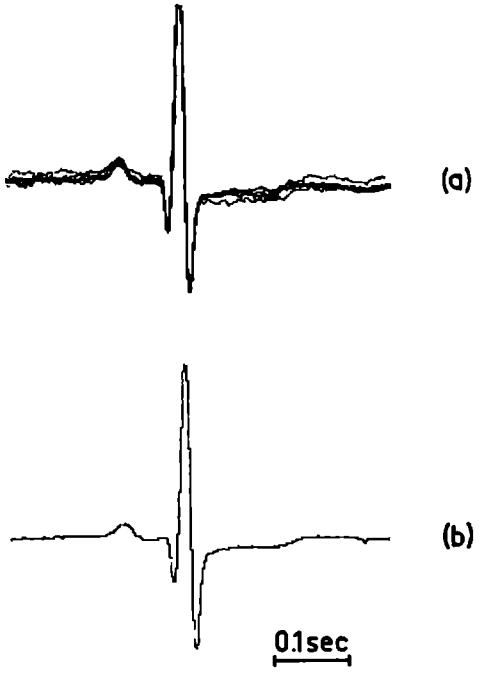


Figure 29. Effect of the number of averaged complexes on the noise variance. The upper curves are 5 averaged FECG complexes each computed from the sum of 10 original complexes. The lower complex is the sum of 100 original complexes.

## References


1. Hon, E. H., "Instrumentation of fetal heart rate and fetal electrocardiography", Am. Journal of Obstetrics and Gynecology, vol. 86, 1963, p.p. 772—784.
2. Larks, S. D. and G. G. Larks, "Resemblance of the foetal ECG complex to the standard lead II QRS of the newborn", Obstetrics and Gynecology, vol. 24, 1964, p.p. 1—5.
3. Van Bemmel, J. H., L. A. M. Peeters and S. J. Hengeveld, "Influence of maternal ECG on the abdominal foetal ECG complex", Am. Journal of Obstetrics and Gynecology, vol. 102, 1968, p.p. 556—562.
4. Hon. E. H., and S. T. Lee, "Averaging techniques in fetal electrocardiography", Med. Electr. and Biol. Engng., vol. 2, 1964, p.p. 71—75.
5. Favret, A. G. and A. A. Marchetti, "Fetal electrocardiographic waveforms from abdominal wall recordings", Am. Journal of Obst. and Gynec., vol. 27, 1966, p. 355.
6. Van Bemmel, J. H. and H. van der Weide, "Detection procedure to represent the foetal heart rate and electrocardiogram", IEEE Trans. on Bio-Med. Engng., BME 13, 1966, p.p. 175—182.
7. Kendall, B., D. C. Amoss, H. H. Sun, A. W. Hahn and D. M. Farrel, "The noise-free fetal electrocardiogram recorded from the maternal abdomen", Am. Journal of Obst. and Gynec., vol. 97, 1967, p.p. 1129—1134.
8. Van Bemmel, J. H., "Waveform detection from abdominal foetal electrocardiograms", Progress Report, Institute of Medical Physics, PR 1, 1968, p.p. 57—62.
9. Selin, I., "Detection theory", Princeton University Press, 1965.
10. Bendat, J. S., "Mathematical analysis of average response values for nonstationary data", IEEE Trans. on Bio-Med. Engng., BME 11, 1964, p.p. 72—81.
11. Zadeh, L. A. and J. R. Ragazzini, "Optimum filters for the detection of signals in noise", Proc. IRE, vol. 40, 1952, p.p. 1223—1231.

# CHAPTER VI

# DETECTION OF THE RR-INTERVAL WITH CORRELATION TECHNIQUES

## 6.1 Statement of the problem

When recording the foetal electrocardiogram (FECG) from the abdominal wall of the mother, it is often difficult, during some stages of pregnancy, to find a regularly occurring R-wave. Different causes have been mentioned (see chapter II).

During the second half of the pregnancy it may even happen that a good phonocardiogram can be recorded, although no foetal R-waves are visible in the abdominal FECG. The reverse, however, is just as easily possible. In such cases it is of value to find some method that gives more certainty that there is a living foetal heart present and by which the foetal heart rate can be determined.

A serious problem arises in those recordings in which neither the phono- nor the electrocardiogram reveals any sign of a living foetal heart or in which much disturbance is present.

To improve the detection of the foetal signal, one may resort to recording the FECG over periods of hours. However, even then it is certainly not always possible to extract information about the foetus by visual inspection.

The fundamental problem is, therefore, to develop a method that will permit detection of the weak foetal ECG imbedded in a background of disturbing signals.

For this purpose correlation techniques, commonly used for the detection of weak signals buried in noise, will be used.

The abdominally recorded electrocardiogram was described in (3.1) as:

$$a(t) = r(t)\,\{m(t) + f(t) + n(t)\} \tag{6.1}$$

Figure 22 gives a good example of the signal (6.1).

It is important that the periods $T_M$ and $T_F$ (see chapter 5.4) are reasonable constant during the observation time, since the only information that can be extracted from a very noisy signal is the mean heart rate of mother and foetus. The constancy of the RR-interval will appear to be important also with respect to the gain in SNR following the procedure that will be described below. It will

further appear that, in order to obtain an optimal discrimination between foetal signal and the rest of the signal components, the shape of the maternal ECG should be rather invariant during the processing of the signal. For the present, the factor r(t) will be taken equal to 1, but its influence will be discussed at the end of section 6.3.

## 6.2 Detection procedure

*Power density measurement*

Arising from the information about the abdominal signal acquired in chapter III, a detection procedure has been developed. It will be assumed that the wave shape of the foetal signal is unknown. The SNR has to be enhanced in favour of the foetal signal.

Most problems involving the detection of weak signals in the midst of noise, can be studied by measuring power densities. Decisions about the presence of f(t) based on the measurement of power densities can also be effected in this case, provided that one can use some reference signal:

$$s(t) = m(t) + n(t)$$

From the difference in power between the original (6.1) and the reference signal, the decision could then be made if in a(t) a signal f(t) was present or not. Of course, it is impossible to obtain such a signal s(t) of suitable properties from the abdomen, with the same signal parameters as present in a(t).

It will be assumed for the moment that the reference signal can be obtained except for its term n(t). So the reference signal will be:

$$s(t) = m(t) \tag{6.2}$$

A difference power measurement between (6.1) and (6.2), gives uncertain results now; this is due to the large noise power density, which is determined in a(t) at the same time. The large effect of the noise-power is mainly caused by the fact that the weak foetal QRS-complex lasts so short a time in relation to the total period of the cardiac cycle.

*The autocorrelation function of an ECG*

Another stochastic signal approach offers possibilities in surmounting these difficulties: the autocorrelation function (ACF) of a(t) reveals the sum of three correlation functions:

$$C_{aa}(\tau) = \overline{a(t) \cdot a(t-\tau)} = C_{mm}(\tau) + C_{ff}(\tau) + C_{nn}(\tau) \qquad (6.3)$$

where it is known that $C_{nn}(\tau)$ is small for $\tau$ large enough and it is supposed that the crossterms $C_{mf}(\tau)$ and $C_{fm}(\tau)$ are small in relation to $C_{ff}(\tau)$.

Since m(t) and f(t) are both almost periodic functions, maxima in $C_{mm}(\tau)$ and $C_{ff}(\tau)$ are expected for respectively

$$\tau = k\ T_m \text{ and } \tau = l\ T_f \text{ with k and l integers.}$$

For $\tau = kT_m$ or $lT_f$ (k and l now unequal to zero), generally no maxima will be expected in $C_{nn}(\tau)$; there is, however, a "residual power" measurable in terms of $C_{nn}(\tau)$ and the finite integration time (variance).

When, in the $\tau$-domain, a comparative power measurement is taken between a(t) and s(t), the following can be stated. Maxima in $C_{aa}(\tau)$ will be measured for $\tau = 0$, $T_f$ and $T_m$. The first peak is as high as the total power present in a(t), the second is caused by the maximum in $C_{ff}(\tau)$ for $\tau = T_f$ and the third by the first maximum in $C_{mm}(\tau)$ for $\tau = T_m$, when $T_f < T_m < 2\ T_f$.

In $C_{ss}(\tau)$ maxima are also observed as $\tau = 0$ and $\overline{T}_m$: the first is the total power of s(t), (a peak for $\tau = T_f$ is not present because s(t) lacks any foetal signal) and the maximum at $\tau = T_m$ is the one caused by the maternal ECG.

Comparison of the two correlation functions finally results in the following difference: for $\tau = T_f$ a peak in $C_{aa}(\tau)$ and no peak at all in $C_{ss}(\tau)$.

The detection procedure can then be summarized as follows:

1) recording and filtering of a(t)
2) "recording" and filtering of s(t)
3) } will be introduced
4) } in section 6.3
5) power measurement in a(t) via the ACF $C_{aa}(\tau)$
6) power measurement in s(t) via the ACF $C_{ss}(\tau)$
7) comparison between $C_{aa}(\tau)$ and $C_{ss}(\tau)$ for $\tau \approx T_f$.

Analyzing the ACF of a (filtered) ECG offers some difficulties, which do not occur when wholly periodic signals are involved. The computation of an autocorrelation function of a truly periodic signal results in a periodic function. In contrast, the ACF of an arrhythmic signal as described here yields a function with decreasing and broadening maxima for increasing $\tau$. The peak amplitude for $\tau = k\ T_f$ in the correlation function $C_{ff}(\tau)$ thus depends on the arrhythmicity of f(t), indeed, on the distribution of intervals between events in f(t), and on any interval serial correlation coefficient which might exist.

There is another, more important reason why maxima for $\tau = kT_f$ with $k \geqq 1$ in $C_{ff}(\tau)$ can be much smaller than the maximum for $C_{ff}(0)$.

When the mean of all present signals equals zero:

$$a(t) = m(t) = f(t) = n(t) = 0 \tag{6.4}$$

and further:

$$\int_{QRS} f(t)dt \approx 0 \tag{6.5}$$

which means that the averaged QRS-complex of the filtered (foetal) ECG equals zero, an extra complication appears.

Because of the fluctuation in $T_f$ and due to the matter expressed by equation (6.5) is it now possible that in the vicinity of $\tau = T_f$ in $C_{ff}(\tau)$ the correlation function becomes very small or even zero. This phenomenon is due to the interference of the several products $f(t) \times f(t-\tau)$ (also remarked by Favret)[2]. This product, at some $\tau \approx T_f$, can reveal positive and negative results when $T_f$ is subject to change. So, the integral of this product may be zero for some region around $\tau = T_f$, and the proposed power-difference measurement can be an unusable procedure.

It is not possible to express the shape of a foetal QRS-complex in simple mathematical form; however, the effect of the interference mentioned can be simulated with a pulse series y(t), which consists of pairs of a positive and a negative Dirac comb[3] at a constant distance $\Delta$ from each other, whereas the intervals between the pairs are distributed according to a function g(t), which is for example the normal distribution (see Figure 30). $\Delta$ is assumed to be small in relation to the mean interval $T_f$.

The pulse series can be written as

$$y(t) = \tfrac{1}{2} \sum_k \left\{ \delta\left(t - \nu_k + \frac{\Delta}{2}\right) - \delta\left(t - \nu_k - \frac{\Delta}{2}\right) \right\} = \tfrac{1}{2} \sum_k (\delta_{1k} - \delta_{2k}) \tag{6.6}$$

$\nu_k$ is the phase of the pairs of pulses.

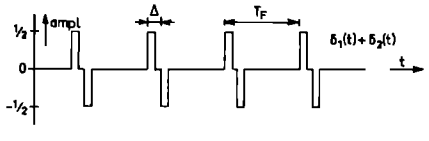


Figure 30. Simulation of a series of foetal QRS-complexes by pairs of positive and negative Dirac combs.

The autocorrelation function of a series of single Dirac combs $\delta(t)$ is:

$$C_{\delta\delta}(\tau) = \sum_k \sum_l \delta(t - \nu_k) \,.\, \delta(t - \nu_l - \tau) \tag{6.7}$$

which yields maxima for $\tau = kT_f$, where

$$\sum_k \delta(\tau - kT_f) = 1 \tag{6.8}$$

The peak for $\tau \approx T_f$, when the variance of the interval distribution is not too large, is the distribution function $g(\tau)$ shifted over $\tau = T_f$.

Similarly, the ACF for y(t) yields:

$$C_{yy}(\tau) = g(\tau - T_f) - \tfrac{1}{2}\{g(\tau - T_f + \Delta) + g(\tau - T_f - \Delta)\} \tag{6.9}$$

It is easy to see from (6.9) that $C_{yy}(\tau) \to 0$ when we take $\lim_{\Delta \to 0} C_{yy}(\tau)$.

Thus for small $\Delta$ a very small power contribution can be expected for all peaks in the ACF except for $\tau = 0$.

When, however, the squared signal $y^2(t)$ instead of y(t) is auto-correlated, we obtain using (6.6):

$$\begin{aligned} y^2(t) &= \tfrac{1}{4} \sum_k \sum_l (\delta_{1k} - \delta_{2k})\ (\delta_{1l} - \delta_{2l}) \\ &= \tfrac{1}{4} \sum_k (\delta_{1k} + \delta_{2k}) \end{aligned} \tag{6.10}$$

So that for $\tau \approx T_f$ :

$$C_{y^2y^2}(\tau) = \tfrac{1}{4}[g(\tau - T_f) + \tfrac{1}{2}\{g(\tau - \bar{T}_f + \Delta) + g(\tau - T_f - \Delta)\}] \tag{6.11}$$

For $\Delta \to 0$ (6.11) becomes around $\tau = \bar{T}_f$:

$$C_{y^2y^2}(\tau) = \tfrac{1}{2} g(\tau - T_f) \tag{6.12}$$

which is a satisfying result, since it appears possible to obtain a peak around $\tau = T_f$, even when the intervals between the pulse pairs are inconstant.

## 6.3 Envelope of the filtered ECG

It is argued that it is impossible, when using signals of the f(t) type, obeying (6.5), to determine whether there is a foetal signal present at all.

Yet the $\tau$-domain is pre-eminently suited to perform the power measurement, since the noise component plays no important role for large $\tau$. It appears from (6.5), that the interference is caused by the fact that some parts of the filtered QRS-segment have an opposite phase. By squaring the filtered f(t) one acquires a positive signal $f^2(t)$. When from the envelope of the new signal, $f_1(t) = \text{Env}\{f^2(t)\}$, the autocorrelation function is determined, there is no interference

between positive and negative parts of the signal, because after squaring there are no signal parts in opposite phase; the expression (6.5) for $f_1(t)$ is unequal to zero. The envelope has been taken since only the low frequency part of the signal $f^2(t)$ is of importance and since the procedure is carried out digitally (see chapter VIII) and a low sampling rate is desired to allow the whole correlation function to be computed at least up to $\tau = T_m$.

The detection procedure from section 6.2 is now extended by

3) square law envelope dectection of $a(t) : a_1(t)$
4) square law envelope detection of $s(t) : s_1(t)$.

Now the ACF will be computed for the signals $a_1(t)$ and $s_1(t)$ in points 5) and 6) of section 6.2:

$$C_{a_1a_1}(\tau) = C_{f_1f_1}(\tau) + C_{m_1m_1}(\tau) + C_{n_1n_1}(\tau) \tag{6.13}$$

and

$$C_{s_1s_1}(\tau) = C_{m_1m_1}(\tau) \tag{6.14}$$

with, when $\tau$ is large enough,

$$\Delta C(\tau) = C_{a_1a_1}(\tau) - C_{s_1s_1}(\tau) \approx C_{f_1f_1}(\tau) + C_{nn}^2(0) \tag{6.15}$$

The term $C_{nn}^2(0)$ is a constant and equal to the square of the noise power. It has been assumed that the autocorrelation function $C_{nn}(\tau)$ is zero for $\tau$ large enough. The variance for finite integration time will be treated in the next section.

The function $C_{m_1m_1}(\tau)$ can also be obtained by another method, viz. that of the crosscorrelation function (CCF) of $a_1(t)$ and $s_1(t)$:

$$\begin{aligned} C_{s_1a_1}(\tau) &= \bar{s}_1(t).\, a_1(t-\tau) \\ &= m_1(t)\,.\, a_1(t-\tau) \approx C_{m_1m_1}(\tau) \end{aligned} \tag{6.16}$$

The practical advantage of (6.16) over (6.14) is that in (6.13) as well as in (6.16) the factor $a_1(t-\tau)$ occurs, so that only the signal $a_1(t)$ must be delayed, whereas in (6.14) the term $s_1(t)$ also must be delayed.

The procedure is closely related to the well-known fact in the statistical detection theory, that the optimum receiver for small signals buried in noise is a square-law detector, followed by an integrator [1]. As similar method has been found here too; the integration of the auto-product has been replaced by integration of the cross-product between the signal and its delayed version. The correlator is here the only possible integrating device, necessary because of the

unknown noise power and applicable because of the quasi repetitive character of the foetal signal.

Formula (6.15) is the final result of the detection procedure. The fact that (6.15) has been acquired by subtraction of $C_{s_1 s_1}$ from $C_{a_1 a_1}$ instead of the more plausible method, the ACF of the squared signal

$$a(t) - s(t) = f(t) + n(t),$$

finds its origin in the modulating factor r(t) from (6.1). When there is a multiplicative disturbance present, (6.1) diminished by (6.2) would give:

$$a(t) - s(t) = r(t)\,\{m(t) + f(t) + n(t)\} - m(t) \tag{6.17}$$

The ACF, computed for the squared signal from (6.17), yields among other things, the term $(C_{r_1 r_1} - 1)\, C_{m_1 m_1}$. This term is unequal to zero, because of the low frequency properties of the multiplicative noise r(t). On the other hand the ACF $C_{m_1 m_1}(\tau)$ of (6.13) is modulated by $C_{r_1 r_1}(\tau)$. It is statistically, however, much better to correct for $C_{r_1 r_1}(\tau)$ in the final result, than for r(t) in the original signal. In practice it was never necessary to carry out such a correction numerically since the ACF $C_{m_1 m_1}(\tau)$ could easily be traced in $C_{a_1 a_1}(\tau)$ with help of $C_{s_1 a_1}(\tau)$.

## 6.4 Practical limitations, variance

In practice the computation of a Formula like (6.13) requires a very large number of multiplications and integrations for about fifty different delays. Of course these computations can easily be carried out on a digital computer. However, when the signal is processed in real time a huge installation will be occupied during all the time that the signal is fed to the computer, which might be a long period. For that reason a practical realization of the processing equipment is very important and the advantage of a special purpose computer is obvious. For this reason an instrument has been developed and constructed based on the polarity-coincidence correlation method [4–7], described in chapter IX. In the polarity-coincidence correlator the function

$$C_{xy}(\tau)_{pol} = \{\overline{\text{sign}\; x(t)}\} \cdot \{\overline{\text{sign}\; y(t-\tau)}\} \tag{6.18}$$

is computed in place of

$$C_{xy}(\tau) = x(t) \cdot y(t-\tau) \tag{6.19}$$

(the "analog" correlation function). By means of auxiliary functions the output of the polarity-coincidence correlator can be made almost the same as that of the analog correlator [6–8].

The use of this correlator is very practical since the ACF and the CCF are

directly available during and after the integration period, but the detection procedure can be carried out with other types of correlators as well.

For the rectified or squared signals x(t) and y(t) a new zero level $\lambda$ can be calculated [9].

When it is given that:

$$C_{|x'\ y|}(\tau)_{pol} = \overline{sign}\ \{|x| - \lambda\} \cdot sign\ \{|y| - \lambda\} \tag{6.20}$$

and a Gaussian joint distribution applies for x and y:

$$f(x,y) = \frac{1}{2\pi\sigma^2(1-\varrho^2)} \exp\left\{\frac{x^2 - 2\varrho xy + y^2}{2\sigma^2(1-\varrho^2)}\right\} \tag{6.21}$$

with a zero correlation coefficient (large $\tau$):

$$\varrho = \varrho_{xy}(\tau) = \frac{C_{xy}(\tau)}{C_{xy}(0)} = 0 \tag{6.22}$$

it can be calculated [10] that:

$$C_{|x|\,|y|}(\tau)_{pol} = 0 \quad \text{for} \quad \lambda = 0.675\left[C_{xy}(0)\right]^{\frac{1}{2}} \tag{6.23}$$

The level $\lambda$ so determined seems to be suited to small foetal SNR's, where the foetal ECG is invisible in the midst of a noisy background.

For higher SNR's, where it is still impossible to compute the instantaneous foetal heart rate it seems better to compute the level $\lambda$ with the method described in chapter IV, where $\lambda$ lies at half the peak of the squared foetal ECG. The correlator delivers in that case the mean foetal heart rate, computed from a signal part of length T, where T has to be long enough to obtain a clearly visible peak in the correlation function.

In an ideal recording without much disturbance one obtains in this way (using the PCCF correlator) a result that is comparable to the expectation density function of the pulse series

$$\mu(t) + \varphi(t)$$

of chapter V. The only exception is, that the pulses $\mu$ and $\varphi$ are no Dirac combs and that one measures also a peak for $\tau = 0$.

*Finite integration time, variance*

As a consequence of the always finite integration time T for the abdominal signal the correlation function has never a zero variance. This disturbance superimposed on the correlation function is mainly due to the finite integration of the ACF of the noise term n(t) and partly due to the crossterms of f(t) and m(t) with n(t).

To gain an impression of the total integration time necessary to obtain a desired SNR, it will be assumed that the clipping, rectification, smoothing, and correlation method (PCCF, with or without auxiliary signals) have only a slight influence — see e.g. (9.12) and (9.13) — on the size of the variance in the correlation function of the signal a(t), which for the time being is thought to consist only of the terms f(t) and n(t).

The SNR's are defined for the input signal as:

$$SNR_0 = \frac{S_0}{N_0} = \frac{f^2(t)}{n^2(t)} \tag{6.24}$$

and for the correlator output $C_{aa}(\tau)$ after integration over T seconds as

$$SNR_1 = \frac{S_1}{N_1} = \frac{E\left\{\int_0^T f(t) \cdot f(t-\tau)dt\right\}^2}{E\left\{\int_0^T n(t) \cdot n(t-\tau)dt - C_{nn}(\tau)\right\}^2} \tag{6.25}$$

with E the expectation operator.

Assuming that the noise has passed a low pass RC filter with bandwidth $W = (RC)^{-1}$ it can be shown that

$$C_{nn}(\tau) = N_0 \cdot \exp\left[-W|\tau|\right] \tag{6.26}$$

whereas generally it is true [11], (9.12) that

$$N_1 = \frac{2}{T^2}\int_0^T (T-\tau)\, C_{nn}^2(\tau)\, d\tau \tag{6.27}$$

so that after evaluation, for small $SNR_0$ and a large integration time-bandwidth product:

$$N_1 \approx N_0^2/WT \tag{6.28}$$

For the signal from the correlator we write for T large enough and assuming stationary signal properties:

$$S_1 = E\{C_{ff}^2(\tau)\} = C_{ff}^2(\tau)$$

When it is further assumed that the signal power at $\tau = T_f$ is the same as at $\tau = 0$, then it follows:

$$S_1 = C_{ff}^2(0) = S_0^2 \tag{6.29}$$

With (6.28) and (6.29), (6.25) becomes:

$$SNR_1 = \frac{S_0^2}{N_0^2} WT = SNR_0^2 \,.\, WT \tag{6.30}$$

The correlator output $SNR_1$ is directly proportional to the integration time. This is the only parameter that can be used to improve the $SNR_1$, because W is determined by the signal itself and it would be irrational no to filter out all high frequency noise components above the signal band, since the input SNR appears in quadratic form in the variance formula (6.30).

To derive a rough estimate of the integration time for a foetal ECG in a background of Gaussian noise, we will apply equation (6.30) to some FECG waveshape with the assumption that all foetal intervals are equal (see Figure 31). The signal power is then

$$S_0 = \frac{1}{N.QRS} \int_{QRS} f^2 dt = \frac{A^2}{3N}$$

in which QRS is the duration of the QRS-complex and $N = T_f/QRS$. When the noise variance for a bandwidth from 0—40 Hz equals $N_0 = \sigma_0^2$ then it follows with $\alpha = A^2/\sigma_n^2$, that

$$SNR_0 = \frac{\alpha}{3N} \tag{6.31}$$

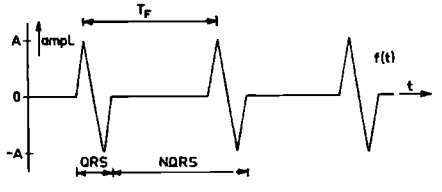


Figure 31. Schematic representation of foetal ECG to calculate the variance after autocorrelation.
QRS is the duration of the QRS-complex and NQRS equals the RR-interval $T_f$.

The integration time is, for a practical value of N = 10, with (6.30):

$$T = \frac{90}{4} SNR_1 \,.\, \frac{1}{\alpha^2} \tag{6.32}$$

If an output SNR of 4 is required it can be calculated that for $\alpha$ = 30, 10, 3, 1, 0.3, 0.1 an integration time of T = 100 msec., 0.9 sec., 10 sec., 90 sec., 17 min., 2.5 hours must be used.

For a directly visible foetal ECG it is necessary that the foetal peak is

approximately 5 times the noise dispersion, which means that $\alpha$ must be larger than 25. For the application of an instantaneous heart rate meter this factor must be even much higher, since the noise power may vary considerably from moment to moment. The computation of mean foetal heart rates and detection of weak foetal ECG's can thus be applied practically for $0.25 < \alpha < 100$.

This means, with the assumptions and approximations used here, a lower limit for the $SNR_0$ of about $10^{-2}$. This limit could be made somewhat lower when, before processing, knowledge can be gained about the signal shape and a matched filter used. The use of such a filter, in fact the use of more a priori information about the signal than only the repetitive character of the foetal ECG, yields a further improvement of the SNR. See Figure 26 for an example of the matched filtering.

Assuming a bandwidth of the FECG of 40 Hz and a QRS duration of 50 msec., it can be calculated using (9.20) that a factor of 4 improvement of the SNR can be reached. Since in (6.30) we have a squared input SNR, the final improvement of the optimal filter can be estimated to be roughly 16, which yields a reduction in the integration time.

## 6.5 Processing sequence

Following the same order of processing as summarized in section 6.2, the result (6.15) can now be calculated for the abdominal FECG [12], [13], see Figure 32 and chapter VIII.

1. The FECG is filtered and recorded with the original signal (Fig. 32(1) and (2)) and, when available, with a separate maternal ECG $m^*(t)$ on analog tape.
2. From this tape-recording the envelope of the signal is determined after clipping and rectification. Since the maternal ECG, which is much larger in amplitude, does not give useful information at all in (6.13), all amplitudes in the maternal filtered ECG of the abdominal signal, that are larger than the maximal foetal or noise amplitudes are clipped. This clipping is also convenient with respect to the finite accuracy of the analog equipment used (32 (3)). The amplitude distribution of a clipped and filtered signal is shown in Figure 33. The envelope is then determined from this signal after rectification (32(4) and (5)).
3. The reference signal $s_1(t)$ will be computed from the latter signal. To this end the maximum amplitudes of the filtered maternal R-waves are determined in the original signal a(t). A pulse is generated at these locations (32(6)). With

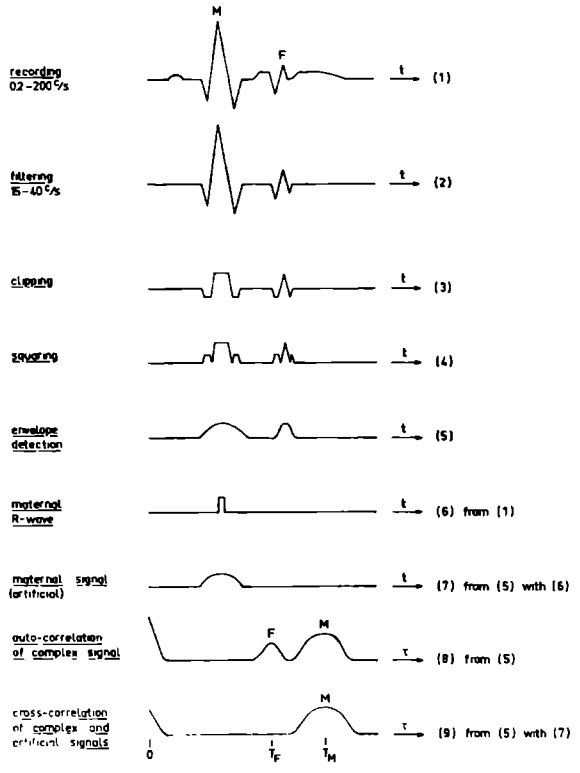


Figure 32. Processing sequence for auto- and crosscorrelation of foetal electrocardiograms. (See also the block diagram of Figure 54).

these pulses the artificial maternal signal $s_1(t)$ is now constructed in the same manner as treated in chapter V (32(7)). Finally we have then available the signals

$$a_1(t) = \text{Env. } \{a^2(t)\}$$

and

$$s_1(t) = m_1(t) = \text{Env. } \{m^2(t)\}$$

while it is known that a(t) as well as m(t) are the filtered and clipped original abdominal signals.

In Figure 22 an example was given of an original signal a(t) and a reference signal s(t) associated with it, but without filtering and envelope detection.

4. From $a_1(t)$ we then compute the ACF, which is represented in Figure 32(8). The CCF between $a_1(t)$ and $s_1(t)$ is shown in Figure 32(9). The difference between ACF and CCF indicates the presence of a foetal ECG.

In the Figures, explained in the next paragraph, some differences between ACF and CCF are due to the covariance of the noise as well as to the factor r(t). In the Figures the normalized correlation function $C(\tau)/C(0)$ is shown in each case.

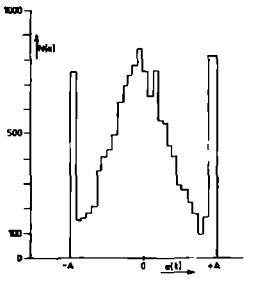

Figure 33. Amplitude distribution of a 20 second part of an abdominal filtered signal (that of Figure 38) after clipping of all amplitudes $|a(t)| \geqq A$.

## 6.6 Results of the processing

### 1. *Visible foetal electrocardiogram*

For visible foetal ECG's in abdominal signals, however small they may be, the method described has always met expectation. Figure 34 gives an example.

For illustration, the filtered signal is reproduced in the upper trace. Also the correlation function, without envelope detection beforehand, is shown. Often the presence of a maximum in the correlation function of the envelope is so clear that calculation of the crosscorrelation function (6.16) can be omitted.
Figure 35 gives an example of the ACF as well as the CCF for the same signal as in Figure 34.

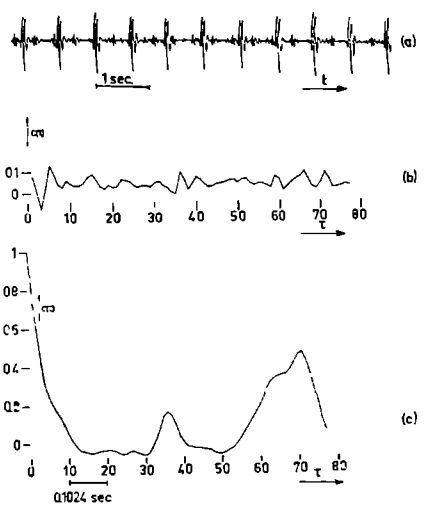


Figure 34. Autocorrelation of an abdominal signal with small but still visible foetal complexes.
(a) shows the filtered signal a(t).
(b) ACF computed from the filtered a(t) but without envelope detection.
(c) ACF from a(t) after envelope detection. The integration time for both ACF's was 30 seconds. Note that even the ACF of the maternal signal in (b) is very small because of the irregularity in the maternal heart rate.

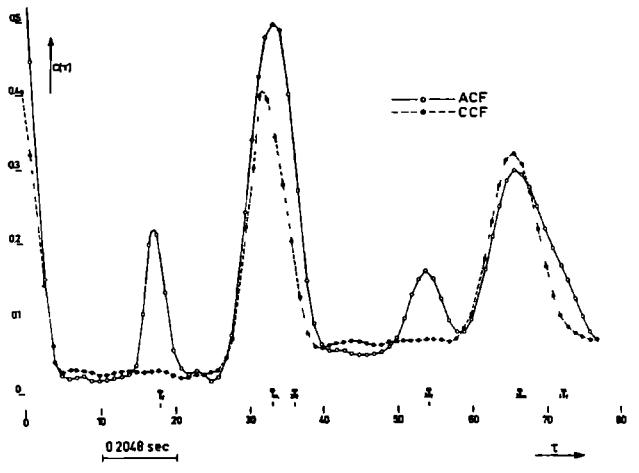


Figure 35. Autocorrelation and crosscorrelation functions computed for an abdominal FECG. The functions are computed for the same signal as in Figure 34, but for a longer part of the recording (5 minutes) Even the fourth foetal complex at 4 $T_f$ is discernable.

One can sometimes, in circumstances of almost constant foetal heart rate, decide without the need for square law detection if a foetal signal has been

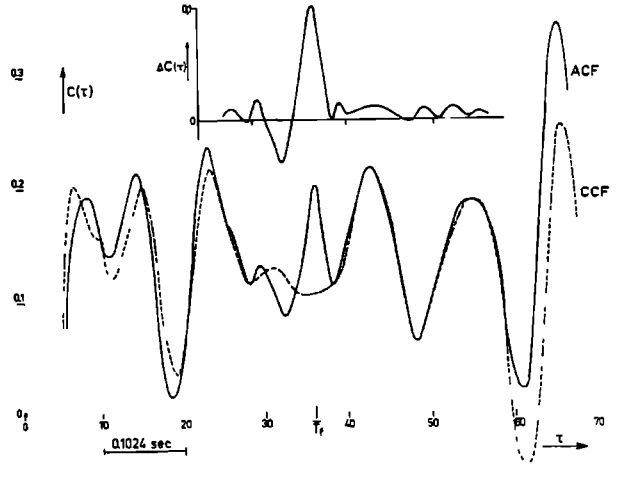


Figure 36 Detection of an abdominal FECG without envelope detection, but with artificial signal s(t), computed from a(t) Also the subtracted result $\Delta C(\tau)$ is shown. The signal is that of Figure 34 and the integration time was 10 minutes The difference between the ACF and CCF for $\tau \approx 65$ is due to the second foetal peak and the factor r(t).

present or not. Figure 36 shows how, by means of the auto- and crosscorrelation of non square law detected signals a(t) and s(t), the presence of a foetal signal can be decided. For the rest, the benefit of the squaring clearly appears.

## 2. *Invisible foetal electrocardiograms*

It is impossible to predict how large an invisible foetal R-wave in an abdominal recording will be. Only afterwards does the integrated foetal peak in the correlation function give an indication about the original foetal signal power and the original SNR. It is sometimes important to use the reference signal since one can then decide, if any foetal signal has been present in the abdominal lead. Thus it can be determined in an early stage of the computing process whether a growing maximum in the ACF is a foetal peak or not. Once again, the signal of Figures 34, 35 and 36 has been taken for illustration.

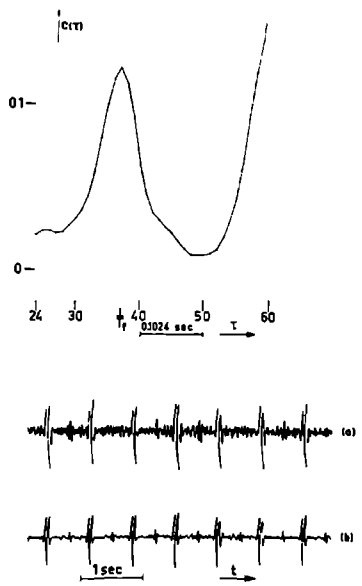


Figure 37. Simulation of the SNR improvement of the detection method by adding noise to the signal a(t). The two lower traces show respectively the filtered signal a(t) with noise added to it (a) and the filtered signal itself (b). The upper curve is a part of the ACF computed from (a). The integration time was 50 sec.

Gaussian noise has been added to the original signal to simulate the presence of much noise in the abdominal signal or to simulate small foetal R-waves. When taking the integration time for the correlation function constant, the results of Figures 37 and 38 are obtained.

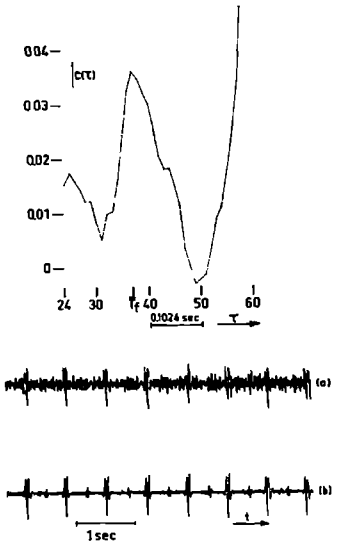


Figure 38. Same legends as Figure 37. Note the increased noise amplitude and larger variance in the ACF.

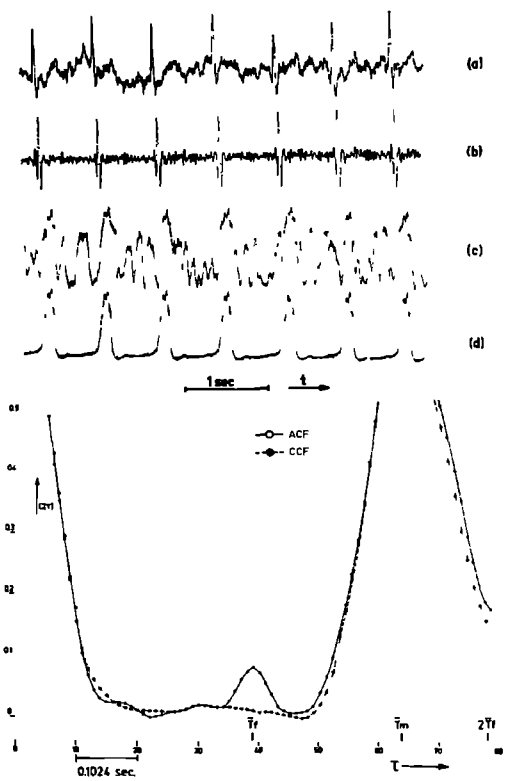


Figure 39. ACF and CCF of an abdominal signal with invisible foetal R-waves.
(a) the abdominal signal a(t).
(b) a(t) after filtering.
(c) the filtered and clipped signal after envelope detection.
(d) the artificial signal s(t).
The difference between ACF and CCF indicates the presence of f(t) in a(t), even for $\tau = 2\ T_f$. The integration time was 17 minutes.

In Figure 39 an illustration is given of the method when the foetal complexes are totally invisible (also after long duration recording)

It therefore appears that it is, in principle, possible to detect weak foetal ECG's from abdominal leads by computing the autocorrelation function of the rectified signals.

For visible FECG's the method never fails Also when (much) noise is added to the abdominal signal (with visible foetal peaks), the presence of a foetal complex in the abdominal recording could always be demonstrated, after some integration time.

So, when the abdominal FECG is masked by muscle disturbance the FECG and, at the same time, the mean heart rate can, in principle, still be traced. When no R-waves could be seen at all in the abdominal ECG, this method proved to be useful too, of course within the limits stated above.

## References


1 Middleton, D, "Introduction to statistical communication theory", McGraw Hill, New York, 1960, ch 18

2 Favret, A G and A F Caputo "Evaluation of auto-correlation techniques for detection of the foetal electrocardiogram", IEEE Trans on Bio Med Engng, BME 13, no 1, 1966, p p 37—43

3 Blackman, R B and J W Tukey, "The measurement of power spectra", Dover publications, New York, 1958

4 Van Vleck, J H and D Middleton, "The spectrum of clipped noise", Proc IEEE, vol 54, 1966, p p 2—19

5 Veltman, B P Th and H Kwakernaak, "Theorie und Technik der Polaritats Korrelation fur niederfrequente Signale", Regelungstechnik, vol 9, 1961, p p 357—364

6 Van Bemmel, J H, "Calculation and Measurement of correlation functions with the aid of auxiliary signals", Res Report, Dept of Applied Physics, Techn Univ Delft, 1963

7 Veltman, B P Th, "Quantisation, sampling and frequency dispersion with correlation measurements", Rept 65—2, Dept of Applied Physics, Techn Univ Delft, 1965

8 Peek, H, "The measurement of correlation functions, using shift independent function", Thesis, Techn University, Eindhoven, 1967

9 Price, R, "A useful theorem for nonlinear devices having Gaussian inputs", IRE Trans on Inform Theory, IT 4, 1958, p p 69—72

10 Van den Bos, A, "Relay- and polarity coincidence correlation of Gaussian signals that have passed a zero memory square or fourth law device", Res Rept, Dept of Applied Physics, Techn University Delft, 1965

11 Bendat, J S, "Principles and Applications of random noise theory", Wiley, New York, 1958, ch 7.

12. Van Bemmel, J. H. and L. A. M. Peeters, "Detection of foetal R-waves by correlation techniques", Proceedings 7th conference on Bio-Medical Engineering of the IFMEBE, Stockholm 1967.

13. Van Bemmel, J. H., "Detection of weak foetal electrocardiograms by autocorrelation and crosscorrelation of envelopes", IEEE Trans. on Bio-Med. Engng., BME 15, no. 1, 1968, p.p. 17—23.

# CHAPTER VII

# SOME CLINICAL AND PHYSIOLOGICAL ASPECTS OF THE PROCESSING METHODS

It is the aim of this study to determine the analytical basis for the relationship between certain measured physiological parameters and the clinical conditions of foetuses. It is not the aim to discuss in detail the clinical and physiological aspects of the methods described in other chapters. This has already been done by others and it is hoped that the material as proposed here will be a further stimulation for future medical and physiological investigations into the condition of the unborn child and the functioning of its heart. A quantitative account has been presented here on which to base an investigation of the correlation between the foetal [1] and perinatal condition of the child and the results of the information processing.

Some clinical aspects will be mentioned very briefly to show some representative examples of the results of the processing methods.

## 7.1 The on-line instantaneous heart rate

Bradycardia and tachycardia as well as irregular heart rates are during birth thought to be mainly caused by nervous (vagal and sympathical) influence on the heart muscle resulting in a duration of the foetal RR-interval that changes as a function of time [2]. It appears to be important to represent continuously the instantaneous heart rate (cardiotachogram) by computation of the reciprocal of the foetal RR-intervals, since the foetal heart rate may alter very suddenly, e.g. during contraction of the uterine muscle. This alteration describes some function of the underlying processes, which control the rate as for example baroceptor activity [3]. It is thus important to measure each interbeat interval separately so that rapidly varying information is not destroyed.

Foetal distress [4] can be accompanied by abnormal patterns in the foetal cardiotachogram, although foetal distress is an entity which is very difficult to define because of the inaccessible nature of the foetus itself. It has been shown that such distress might be caused by compression of the umbilical cord [5], by a high intra-uterine tension, by alterations in the exchange of oxygen and carbon-dioxyde between mother and foetus, resulting in a lowering pH and changing blood gas values [6], [7].

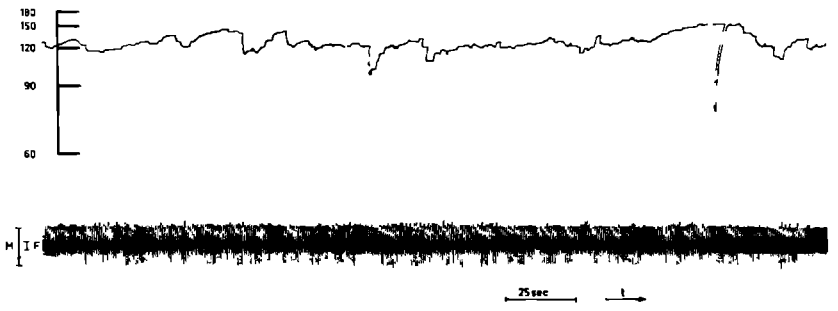


Figure 40. Part of a foetal cardiotachogram, computed from abdominal FECG during birth. The filtered abdominal FECG is shown in the lower trace.

Figure 40 shows an apparently normal cardiotachogram, recorded with abdominal electrodes during birth. Note that foetal heart rate can be traced instantaneously, although many foetal R-waves are masked by maternal QRS-complexes.

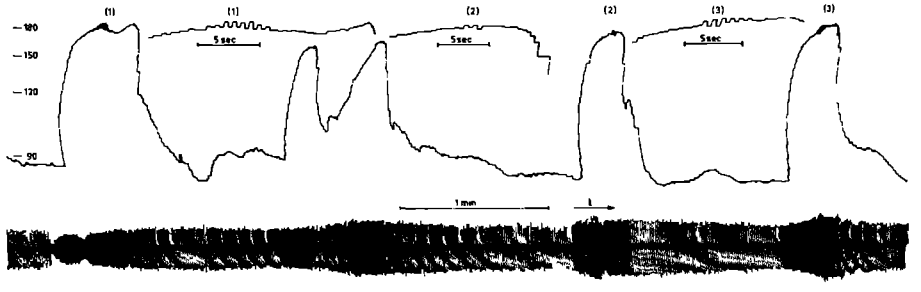


Figure 41. Part of an abnormal foetal cardiotachogram computed from FECG recorded with scalp electrode. Note the reducing basic heart rate and the tachycardial patterns. On the top of these patterns are seen irregularities, shown enlarged in the same Figure. The filtered FECG is shown in the lower trace.

Trends in foetal cardiotachograms may give an indication of developing foetal distress. Figure 41 gives a part of a record in which the patterns of bradycardia during contractions were gradually changing into patterns of tachycardia (shown in the Figure), whereas the basic heart rhythm was continuously reducing. At the top of some of these tachycardial bursts some irregularities are superimposed on the basic heart rate, giving an indication of an instability in the nervous control of the foetal heart (inset). It can further be noted that

the heart rate became more uncontrolled i.e. more stable between contractions than before. An example of extrasystoles superimposed on an apparently normal basic rhythm during delivery is illustrated in Figure 42. The methods described in chapter IV (the computation of a reliable RR-interval by comparison of sequential foetal RR-intervals) would now certainly not result in the heart rate curve as shown in this Figure, so it was necessary to switch off the memory function of the instrument (the lock-in property). Figure 43 shows a part of a foetal cardiotachogram during uterine contractions in which a regular heart rate can be seen instead of bradycardia.

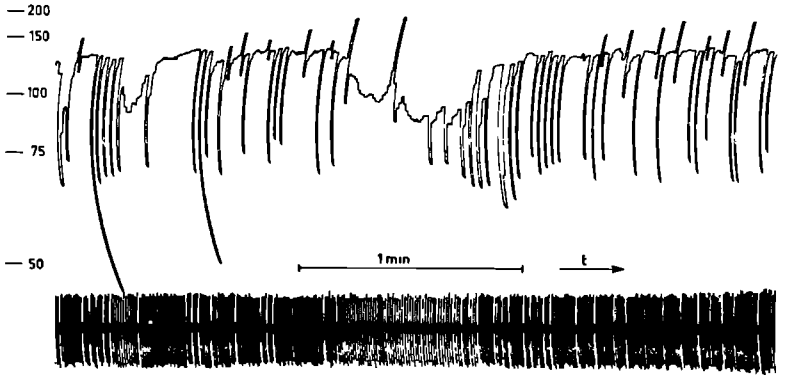


Figure 42. Part of a normal basic foetal cardiotachogram, computed from a scalp lead FECG. Superimposed on the bradycardial patterns are extra-systolic intervals. The comparative method was no longer usable in this case because of the large fluctuations from beat to beat (see also Figure 51). The lower trace is the filtered FECG.

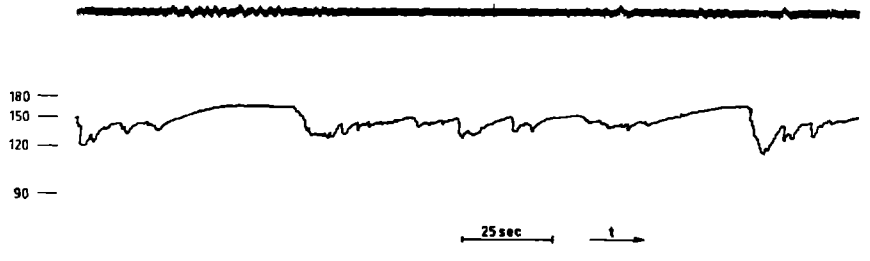


Figure 43. Part of a foetal cardiotachogram from scalp leads. Instead of bradycardia during uterine contractions the heart rate becomes regular. The upper trace shows the unfiltered FECG. During contractions much more low frequency disturbance is present in the original signal.

During pregnancy it is quite easy to follow the instantaneous foetal heart rate with abdominal leads (as shown in Figure 40), when the foetal QRS-complex is clearly visible since then no uterine contractions, muscle disturbances or maternal movements hamper the recording of the foetal ECG, so that the SNR is not influenced by external factors. During some stages of the pregnancy it is thus possible to investigate foetal responses for instance to drugs given to the mother. The condition of the foetus can be followed by this method in cases of complicated pregnancies too.

## 7.2 The foetal PQRST-complex

No matter what is the stage of pregnancy, whenever the foetal SNR is sufficiently high (see chapter V), it is wholly feasible to compute the shape of the foetal PQRST-complex from abdominal recordings. This will, however, not always reveal useful information for the obstetrician since for instance some congenital malformations of the heart, possibly correlated with the shape of the FECG complex, have mostly no consequences for obstetrical practice. It might however be worthwile that the obstetrician knows in advance that some complications with the child could occur during birth or that an abnormal foetal heart rate might be originating from such abnormalities.

At birth sometimes a change can be seen in the shape of the FECG complex; during foetal distress such a change may be caused by pathological alterations in the de- and repolarization of the cardiac muscle, for instance caused by a diminished oxygen flow in the placental circulation. This can result in alterations in the ST-T complex and a prolonged RR-interval. Figure 3 shows an example

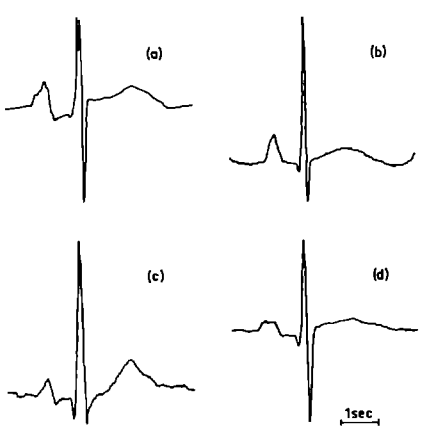


Figure 44. (a) — (d) are examples of FECG complexes computed from scalp lead recordings of different patients. All results are the sum of 100 original complexes.

of the latter. Figure 44 gives some examples of FECG complexes computed from scalp lead recordings.

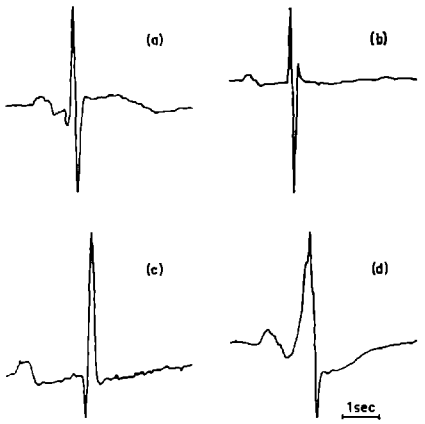


Figure 45. (a) — (d) are examples of FECG complexes computed from abdominal recordings of different patients. The results are computed from 100 complexes.
Note the different shapes that might be obtained.

During pregnancy many possible wave shapes can be discerned for different patients, dependent on the position of the abdominal electrodes in relation to the foetal heart (see chapter II). The wave-form generated in any lead can be thought to be a projection of a spatial foetal vectorcardiogram on the plane that is defined by the chosen electrode positions. Although amplitude relationships are not valid in these leads, unless some a priori information is acquired about the position of the child, the conduction time information present in the PQRST wave form remains of value and largely independent of the electrode positions.

The durations of the atrial and ventricle complexes as well as the conduction times between sino-auricular and atrio-ventricular nodes increase with the duration of the pregnancy. This results in small P-waves and short PR-intervals early in pregnancy and often notched QRS-complexes at later stages, the latter probably caused by unequal conduction times of the excitation pulse in the branches of the bundle of His-Tawara.

The repolarization wave, which is the main source of low frequency components as compared with the other parts of the ECG complex, is nearly always filtered out largely by the tissues between the foetal heart and the recording electrodes (see chapter II). Only sometimes can a clear T-wave be discerned. Figure 45 shows four examples of abdominal FECG complexes recorded during pregnancy in which some of the peculiarities mentioned above are visible.

Using intra-uterine electrodes [8] (brought into the uterus after a transabdominal puncture for purpose of intra-uterine pressure recording) the SNR is much better.


Figure 46. Series of averaged FECG complexes computed from intra-uterine leads. The time lapse between the complexes was about one hour.

Figure 46 shows a series FECG complexes computed from these trans-abdominal leads. The foetus changed its position below the electrodes during the recording of this FECG so that the projection of the foetal VCG onto the lead plane altered as a function of time.

Congenital malformations of the heart having consequences for the electric field potential generated by the heart can be detected by this procedure (see Figure 45c and d) and its development can be followed during pregnancy, when the SNR has become large enough to apply the processing method.

## 7.3 The mean RR-interval

When the additive noise component is too strongly present in the signal, it is no longer possible to compute the foetal heart rate instantaneously. A reliable result cannot then be acquired, even when sequential intervals are compared with each other. This is the case when $^{2}\log \beta$ (see Figure 19) is large. In chapter VI several results of auto- and crosscorrelation functions have been shown, by which it became clear that even in a noisy environment it is still possible to trace

the mean foetal heart rate. With a continuous display of the running correlation function of the preprocessed abdominal signal and integration over short time (by RC-circuitry) one can follow continuously the change in the mean foetal heart rate.

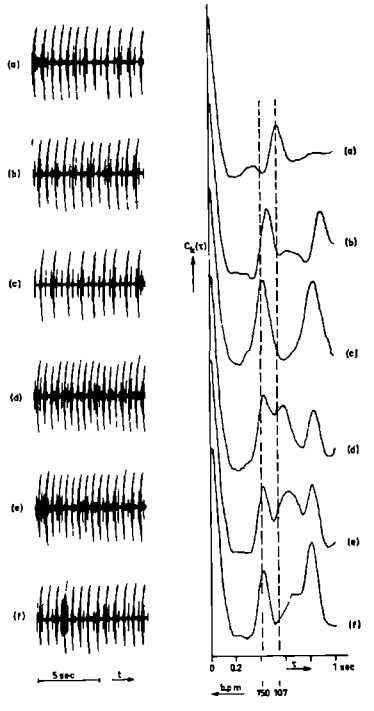

Figure 47. A series of autocorrelation functions, subsequently computed from 20 second parts of an abdominal FECG. Parts of the filtered original signal are also shown.

Figure 47 shows a series of autocorrelation functions after envelope detection of the rectified and filtered abdominal FECG. The peak for $\tau \approx \bar{T}_f$ (the foetal RR-interval) changes gradually as a function of real time. The time constant for each integrator was 20 seconds, whereas the functions have been plotted every 30 seconds.

It is quite possible to follow the mean foetal heart rate in those cases where it is desired to detect any trend in the mean RR-interval. This may be important in seriously complicated pregnancies or as a help in the investigations of the long term influence of drugs.

## 7.4 Irregularities in foetal RR-intervals

Many processing methods can be devised to obtain an insight in the instability of the foetal heart rate. In one of the preceding sections (7.1) an on-line method was described by which the foetal RR-intervals were represented as a function of time (the foetal cardiotachogram) and in chapter III two interval distributions (histograms) were given for signal parts recorded during birth. Whereas the first method gives a signal as a function of real time (the cardiotachogram), all time information is lost with the second representation. Even the variance around the mean of the histogram gives no measure of the short term irregularity of the heart rate, since a broad histogram might also be caused by slowly changing RR-intervals. The advantage of second order interval distributions (also called scatter diagrams) for N sequential intervals lies in the fact that the interval information is condensed into a single picture in which still some relationship with the time domain is kept.

Serial correlation coefficients can also easily be calculated for such distributions to produce a quantitative measure of the irregularity of the heart (see chapter VIII for definition and practical realization).

The ordering (correlation) or randomness can also be tested by comparison of the original second order interval distribution with a second order distribution of the N shuffled intervals. This shuffling can be carried out for instance by using random number tables, but for small N it is desired that all present intervals are utilized but only once, in order to compare the obtained result with the original unshuffled data. To this end a shuffling procedure has been developed for N intervals, with N a power of two.

Although such second order interval distributions offer advantages in information compression one has, taking many intervals during a long observation time, still the disadvantage, that the phenomenon of short term irregularity is masked when the mean RR-interval changes gradually. This causes the serial correlation coefficients to say nearly nothing about short term irregularities. For that reason all intervals are first normalized by division by the preceding interval, so that instead of the interval itself its percentage fluctuation is used (see chapter VIII for definition).

One can compute then another histogram: that of the percent fluctuations. The latter histogram can then again be compared with a histogram of intervals that has been computed after shuffling, to obtain an impression of the kind of instability of the foetal heart rate.

The variance of these interval distributions gives a quantitative measure for the irregularity of the heart. Of course this variance is related to the variance of the earlier described second order intervals, which is indicated in chapter VIII.

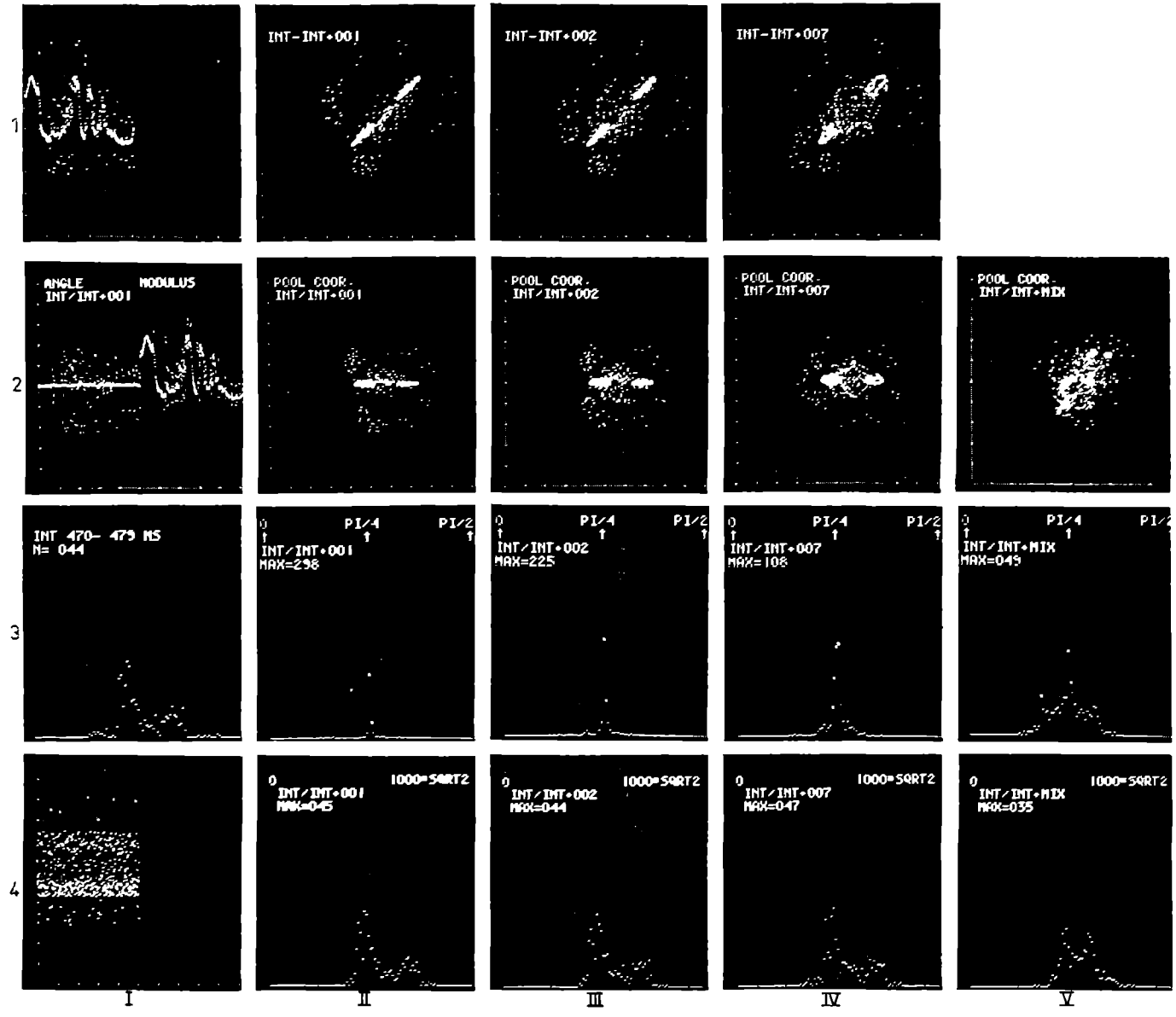
INT-INT•001
INT-INT•002
INT-INT•007
ANGLE MODULUS
INT/INT•001
POOL COOR.
INT/INT•001
POOL COOR.
INT/INT•002
POOL COOR.
INT/INT•007
POOL COOR.
INT/INT•MIX
INT 470- 479 MS
N= 044
0 PI/4 PI/2
INT/INT•001
MAX=298
0 PI/4 PI/2
INT/INT•002
MAX=225
0 PI/4 PI/2
INT/INT•007
MAX=108
0 PI/4 PI/2
INT/INT•MIX
MAX=049
0 1000=SQRT2
INT/INT•001
MAX=045
0 1000=SQRT2
INT/INT•002
MAX=044
0 1000=SQRT2
INT/INT•007
MAX=047
0 1000=SQRT2
INT/INT•MIX
MAX=035
1
2
3
4
I
II
III
IV
V

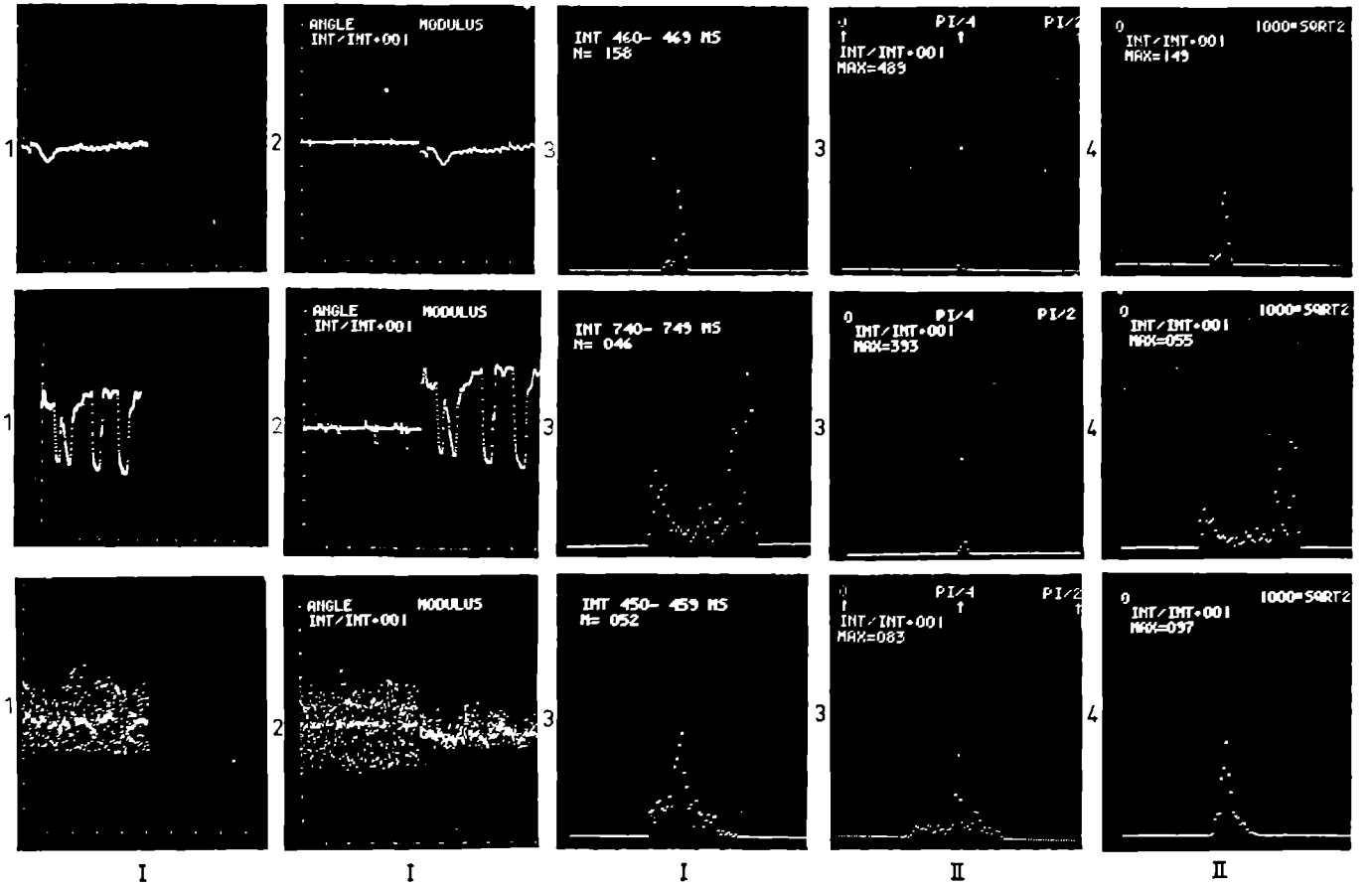
1
2
ANGLE
MODULUS
INT/INT*001
3
INT 460- 469 MS
N= 158
3
0
PI/4
PI/
INT/INT*001
MAX=489
4
0
1000*SQRT2
INT/INT*001
MAX=149
1
2
ANGLE
MODULUS
INT/INT*001
3
INT 740- 749 MS
N= 046
3
0
PI/4
PI/2
INT/INT*001
MAX=393
4
0
1000*SQRT2
INT/INT*001
MAX=055
1
2
ANGLE
MODULUS
INT/INT*001
3
INT 450- 459 MS
N= 052
3
0
PI/4
PI/2
INT/INT*001
MAX=083
4
0
1000*SQRT2
INT/INT*001
MAX=097
I
I
I
II
II

Figure 48. (See page 91). Some representations of a series of 512 sequential foetal RR-intervals by compression of the information into one picture. The RR-intervals have been measured from a foetal ECG, recorded during delivery with a scalp electrode.

1.I. The lengths of the 512 intervals $T_i$ (ordinate) as a function of number. Note the bradycardial patterns with irregularities.

1.II. Second order interval distribution for sequential intervals $T_i$ and $T_{i+1}$. All scales have a length of 1.0 second. The pattern can easily be fitted with a regression line through the origin. This is possible because of the gradual changes (the bradycardia) in the heart rate. For that reason a correlation coefficient gives no information about the short term irregularity. The distance between the brightest dots along axes is 100 msec.

1.III. Same as 1.II. for $T_i$ and $T_{i+2}$.

1.IV. Same as 1.II. for $T_i$ and $T_{i+7}$.

1.V. Same as 1.II. for shuffled intervals.

2.I. The angle $\varphi_i = \text{arctg}(T_{i+1}/T_i)$ and the modulus $r_i^2 = (T_i^2 + T_{i+1}^2)$ as a function of number. Note the rather stable $\varphi_i$-signal and the resemblance between the modulus $r_i$ and $T_i$ in 1.I.

2.II. Transformation of 1.II. from Cartesian coordinates $T_i$ and $T_{i+1}$ to polar coordinates $\varphi_i$ (ordinate) and $r_i$ (abscissa).

2.III—V. Same as 2.II. for 1.III—V.

3.I. The interval histogram of 1.I. or the projection of 1.II.—1.V. on the $T_i$ — or $T_{i+k}$ — axes. The maximum N is reached for $T_i = 0.475$ sec and indicated in the Figure.

3.II—V. The projections of 2.II—V. on the $\varphi$-axis. The maxima are reached for $\varphi = \pi/4$ and indicated in the Figures. Note the narrow histogram 3.II., a measure for the short term irregularity in the heart rate although 3.I is very broad.

4.I. The lengths of the 512 RR-intervals as a function of number after shuffling.

4.II—V. The projections of 2.II—2.V on the r-axis. The lengths of the abscissae are $\sqrt{2}$ second and the maxima of the histograms are indicated in the Figures. Note the resemblance between 3.I. and 4.II.

Figure 49. (See first row on page 92). Same notation as Figure 48.
Severe bradycardia during labour. Note the stable $\varphi_i$-signal in 2.I. and the narrow histogram 3.II.

Figure 50. (See second row on page 92). Same notation as Figure 48.
Normal heart rate with slight bradycardia during labour. There are nearly no short term irregularities. This can be seen from the $\varphi_i$-signal in 2.I. and the very narrow histogram in 3.II.

Figure 51. (See third row on page 92). Same notation as Figure 48.
Bradycardia with extrasystoles during labour.
From 2.I. it is remarkable that the $\varphi_i$-signal is very irregular, whereas the $r_i$-signal is different from 1.I. Note the broad $\varphi_i$ histogram in 3.II.

The Figures 48—51 show histograms and distributions for four different kinds of heart irregularity, recorded during delivery, of which the cardiotachograms are shown in the same Figures. Figure 48 shows also the second order interval distributions for these intervals as well as for the shuffled distributions and shows finally the histograms, computed after normalization for subsequent and shuffled intervals.

As stated in the Introduction (chapter I) a physiological process is often very complex so that much information is needed for its understanding and for the interpretation of the signals that flow from it to the outside world. This offers difficulties in practice since far from all desirable information can be acquired.

Consequently, it is difficult to acquire much information about the condition of the unborn child, and that only with great effort. The FECG is one of the few signals that can be recorded continuously during pregnancy and delivery and this is one of the main reasons that the processing of foetal electrocardiograms is valuable in obtaining insight into the condition of the foetus. But it must be stressed that this is only true when the results are carefully examined and investigations undertaken to correlate them with other available information about the foetus. For this purpose various procedures are very well suited such as: biochemical evaluation before and during delivery (e.g. Saling's method), intra uterine pressure recordings, foetal phonocardiograms and ultrasonic techniques. Of course it is very valuable to follow the neonatal condition of the child and to relate it to the condition in utero [6-10].

Taking into account the difficulties of information acquisition and interpretation in the intensive care of adults one can readily imagine that this holds even more for the distressed foetus. This is the reason why especially from both medical — obstetrical and cardiological — and physiological sides much research is still needed for a better understanding of the few signals that can be recorded from the unborn child during pregnancy and delivery.

## References

1. Peeters, L. A. M., "The foetal Electrocardiogram", Thesis, Nijmegen 1968.
2. Caldeyro-Barcia, R., C. Mendez-Bauer, J. J. Poseiro, L. A. Escarcena, S. V. Pose, J. Bieniarz, I. Arnt, L. Gulin and O. Althabe, "Control of human fetal heart rate during labor — The heart and circulation in the newborn and infant", New York, 1966.
3. "Baroreceptors and hypertension", Proceedings of an International Symposium, Ohio, 1965, P. Kezdi, editor, Pergamon Press 1967.
4. Hon, E. H., "The fetal heart rate patterns preceding death in utero", Am. J. Obstet. and Gynec, vol. 78, 1959, p. 47.

5. Lee, S. T. and E. H. Hon, "Fetal hemodynamic response to umbilical cord compression", Obstet. and Gynec., vol. 22, 1963, p. 553.
6. Dawes, G. S., "Foetal and neonatal physiology", Yearbook medic. publ. Inc., 1968.
7. Quilligan, E. J. and E. B. Katigbak, "Correlation of fetal heart rate and acid-base balance at birth", Obstet. and Gynec., vol. 25, 1968, p. 371.
8. Vasicka, A., H. T. Hutchinson, W. J. Rylander and C. Murray, "Simultaneous recording of uterine contractility and fetal heart rate using an intra-amniotic platinum electrode", Obstet. and Gynec., vol. 22, 1963, p. 271.
9. Prechtl, H. and D. Beintema, "The neurological examination of the full-term newborn infant", W. Heinemann Medical Books Ltd, London, 1964.
10. Assali, N. S., G. A. Bekey and L. W. Morrison, "Biology of gestation", vol. II, Acad. Press, New York, 1968, chapter II.

# CHAPTER VIII

# THE PROCESSING OF THE FECG IN PRACTICE

In this chapter the practical set-up for the processing of the foetal ECG by analog, hybrid and digital equipment will be outlined briefly.

While for the detection of the instantaneous heart rate it is demanded that the results are available in real-time, for computation of the undistorted foetal ECG complex during pregnancy there is no need to present the results of the processing on-line. This is the reason that for the presentation of the foetal RR-interval a method has been sought, realized in an instrument with a high degree of automation, which utilizes only a small part of the signal and accepts all kinds of abdominal-, scalp- and intra-uterine foetal waveforms as well as phonocardiograms or even preprocessed ultrasonic doppler signals. As far as the off-line computation of the noise-free FECG waveform is concerned, it is possible to optimize for every separate problem the detection level and the filtering method, as well as the choice of signal parts to be processed etc.; but in this situation the level of automation is lower than in the first case.

Some further detailed information will now be given about the block diagrams and the processing schemes to achieve the methods explained analytically in chapters IV to VII, to provide an impression of the amount of computation to be done and the equipment needed. It is stressed that it is very useful to pre-process the physiological signals as far as can be done by hybrid or special purpose computers so that the programming of and computations in the general purpose digital computer itself can be limited. The use of the digital computer is of course very dependent on the kind of machine available.

## 8.1 The instantaneous foetal heart rate

The flow diagram for the on-line processing of foetal ECG's to obtain the instantaneous RR-interval has been given in Figure 16. A block diagram of the instrument that carries out the computations will now be discussed; see Figure 52.

The instrument is constructed with logic elements such as flip-flops, gates and so on for its digital part which is completely controlled by clock pulses, so that dissimilar internal delays give no difficulties [1].

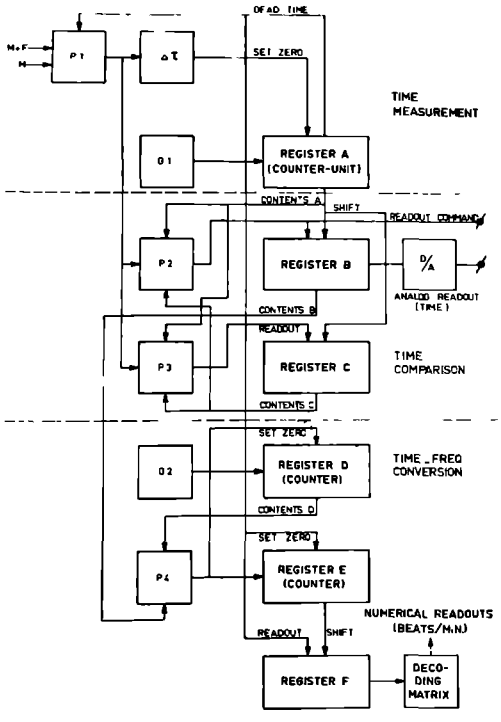


Figure 52. Block diagram for the extraction of correct foetal RR-intervals from a noisy abdominal pulse sequence from $P_1$ (see Figure 15).
The diagram is a practical realization of the flow diagram in Figure 16.

The analog signals are converted to a single pulse series in a hybrid part of the equipment, which consists of filters, automatic gain control circuitry, comparators for threshold detection, pulse shapers and delaying monostable multivibrators (see Figure 15).

The digital part operates as follows.

*Register A* is a nine bit counter unit which measures a foetal RR-interval $T_F$. The register A continuously counts the pulses from a generator G1 (320 Hz) and is reset every time that a pulse arises from $P_1$ (see chapter IV and Figure 15). It also sends a blocking signal to $P_1$ for 0.200 second after resetting. Besides the main counter, A contains two parallel counters $A^+$ and $A^-$, to provide the appropriate time window for the interval $T_F$. The contents of the interval preceding $T_F$, have been stored in register C: when $A^+$ (a counter that runs a fraction of $\Delta A/A$ faster than counter A) equals the contents of register C, a pulse is given to open gate $P_2$. When the contents of $A^-$ (which runs the same fraction slower) equal that of C and when in the mean time no pulse came from $P_1$, the gate $P_2$ is closed. The gate $P_2$ is also closed at the instant, during the time between the

setting and resetting of $P_2$ (the window), when a pulse arises from $P_1$. The basic frequencies for A ' and A are respectively $(A + \Delta A)'A$ and $(A-\Delta A)/A$ times 320 Hz. A normal value for $\Delta A$ is A/10, which will be used in explaining the following aspect of the operation.

*Register B.* Register B takes over the state of A via $P_2$, just before A will be reset, provided that (see chapter IV):

$$0.9\, T_{F_i} \leqq T_{F_{i+1}} < 1.1\, T_{F_i} \tag{8.1}$$

The contents of B are available as a voltage via an Analog to Digital converter or as a direct output for punching or printing.

*Register C.* This has the same function as B, without the condition (8.1). The requirement for the shift of A into C is now however:

$$0.55\, T_{F_i} \leqq T_{F_{i+1}} < 1.8\, T_{F_i} \tag{8.2}$$

the relation being determined by $P_3$, which follows very large deviations from a basic instantaneous foetal heart rate.

When 8 times a pulse has arisen from $P_1$ and no shift from A into C has taken place, the 9th interval is always carried into memory C. Indeed, during these 8 pulse intervals the instantaneous foetal heart rate might have changed so considerably, that the unequality (8.2) would never again be applicable, so that all measurements would stop once and for all. Such a safety procedure is also necessary for the start up period of the instrument. A 3 bit counter takes care of it.

*Register D* is another 9-bit counter that continuously counts the pulses from generator G2 (96 kHz). Its function is to compute the reciprocal value of the time, present in B. As soon as the contents of D are the same as those of B, D will be reset to zero (via $P_4$). In fact $P_4$ repeates very fast the foetal pulse rate and E simulates the measurement carried out by register A, and offers some kind of time compression.

*Register E.* This register is a decimal counter which counts the reset commands of D from $P_4$ during the dead time (0.200 second) after a pulse from $P_1$. It can be proved simply, that after this counting, the foetal heart rate is computed in E in beats per minute, from the instantaneously measured RR-interval. The contents of B can be written after measurement of $T_F$: $B = 320\, T_F$, so that during an interval of 0.200 second in E can be measured:

$$\frac{(\text{dead time}) \times (\text{freq. of } G_2)}{(\text{freq. of } G_1) \times T_F} = \frac{0.200 \times 96.000}{320 \times T_F} = \frac{60}{T_F} \text{ pulses} \tag{8.3}$$

This last number equals exactly the foetal heart rate per beat in beats per minute, computed from the reciprocal value of $T_F$.

*Register F* takes over the state of E after counting. By means of a decoding matrix and indicator tubes the contents of F are represented as a number, the foetal heart rate.

When for $G_2$ a frequency of 960 kHz is chosen, the register F can even be omitted, since computation of $60/T_F$ is now carried out in 0.02 second, which is amply sufficient for reading the status of the indicator tubes from register E itself in the rest of the free time during the following interval $T_F$.

*Practical use*

The use of the instrument is very simple, owing to the nearly complete automation, since only for abdominal foetal ECG's is a choice involved of the detection level $V_F$ (see chapter IV). Foetal phonocardiograms can also be processed by the instrument, although the interval accuracy of a measurement with heart sounds is much lower than with R-waves. This is caused by the fact that the envelope of the phonocardiogram has mostly very low frequency contents.

## 8.2 Foetal ECG waveforms

A processing scheme for the computation of foetal ECG waveforms is represented in Figure 53, a practical realization of the general diagram of Figure 25.

The possible locations of foetal R-waves are predicted by the window similar to that treated in chapter IV and 8.1, where it was used for a reliable computation of RR-intervals. The detection of both the foetal and maternal R-waves consists here of four stages: filtering of the signals, level detection, analog gating and zero crossing detection after differentiation (or determination of maxima). In this way the maxima of foetal and maternal ECG-complexes are computed. Since we do not want to detect foetal pulses that coincided with maternal ones, it is decided that a foetal R-wave was present only when it falls outside $\pm$ T/2 from a detected maternal pulse. This time T can be optimized for each signal, and needs not be specifically 110 msec as for the interval computation (see Figure 15).

Since we know the locations of maternal QRS-complexes from the abdominal record or a separate maternal signal $m^*(t)$, it is possible to construct the artificial

maternal ECG m(t). To this end an appropriate sampling rate and delay is chosen so that the sum of a number of maternal complexes can be stored in an average response computer (ARC2 in Figure 53).

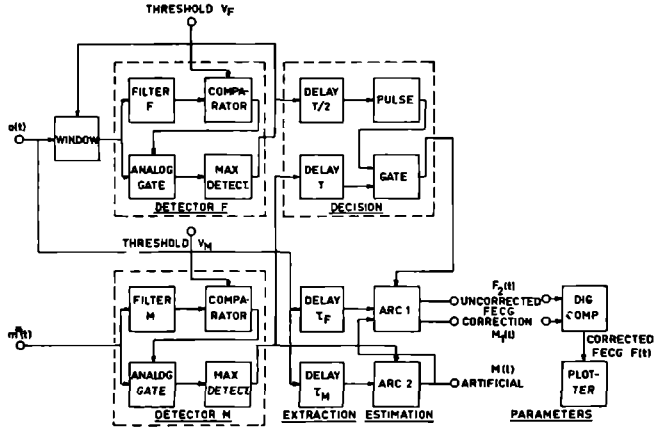


Figure 53. Block diagram for the computation of the FECG wave-form (see for comparison the general detection scheme of Figure 25).

When the ARC2 is triggered next by the same maternal pulse series and the instrument is read out via a Digital to Analog converter, we obtain the artificial ECG of Figure 22. The ARC2 is in fact used as a function generator yielding m(t).

This signal is normally stored temporarily on tape together with the original signal a(t) and subsequently processed in the same ARC2. But in Figure 53 we assume for simplicity that we use two ARC's, as also can be done in practice.

The signal, together with that from ARC2, is fed to ARC1 which is then triggered by the foetal pulse series. At the end of the processing we obtain the uncorrected foetal ECG, $F_2(t)$, and its correction, $M_1(t)$, from the maternal ECG (see (5.13) and (5.18)).

In the same manner we can compute the means of the maternal ECG's, $M_o(t)$ and $M_a(t)$, from the original and the artificial signals (see Figure 24 c,d and f,g).

After this data reduction and preprocessing, the signals are fed to the digital computer, in which the phase- and amplitude correction is performed.

This amplitude correction $\alpha$ is computed from the relation

$$a = \left[ \frac{\sum\limits_{T_i} M_0^2(t_i)}{\sum\limits_{T_i} M_1^2(t_i)} \right]^{\frac{1}{2}} \tag{8.4}$$

Hereafter the phase $\tau_a$ is computed from the minimum of the function

$$\Phi(\tau) = \sum_{T_i} \{M_0(t_i) - aM_1(t_i - \tau)\}^2 \tag{8.5}$$

which is reached for $\tau = \tau_a$.

The final corrected foetal ECG waveshape is then:

$$F(t) = F_2(t) - aF_1(t - \tau_a) \tag{8.6}$$

which is represented in Figure 24e.

## 8.3 Auto- and crosscorrelation after envelope detection

The computation of the ACF and CCF of abdominal FECG's is done according to Figure 54. After filtering the signal a(t) is clipped, rectified and low-pass filtered, so that the envelope is obtained. The cut-off frequency of the envelope filter is at 25 Hz and it has a slope of 18 dB/oct. The artificial signal is constructed by feeding the signal envelope to an ARC after delaying. When a good estimation of one complex of the undistorted maternal signal envelope is obtained, both the output of the ARC and the signal envelope are fed into the correlator. In this instrument the signals are auto- and crosscorrelated. The correlator itself will be briefly outlined in the following (see Figure 55).

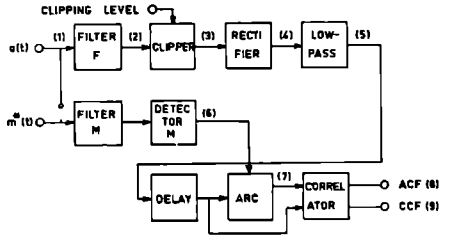


Figure 54 Block diagram for the computation of the autocorrelation function (ACF) and crosscorrelation function (CCF) from abdominal FECG's
The numericals between brackets refer to Figure 32
For detector see Figure 53 and for correlator Figure 55

It is constructed from three basic sections, all completely identical [2]. The signal $x_1$ is fed to unit $S_1$, where it is sampled. In fact the sampler consists of an adder, in which the signal $x_1$ is added to an auxiliary signal $h_1$ or $h_2$, and a hard limiter. The signal sign $\{x_1 + h_1\}$ thus acquired is then delayed in a shift register with units SR. The SR outputs are multiplied with the undelayed signal

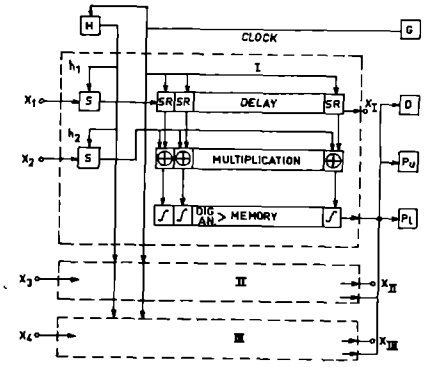


Figure 55. Basic scheme for the correlator described in section 8.3. In S the signal is sampled and H generates the auxiliary signals. D, Pu and Pl refer to CRT-display, punch and plotter respectively.

sign $\{x_2 + h_2\}$ in modulo-2 adders. Finally the product is integrated over a short or a long time.

These integrations are respectively carried out by RC-circuitry with adjustable time constants and by parallel 20 bit counters. The memory can be read out by a scanner and displayed on a CRT screen or be printed, punched or plotted. The sampling rate can be chosen from dividers following a crystal oscillator or be programmed from an external generator. The auxiliary signals are also clocked by the sampling frequency. When only one auxiliary signal is chosen we obtain, instead of the true correlation function, the relay correlation function. An auxiliary signal is generated by dividers and a D/A converter so that we obtain an uniform distribution, whereas the signal itself has an as high as possible frequency content (see Figure 56). It can be proved that for most applications a quantization degree of 16 levels is amply sufficient. The correlator is usable for all kinds of correlation problems because of its general set-up and its application is thus not only restricted to the processing of FECG's.

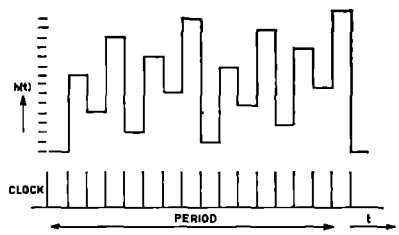


Figure 56. Shape of an auxiliary signal for the correlator with 16 quantization levels. See for the construction of it Figure 57.

## 8.4 Observations of multiple RR-intervals

A series of sequential measurements of foetal RR-intervals can be condensed to some form of interval distribution (histogram) or to a second order distribution for subsequent intervals, to obtain a visible result of the information compression (see Figures 48—51). For the latter distributions normalized serial correlation coefficients can be calculated with (9.11) as

$$\varrho_N(k) = \sum_{i=1}^{N} (T_i - T)\ (T_{i+k} - T) \Big/ \sum_{i=1}^{N} (T_i - T)^2 \qquad (8.7)$$

in which $\varrho_N(k)$ is the $k^{th}$ correlation coefficient for a total of N intervals and where the $i^{th}$ interval lies k—1 intervals apart from the $(i + k)^{th}$ interval. These intervals can be combined in the second order distribution density function mentioned above (T is the mean of all intervals $T_i$). In this way one obtains not only an impression of the stability of the foetal heart rate by the picture of the distribution function but one acquires also a numerical answer, which is correlated with the shape of the distribution function.

After randomizing or reordering of all intervals the histogram is unaltered of course but the second order distribution then generally has a completely different shape and the correlation coefficient is zero. The randomizing is done utilizing a shuffling table, which has been devised for N intervals, with N a power of two, in order that this table can easily be extended, dependent on the number of available RR-intervals. All measured intervals are then only used

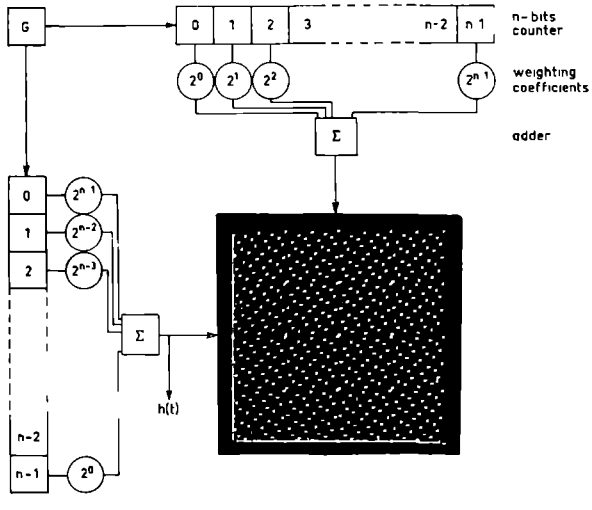


Figure 57. Construction by hardware of the shuffling table for the reordering of $N = 2^n$ RR-intervals.
The auxiliary signal h(t) of Figure 56 for $n = 4$ can be acquired from the side counter.

but once. The table has been constructed by the mixing of two uniform density functions, of which the first one consists of all natural numbers from 1 up to and including $N = 2^n$ and the second one is comparable with the function as shown in Figure 56, but now for N levels instead of 16. The table itself is shown in Figure 57 for $N = 512$, where it is thought to be generated by hardware. Naturally, in practice it is done by a software program. To overcome the effect of a gradually changing heart rate on the second order distribution function, a further procedure is developed to obtain insight in the short term irregularity of the heart beat. Instead of using the intervals $T_i$ the percentage fluctuation $\vartheta_i$ of this interval is defined as

$$\vartheta_i = T_i/T_{i-1} \tag{8.8}$$

so that all intervals $T_i$ are normalized according to the immediately preceding interval. $\vartheta_i$ can also be expressed in terms of the second order distribution, for which $\varphi_i$ is the angle between the abscissa and the point $(T_{i-1}, T_i)$, so that

$$\vartheta_i = \mathrm{tg}(\varphi_i) \tag{8.9}$$

In fact the second order distribution with cartesian coordinates (x, y) is transformed to polar coordinates $(\varphi, r)$ with $r_i$ the length of the vector $(x_i, y_i)$. Just as the interval histogram is a projection of the second order distribution on the x- or y-axis, the fluctuations $\varphi_i$ and the vector length $r_i$ can also be plotted in histograms, a projection of the $(\varphi, r)$ distribution on the $\varphi$-axis and the r-axis.

This has the advantage that in the $\varphi$-histogram now no effect is seen due to a gradual slope in the cardiotachogram. The abscissa of the histogram of fluctuations is then expressed in degrees from 0 to $\pi/2$ because of relation (8.9) with a maximum at $\pi/4$.

The formula (8.8) can also be applied to the shuffled series of intervals $T_i$ which gives an impression of the total variation in the present RR-intervals $T_i$. Several results of the shuffling and normalization were shown in the Figures 48—51. The time window $P_2$ from chapter IV is now comparable with a window in the histograms for fluctuations between arctg 0.9 and arctg. 1.1.

## References

1. Bartee, T. C., L. L. Irwin and S. R. Reed, "Theory and design of digital machines", McGraw Hill, New York, 1962, chapters 7 and 8.

2. Van Bemmel, J. H. and S. J. Hengeveld, "Cobra, an on-line correlator", Int. Report, Institute of Medical Physics TNO, Utrecht, 1966.

# CHAPTER IX

# APPENDIX

## Basic theory of statistical processing methods

1. *Convolution*

The convolution between two time series x(t) and h(t) is defined as [1]:

$$y(t) = \lim_{T\to\infty} \int_{-T}^{T} x(\tau)\, h(t-\tau) d\tau = x(t) * h(t) \tag{9.1}$$

This is the basic formula, that can be applied, to describe sampling, filtering, correlation, coherent averaging, interpolation, prediction etcetera. It can be interpreted as the effect of a linear operator H (the Fourier transform of h) on the signal X (the transform of x).

When the signals are processed digitally, the formula has to be rewritten for discrete signals:

$$y_i = \lim_{N\to\infty} \Delta t \sum_{k=-N}^{N} x_k\, h_{i-k} = x_i * h_i \tag{9.2}$$

The sampled signal $x_i$ can be computed from the band limited signal x(t) by convolution of x(t) with a series of Dirac pulses:

$$x_i = \lim_{T\to\infty} \int_{-T}^{T} x(\tau)\ \ \delta(t - i\Delta\tau)\ d\tau = x(t) * \delta_i \tag{9.3}$$

where $\delta(t) = 1$ for $t = 0$ and elsewhere zero and $\Delta\tau$ is the Nyquist sampling interval.

*Smoothing*

In several circumstances (computation of the derivate, power spectrum estimation from the correlation function) the signals must be smoothed, either before digital processing or in the computer itself. The reasons for smoothing are the presence of unwanted high frequencies or the effect of a finite signal length which leads to uncertainties in spectral estimates.

The smoothing can be thought either as a multiplication in the frequency domain or as a convolution in the time domain.

It is only a matter of elegance and computing time, in what domain the filtering is performed. The smoothing can be carried out by specially developed or generally accepted smoothing filters or "windows" [1]. The widely used "Hamming" window is written for continuous signals (in the time domain) as:

$$h(t) = 0.54 + 0.46 \cos \frac{\pi t}{T}, \quad |t| \leqq T \qquad (9.4)$$
$$= 0 \qquad |t| > T$$

with T the length of the signal part. For discrete signals with convolution in the frequency domain the window is:

$$H_i = 0.23,\ 0.54,\ 0.23 \qquad i = -1,0,+1 \qquad (9.5)$$

## 2. *Correlation, covariance*

The crosscorrelation function (CCF) between two signals x(t) and y(t) is written for continuous signals [2] as:

$$C_{xy}(\tau) = \lim_{T\to\infty} \frac{1}{2T} \int_{-T}^{T} x(t) \,.\, y(t-\tau)dt = x(t) \,.\, y(t-\tau) \qquad (9.6)$$

For ergodic signals this expression can also be written in terms of the second order probability density function for the ensemble elements $x_t$ and $y_{t-\tau}$ [2]:

$$C_{xy}(\tau) = \int_{-\infty}^{\infty}\int x_t \,.\, y_{t-\tau} \,.\, f(x_t, y_{t-\tau})\ dx_t dy_{t-\tau} \qquad (9.7)$$

with f(x, y) the joint distribution function of x and y. For some cases (9.6) can be simplified to [3]:

$$C_{xy}(\tau)_{pol} = \text{sign}\{x(t)\}\ \text{sign}\{y(t-\tau)\} \qquad (9.8)$$

with $\text{sign}\{x(t)\} = \begin{cases} +1 & \text{for } x(t) > 0 \\ -1 & \text{for } x(t) \leqq 0 \end{cases}$

$C_{xy}(\tau)_{pol}$ is called the polarity coincidence correlation function (PCCF).

The relation between $C_{xy}(\tau)$ and $C_{xy}(\tau)_{pol}$ is for ergodic signals with a joint Gaussian amplitude density distribution and zero means (see [3] or [4]).

$$f(x,y) = \frac{1}{2\pi\sigma_x\sigma_y(1-\varrho^2)^{\frac{1}{2}}} \exp\left[-\frac{1}{2(1-\varrho^2)}\left(\frac{x^2}{\sigma_x^2} - 2\varrho\frac{xy}{\sigma_x\sigma_y} + \frac{y^2}{\sigma_y^2}\right)\right]:$$

$$\varrho = \varrho_{xy}(\tau) = \frac{C_{xy}(\tau)}{\sigma_x\sigma_y} = \sin\left\{\frac{\pi}{2} C_{xy}(\tau)_{pol}\right\} \qquad (9.9)$$

with $\sigma_x^2$ and $\sigma_y^2$ the variances of x(t) and y(t).

When the signals are not Gaussian distributed, it is still possible to use the simple computational formula (9.8) although for most cases an analytical expression like (9.9) is not so very simple to obtain (see chapter VI for an example of this).

For all types of joint distributions of the input signals to the correlator it is possible to use a polarity correlator, provided that beforehand certain independent auxiliary signals $h_1(t)$ and $h_2(t)$ are added to the statistical variables x(t) and y(t) (see [4-7]). In such cases it can be derived simply that

$$C_{xy}(\tau) = \alpha \,.\, C_{x+h_1,\ y+h_2}(\tau)_{pol} \qquad (9.10)$$

where $h_1(t)$ and $h_2(t)$ each have an uniform amplitude density distribution with zero mean and $\alpha$ is a constant, dependent on the second moments of the distribution functions of the signals. The maximal amplitudes of $h_1(t)$ and $h_2(t)$ have to be larger than the maximum amplitudes in the signals x(t) and y(t) respectively.

For discrete signals (9.6) may be written as

$$C_{xy}(i \,.\, \Delta\tau) = \lim_{N\to\infty} \frac{1}{2N+1} \sum_{-N}^{N} x_k \,.\, y_{k-i} = x_k \,.\, y_{k-i} \qquad (9.11)$$

$C_{xy}(i\Delta\tau)$ is exactly the sampled continuous correlation function (9.6).

To get an idea of the effect of the correlation process on the signals, e.g. in SNR terms, it is desired to obtain an expression of the variance in the correlation function as a function of integration time and delay $\tau$. It has been shown by Bendat [8], that for the finite correlation function, integrated over T seconds:

$$C_{xy}^{*}(\tau) = \frac{1}{T}\int_0^T x(t) \,.\, y(t-\tau)dt$$

the variance can be written as

$$\sigma_{xy}^2(\tau, T) = \frac{2}{T^2}\int_0^T (T-\nu)\ [P_{xy}^2(\tau, \nu) - C_{xy}^2(\tau)]\ d\nu$$

with $P_{xy}(\tau,\nu)$ a function of the input variables:

$$P_{xy}^2(\tau, \nu) = x(t) \,.\, y(t - \tau) \,.\, x(t - \nu) \,.\, y(t - \nu - \tau)$$

for which it is required to know the fourth order distribution function of the variables.

For a crosscorrelation function $C_{xy}^*(\tau)$ and for those $\tau$-values where $C_{xy}(\tau) \approx 0$ it follows that

$$\sigma_{xy}^2(\tau, T) = \frac{2}{T^2} \int_0^T (T - \nu)\, C_{xx}(\nu) C_{yy}(\nu) d\nu \tag{9.12}$$

Under the same assumptions it can be derived for the PCCF [9] that

$$\sigma_{xy}^2(\tau, T)_{pol} = \frac{8}{\pi^2 T^2} \int_0^T (T - \nu) \{\arcsin \varrho_{xx}(\nu)\} \{\arcsin \varrho_{yy}(\nu)\} d\nu \tag{9.13}$$

when the signals x(t) and y(t) have a Gaussian joint distribution. The last expression gives only a slightly greater variance than (9.12).

### 3. *Matched filtering*

When a signal $x_0(t)$ of known waveshape is buried in white Gaussian noise $n_0(t)$, a filter can be devised, that has an output $x_1(t)$, which best fits, in least squares terms, with the signal $x_0(t)$. Such filters are commonly called optimal or matched filters, in the sense that the output waveform is matched with the known signal.

It appears that the impulse response h(t) of such a filter coincides exactly with the signal shape of $x_0(t)$ for inverted time [10]:

$$h(t) = x_0(-t) \tag{9.14}$$

This means that for the input signal

$$y_0(t) = x_0(t) + n_0(t) \tag{9.15}$$

the following quadratic cost function is a minimum:

$$\int_{-T/2}^{T/2} \{y_1(t) - x_0(t)\}^2 dt \tag{9.16}$$

T is the observation time of the signal and $y_1(t)$ is the filter output:

$$y_1(t) = x_1(t) + n_1(t) = \int_{-T/2}^{T/2} y_0(\tau)\ h(t-\tau)\ d\tau \tag{9.17}$$

When $y_1(t)$ is written in the form of (9.6) then it can be seen that (9.17) is exactly T times the sum of the autocorrelation function of $x_0(t)$ and the cross-correlation function between $x_0(t)$ and $n_0(t)$, integrated over T:

$$y_1(t) = \int_{-T/2}^{T/2} x_0(\tau)\ x_0(\tau - t)\ d\tau + \int_{-T/2}^{T/2} n_0(\tau)\ x_0(\tau - t)\ d\tau \tag{9.18}$$

The first term has its maximum value at $t = 0$. The SNR at the moment of maximum correlation can now be calculated. One must be aware that we have calculated a filter response that optimizes the SNR, in order to distinguish this matched filter from other types of optimum filters, matched on the basis of other criteria.

Assuming that the signal has a bandwidth 2W and a duration of T seconds we will calculate the SNR at the filter output ($SNR_1$) for $t = 0$. With the assumption that the noise has a uniform power density spectrum between —W and +W we may write for the energy per unit bandwidth:

$$N_0 = \frac{1}{2W} \int_{-T/2}^{T/2} n_0^2(t)dt \text{ and } S_0 = \frac{1}{2W} \int_{-T/2}^{T/2} x_0^2(t)\ dt \tag{9.19}$$

Then we can write

$$SNR_1 = \frac{E\{C_{x_0x_0}{}^2(0)_T\}}{E\{C_{x_0n_0}{}^2(0)_T\}} = \frac{(2W \cdot S_0)^2}{(2WS_0)\ (2WN_0)} = \frac{S_0}{N_0} \tag{9.20}$$

All energy of the signal is collected at $t = 0$ by the filtering process. The denominator of (9.20) has been calculated by observing that the sum of independent Gaussian variables is again a Gaussian variable [11]. The above calculations are also of course applicable when the signal $x_0(t)$ is shifted over a delay of $t_0$ seconds, so that $y_1(t)$ has its maximum for $t = t_0$.

### *4. Detection*

The quality of a detection procedure can be expressed in terms of statistical errors in the signals or measurements. The threshold in a binary detection system

is mostly compared with the logarithm of the ratio of weighted a priori probabilities of signal and noise (Bayes criterion), the likelihood ratio [12]. For the case of the detection of a known signal $x_0(t)$ (see preceding section) in the midst of white Gaussian noise $n_0(t)$ the likelihood ratio may be written as

$$L(y_0) = \exp -\frac{S_0}{2N_0} \exp \frac{\int_{-T/2}^{T/2} y_0(t)\, x_0(t - t_0)\, dt}{N_0} \qquad (9.21)$$

When the arrival of the known signal $x_0(t-t_0)$ has to be estimated, then the optimum detection appears to utilize the computation of the maximum of $L(y_0)$: the maximum likelihood ratio. From (9.21), it can be seen that L has a maximum for a maximal integral. The integral is, see (9.18), just the output of the SNR-matched filter with response $x_0(-t)$. When one wants to estimate continuously the arrival of the signals $x_0(t-t_k)$ it is thus sufficient to measure the maxima of the optimally filtered signal $y_0(t)$.

5. *Fourier transformation, power spectrum*

For discrete signals, the Fourier transform is defined as [13]

$$Y_i = \sum_{k\ 0}^{N-1} x_k \exp.(-2\pi jik/N) \qquad i = 0,1,\ldots N-1 \qquad (9.22)$$

This expression is also called the discrete Fourier transform (DFT).

With a recently published computation method, the fast Fourier transform (FFT), it is often much faster to perform a digital convolution process in the frequency domain instead of in the time domain. The power spectrum for discrete signals can be computed either from (9.22) of from (9.6).

For the sampled correlation function the power spectrum becomes [14]:

$$G_i = \Delta\tau \left[ C(0) + 2 \sum_{k=1}^{N-1} C(k \,.\, \Delta\tau) \cos \frac{\pi ik}{N} + C(N \,.\, \Delta\tau) \cos i\pi \right] \qquad (9.23)$$

where the correlation function (9.6) has been sampled for $\tau = 0, \Delta\tau, 2\Delta\tau, \ldots N\Delta\tau$.

6. *Coherent averaging*

The SNR of signals composed of a consistent and recurrent waveform embedded in additive noise can be improved, using coherent averaging techniques. In case of a purely independent disturbance it can be shown that the SNR im-

proves linearly with the number of averaged waveforms [15]. The original SNR for the signal

$$y(t) = x(t) + n(t) \tag{9.24}$$

can be written at $t = t_0$ :

$$SNR_0 = \frac{E\{x^2(t = t_0)\}}{E\{n^2(t)\}} = \frac{E\{x^2(t_0)\}}{n^2(t)} \tag{9.25}$$

x(t) itself is a signal with a waveform w(t) which recurs at the instants of occurrence of the point events in the series $\varphi(t)$, so that

$$x(t) = \varphi(t) * w(t)$$

The minimal interpulse distance of $\varphi(t)$, $T_\varphi$, is normally longer than the duration of w(t), defined for T seconds.

The coherent averaging procedure can be written with (9.1) or (9.6) respectively as a summation or averaging procedure. (9.1) with (9.24) yields for finite time:

$$\begin{aligned} w^*(t) &= \varphi(t) * y(-t) \\ &= \varphi(t) * x(-t) + \varphi(t) * n(-t) \\ &= x^*(t) + n^*(t) \end{aligned} \tag{9.26}$$

The new SNR is then for N added waveforms [11]:

$$SNR_1 = \frac{E\{x^{*2}(t)\}}{E\{n^{*2}(t)\}} = \frac{N^2 E\{x^2(t)\}}{N E\{n^2(t)\}} = N\, SNR_0 \tag{9.27}$$

From (9.27) the improvement, proportional with the number of averaged signals, can be seen.

## References


1. Blackman, R. B. and J. W. Tukey, "The measurement of power spectra", Dover Publications, New York, 1958, p.p. 73—118 and p.p. 14, 95.
2. Doob, J. L., "Stochastic processes", Wiley, New York, 1953, ch. 10, 11.
3. Van Vleck, J. H. and D. Middleton, "The spectrum of clipped noise", Proc. IEEE, vol. 54, 1966, p.p. 2—19.
4. Veltman, B. P. Th. and H. Kwakernaak, "Theorie und Technik der Polaritätskorrelation für niederfrequenter Signale", Regelungstechnik, vol. 9, 1961, p.p. 357—364.
5. Van Bemmel, J. H., "Calculation and measurement of correlation functions with the aid of auxiliary signals", Res. Report, Dept. of Applied Physics, Techn. University Delft, 1963.
6. Peek, H., "The measurement of correlation functions in correlators using shift independent functions", Thesis, Techn. University Eindhoven, 1967.

7. Van Bemmel, J. H. and S. J. Hengeveld, "The Cobra, an on-line correlator", Int. Report, Institute of Medical Physics TNO, Utrecht, 1966.
8. Bendat, J. S., "Principles and applications of random noise theory", Wiley, New York, 1966, ch. 7.
9. Van den Bos, A., "The variance of autocorrelation estimates of clipped Gaussian noise", Res. Report 65—1, Dept. of Applied Physics, Techn. University Delft, 1965.
10. Zadeh, L. A. and J. R. Ragazzini, "Optimum filters for the detection of signals in noise", Proc. IRE, vol. 40, 1952, p.p. 1223—1231.
11. Cramer, H., "Mathematical methods of statistics", Princeton University Press, 1946, ch. 17.
12. Selin, I., "Detection theory", Princeton Univ. Press, 1965, chapter 2.
13. Several authors, "Special issue on Fast Fourier Transform", IEEE Trans. on Audio and Electroacoustics, AU-15, 1967, p.p. 43—114.
14. Blackman, R. B. and J. W. Tukey, op. cit., p.p. 30—37.
15. Bendat, J. S., "Mathematical analysis of average response values for nonstationary data", IEEE Trans. on Bio-Med. Engng., BME-11, 1964, p.p. 1129-1134.

# STELLINGEN

## I

Een bruikbare maat voor de irregulariteit in een reeks van N opeenvolgende hartslagintervallen van duur $T_i$ ($i = 1, 2, \ldots N$) is de hoek tussen de vectoren $T = (T_1, T_2, T_3, \ldots T_N)$ en $E = (1_1, 1_2, 1_3, \ldots 1_N)$.

Dit proefschrift, hoofdstuk VII en VIII.

## II

Indien de constructie van hulpsignalen $h_1$ en $h_2$ voor polariteitscorrelatoren gebaseerd wordt op rademacher functies $r_i$ verdienen gewichtsfactoren $a_i$ die zich verhouden als $a_i/a_{i+1} = 2$ de voorkeur

$$(h_1 = \sum_{1}^{n} a_i r_{2i-1} \text{ en } h_2 = \sum_{1}^{n} a_i r_{2i}).$$

J. B. H. Peek, proefschrift 1967, Eindhoven.
Dit proefschrift, hoofdstuk VIII.

## III

Het ontbreken van de T-golf in abdominale foetale electrocardiogrammen kan verklaard worden uit het capacitief gedrag van het weefsel tussen het foetaal hart en de meetplaatsen.

Dit proefschrift, hoofdstuk II.

## IV

Detectie van gestoorde quasi-periodiek voorkomende signaalcomplexen, van korte duur ten opzichte van de gemiddelde periodelengte en met gemiddelde waarde gelijk aan nul, is mogelijk met een gelijkrichter en een correlator.

Dit proefschrift, hoofdstuk VI.

V

Voor de meting van electrocardiogrammen tijdens fysieke inspanning is het gunstiger om een nieuw stelsel afleidplaatsen te gebruiken dan om cohaerente middelingstechnieken toe te passen op de standaardafleidingen. De matrix voor de transformatie van de nieuwe ECG's naar standaard ECG's is per individu verschillend.

VI

Het model opgesteld door Warner, Cox en Russell dat de invloeden van vagus en sympathicus op de hartslagfrequentie beschrijft is door de vele vrijheidsgraden bij de huidige meetmogelijkheden oncontroleerbaar.

H. R. Warner en A. Cox, J. Appl. Physiol. 17 (1962) 349.
H. R Warner en R. O. Russell, Circ. Res. 24 (1969) 567.

VII

Het begrip over de werking der hersenen neemt niet toe als bij een wiskundige beschrijving, gebaseerd op signalen vanaf de hersenschors, een fysiologische interpretatie ontbreekt.

H. Spekreyse, proefschrift 1966, Amsterdam.
A. Rémond, EEG Journal 26 (1969) 350.

VIII

Inter- en intra individuele variabiliteit bemoeilijken het stellen van een diagnose. Na het vastleggen van iedere patient in een eigen standaard is de digitale rekenmachine van onmisbaar nut bij patientenbewaking en bevolkingsonderzoek.

IX

In de ultrageluidsdiagnostiek verdient het gebruik van electronische aftastmethoden de voorkeur boven mechanische aftasttechnieken.

J. C. Somer, Ultrasonics 6 (1968) 153.

X

Rationalisatie en operationele besliskunde ten behoeve van de Nederlandse ziekenhuizen zullen op den duur leiden tot een minder snel stijgen van de verpleegprijzen. Een systematisch onderzoek hiernaar is te veelomvattend voor één ziekenhuis

J H van Bemmel, Computers in European Hospitals, 1967

XI

De vermeende zelfstandigheid van de — door rekenautomaten vergrote — machten in wetenschap, techniek en organisatie is een gevolg van de onmondigheid en onzelfstandigheid die de mens zichzelf aandoet.

H van Riessen, Mondigheid en Machten, 1967

XII

Aan futurologische uitspraken van beoefenaars van wetenschap wordt vaak ten onrechte dezelfde waarde gehecht als aan hun wetenschappelijke beweringen.

J H van Bemmel

2 oktober 1969